Mineral Replacements in Flooding Experiments Linked to Enhanced Oil Recovery in Chalk

by

Mona Wetrhus Minde

Thesis submitted in fulfilment of
the requirements for the degree of
PHILOSOPHIAE DOCTOR
(PhD)

Faculty of Science and Technology
Institute of Energy Resources
2018

University of Stavanger
NO-4036 Stavanger
NORWAY
www.uis.no

ISBN: 978-82-7644-799-6
ISSN: 1890-1387
PhD: Thesis UiS No. 419

To my parents,

Anne Lise & Per Gunnar,

and my family,

Pål, Espen & Maren

Acknowledgements

The quote “dwarfs standing of the shoulders of giants” has been traced back the 12th century, but is certainly also valid in the 21st century. I feel lucky to have been able to work with the group of researchers at UiS studying chalk. Not only have I been able to learn from the best, building on the work performed over the last decades, I have also had the opportunity to study samples from so many experiments, performed by others and myself, enabling me to work with a wide range of research questions over the last three years.

I would like to thank my supervisors Professor Merete Vadla Madland and Professor Udo Zimmermann for the guidance they have given me, the trust they have put in me and for providing me with chances to work with different people, equipment and in different places around the world I would not have experienced without them. I am truly thankful, this could not have been done without you!

I would also like to thank the engineers at UiS who are always there to help and especially Reidar Inge Korsnes for his sharing of knowledge, his help, patience and good mood, helping me keep the faith. In addition, I want to thank Professor Aksel Hiorth for all his help in modelling and understanding the geochemical theory behind rock-fluid interaction, as well as fruitful discussions on many questions. Among all the colleagues who have helped me on my way, I also want to thank Vidar Folke Hansen for his help in electron microscopy and for support the last years.

I would like to thank the National IOR Centre of Norway and UiS for employing me and all my former and current colleagues and friends at UiS, especially Ema Kallesten, Nina Egeland and Irene Ringen for good companionship and collaboration, as well as Tania Hildebrand-Habel and Ingunn Cecilie Olsen for introducing me to the wonderful world of electron

microscopy. The list of people to thank at UiS, and IRIS, includes many more! Working with the group of PhDs in the National IOR Centre of Norway and at the Faculty of Science and Technology has been wonderful, with good scientific discussions, sharing of knowledge and ideas and lots of fun. The Centre has also been an arena for meeting other researchers and representatives from the industry with the possibility to present our work, discussions and receive valuable feedback.

I also like to thank the many institutions around the world I have had the opportunity to visit during my PhD years. I have learned so much from your work and our discussions. A special thanks to Bernhard Schulz and Sabine Gilbricht in Freiberg and the team in Misasa, Japan.

I would like to thank my parents, Anne Lise and Per Gunnar for their support and making me believe in myself. I would like to thank Maren, Espen and Pål and the rest of my family and friends for all the help, support and cheering on the way. Gry, thank you for cheering and motivating me through numerous coffee-breaks and lunches.

Mona Wetrhus Minde

Summary

Seawater injection into chalk-reservoirs on the Norwegian Continental Shelf has increased the oil recovery and reduced seabed subsidence. In the research-field of Improved Oil Recovery (IOR) the effects of injection of seawater-like brines into chalk have been studied for decades. Particular ions in brines seem to have the power to change the wetting conditions of the rock as well as affecting the strength of chalk. Therefore, when optimizing brines to enhance the production of oil, it is paramount to understand how the injected brine impose alterations in geo-mechanical properties, which in turn affect the strength of the rock. These effects are referred to as "water weakening of chalk" and should be controlled to avoid undesired compaction effects and loss in well stabilities, affecting both safety and costs.

This thesis aims to describe the "the which, the how and the where" of mineralogical alterations in chalk when flooded with reactive brines, with special focus on the Mg^{2+}-ion. The produced changes may directly impact mechanical properties of the rock, and can often only be observed at micron- and sub-micron-scale. The study of these alterations therefore requires methods with possibilities to image and quantify the chemical composition of the rock with resolution below pore-scale, often at nano-scale. The analytical tools used in this study are, on one hand, well-known in terms of their application to rocks and partly on chalk, but on the other hand, this research has developed new methodological approaches for the study of mineralogical changes in Enhanced Oil Recovery (EOR) experiments. This work has resulted in the design of a toolbox which holds the possibility to sufficiently investigate the mineralogical effects of EOR-fluids.

Tests have been performed on several types of outcrop chalk, flooded with different brines, at different stresses and temperatures, and for different periods

of time. In addition, similar experiments on “artificial chalk cores”, made from pure calcite powder, have been completed. The tests were performed on cylindrical core samples and analysed by scanning and transmission electron microscopy, Mineral Liberation Analyzer, electron microprobe analysis, whole-rock geochemistry, stable isotope analyses, nano secondary ion mass spectrometry, X-ray diffraction, along with measurements of the specific surface area, density and porosity, and quantification of the composition of the effluent water.

Thorough core- pore- and nano-scale investigation has been conducted and the results from all scales match. The combination of scales supplement each other to an improved understanding of the data and the following results can be highlighted:

Analyses after flooding with NaCl show very few mineralogical reactions in chalk, however, in silica-rich chalk, the distribution of silicate minerals may be significantly altered. After flooding with $MgCl_2$, the results show dissolution of calcite and precipitation of magnesite. The occurrence and shape of new-grown crystals depend on flooding time and distance from the flooding inlet of the sample cores, together with the primary mineralogy of the chalk and its diagenetic history. Crystals vary in size, from a few nanometres up to over 10 μm and may crystallize as single grains or in clusters. Additionally, non-carbonate phases dissolve and precipitate during flooding, altering the distribution of these minerals within the cores. The type of chalk, with different contents and types of non-carbonate minerals, is found to play a role for the strength of the chalk and is also reflected in the precipitated mineral phases during flooding. These new-formed minerals may alter the permeability, porosity and the reactive surface of the flooded chalk.

All tests show pronounced alteration of texture and mineralogy at the flow-inlet side of the core, along with a decreasing trend in magnesium content towards

the outlet. With longer duration of flooding, the alterations move like a front further into the cores, and for a three year long test, the whole core is altered from the primary mineralogy to newly formed minerals. When studied at core- and pore-scale, the newly formed crystals are found to be magnesite with minor calcium impurities, together with clay minerals. In two slightly shorter tests, flooded for one and a half and two years, respectively, the alteration front is still observable. On the outlet side of the cores, the mineralogy still mainly consists of calcite, primary clay minerals and other non-carbonate minerals together with occurrences of newly formed magnesite and secondary clay minerals. On the inlet side of the cores, the mineralogy consists of magnesite and clay minerals, as observed in the experiment flooded for three years. Dolomite or low to high Mg-calcite, are not observed.

An interesting observation in long-term flooded chalk, is the abrupt transition between the two mineral regimes found on each side of the alteration front. These transition zones have higher porosity than other parts of the cores, a pattern similar to what is observed in single-crystal experiments, where the alterations happen through dissolution and precipitation, driven by the progression of high porosity-zones and the state of equilibrium at the boundary between the primary and secondary mineral phases.

In long-term flooded chalk, the texture of larger macrofossils is often preserved, while their mineralogy is altered. Such pseudomorphism is observed at centimetre- and micrometre-scale, but not at nanometre-scale, pointing to the precipitation rate of magnesite being the rate-limiting factor, found to result in micrometre-scale pseudomorphism. Severe signs of dissolution on calcite grains and high-resolution analyses of precipitation on grain-scale confirm that the formation of new mineral phases is controlled by dissolution and precipitation, and not by molecular solid state diffusion.

Saturation indices modelled along the flooding axis of chalk cores, during flooding with reactive brines, do, in general, not match the form and size of crystals and aggregates observed in these experiments. It seems that smaller crystals precipitate in the fluid-phase at the inlet where nucleation rates are high, and subsequently aggregate and settle downstream in the core, towards the outlet. As such, the crystal shapes and sizes are dictated by a function of nucleation, growth and transport rates within the core. Moreover, the transport includes both transport of ions and nanometre-sized crystals in the fluid-phase. The fluid-flow may also be affected by the primary texture and fractures in chalk, which in turn also concern the mineralogical alterations due to rock-fluid interactions when injecting $MgCl_2$ as well as seawater. Preliminary studies show that mineralogical changes in outcrop chalk from the Niobrara Fm (USA) are similar in water wet and mixed wet systems, suggesting that the observations made in water wet chalk may be used to interpret mixed wet chalk and to understand hydrocarbon reservoir behaviour.

All these points are important input parameters to models and simulators which are used at all scales to predict effects of any EOR fluids. The interaction between laboratory experiments and modelling as well as simulation is essential to understand the underlying mechanisms at play when flooding chalk with non-equilibrium brines as well as to constrain and validate models and simulation of fluid-injection.

These studies have tested numerous analytical methods and the experiences have shown that through application of basic analysis tools such as electron microscopy, X-ray diffraction, whole-rock and stable isotope geochemistry, the major mineralogical changes in flooded chalk-cores may be identified and sufficiently quantified. More detailed information on nano-scale can be provided, as shown, by e.g. transmission electron microscopy on focused ion beam lamellas. For core-scale mapping, scanning electron microscopy mapping

tools, such as Mineral Liberation Analyser or QEMSCAN, can provide helpful results. Together, these tools provide a toolbox for researchers and industry, which may help to understand the effects of injection of reactive brines and how the rocks depositional facies and diagenetic history impact the effects of EOR-fluids in laboratory experiments, pilot projects and field implementations.

List of publications

Paper I:

Minde, M.W., Zimmermann, U., Madland, M.V., Korsnes, R.I., Schulz, B., Gilbricht, S. (In review)
Mineral Replacement in Long-Term Flooded Porous Carbonate Rocks. *Geochimica et Cosmochimica Acta.*

Paper II:

Minde, M.W., Madland, M.V., Zimmermann, U., Egeland, N., Korsnes, R.I., Nakamura, E., Kobayashi, K., Ota, T. (In review)
Mineralogical alterations in calcite powder flooded with MgCl2 to study Enhanced Oil Recovery (EOR) mechanisms at pore scale.
Microporous and mesoporous materials.

Paper III:

Minde, M.W., Zimmermann, U., Madland, M.V., Korsnes, R.I., Schulz, B. and Audinot, J.-N. (2016)
Fluid-flow during EOR experiments in chalk: insights using SEM-MLA, EMPA and nanoSIMS applications.
SCA annual symposium, Snowmass Colorado.

Paper IV:

Minde, M.W., Wang, W., Madland, M.V., Zimmermann, U., Korsnes, R.I., Bertolino, S.R.A. and Andersen, P.Ø. (2018)
Temperature effects on rock engineering properties and rock-fluid chemistry in opal-CT-bearing chalk.
Journal of Petroleum Science and Engineering 169, 454-470.

Paper V:

Andersen, P.Ø., Wang, W., Madland, M.V., Zimmermann, U., Korsnes, R.I., Bertolino, S.R.A., Minde, M.W., Schulz, B. and Gilbricht, S. (2017) Comparative Study of Five Outcrop Chalks Flooded at Reservoir Conditions: Chemo-mechanical Behaviour and Profiles of Compositional Alteration. *Transport in Porous Media* 121, 135–181.

Paper VI:

Zimmermann, U., Madland, M.V., Minde, M.W., Borromeo, L. and Egeland, N. (2017)
Tools to Determine and Quantify Mineralogical Changes During EOR Flooding Experiments on Chalk,
Abu Dhabi International Petroleum Exhibition & Conference. Society of Petroleum Engineers, Abu Dhabi, UAE.

Paper VII:

Borromeo, L., Egeland, N., Minde, M.W., Zimmermann, U., Andò, S., Madland, M.V. and Korsnes, R.I. (2018)
Quick, Easy, and Economic Mineralogical Studies of Flooded Chalk for EOR Experiments Using Raman Spectroscopy.
Minerals 8 (6).

List of additional papers

Borromeo, L., Minde, M.W., Zimmermann, U., Andò, S., Toccafondi, C. and Ossikovski, R. (2017)
A new frontier technique for nano-analysis on flooded chalk: TERS (Tip Enhanced Raman Spectroscopy).
EAGE - 19th European Symposium on Improved Oil Recovery/IOR Norway 2017, Stavanger.

Borromeo, L., Zimmermann, U., Andò, S., Minde, M.W., Egeland, N., Toccafondi, C. and Ossikovski, R. (In press)
Application of Tip-Enhanced Raman Spectroscopy for the nanoscale characterization of flooded chalk.
Journal of Applied Physics.

Egeland, N., Minde, M.W., Kobayashi, K., Ota, T., Nakamura, E., Zimmermann, U., Madland, M.V. and Korsnes, R.I. (2017)
Quantification of Mineralogical Changes in Flooded Carbonate under Reservoir Conditions.
EAGE - 19th European Symposium on Improved Oil Recovery/IOR Norway 2017, Stavanger.

Kallesten, E.I., Zimmermann, U., Minde, M.W. and Madland, M.V. (2017)
Petrological, Mineralogical and Geochemical Constraints on Hydrocarbon Bearing North Sea Reservoir Chalk.
EAGE - 19th European Symposium on Improved Oil Recovery/IOR Norway 2017, Stavanger.

Kjøller, C., Sigalas, L., Christensen, H.F. and Minde, M.W. (2016)
A Fast Method for Homogenous Dissolution of Chalk Specimens for Laboratory Experiments – Documentation by X-ray CT Scanning and Scanning Electron Microscopy.
SCA Annual Symposium, Snowmass, Colorado.

Minde, M.W., Haser, S., Korsnes, R.I., Zimmermann, U. and Madland, M.V. (2017)
Comparative Studies of Mineralogical Alterations of Three Ultra-long-term Tests of Onshore Chalk at Reservoir Conditions.
EAGE - 19th European Symposium on Improved Oil Recovery/IOR Norway 2017, Stavanger.

Neuville, A., Renaud, L., Luu, T.T., Minde, M.W., Jettestuen, E., Vinningland, J.L., Hiorth, A. and Dysthe, D.K. (2017)
Xurography for microfluidics on a reactive solid.
Lab on a Chip 17, 293-303.

Hansen, V., Echevarria-Bonet, C., Minde, M.W., Taftø, J. (In review)
Determination of atomic positions and polar direction in the half-Heusler Sb1-xSnxTi1-y-zHfyZrzCo using Electron channeling.
Journal of Applied physics.

Conference contributions

2018

Korsnes, R.I., Minde, M.W., Madland, M.V., Zimmermann, U. Can we control water induced compaction in chalk reservoirs? Experiences from in-situ core and pore scale studies. *DHRTC – Modified Salinity Water Flooding Workshop*, 2018.

Minde, M.W., Korsnes, R.I., Egeland, N., Madland, M.V., Zimmermann, U. Mineralogical alterations in calcite powder flooded with MgCl2 to study underlying Enhanced Oil Recovery (EOR) mechanisms. *CPM 8*, 2018.

Bredal, T.V., Minde, M.W., Zimmermann, U., Madland, M.V., Korsnes, R.I., Ruud, C. Micro- and nano-analyses of fracture-filling after flooding on-shore chalk with different IOR fluids. *IOR NORWAY 2018*.

Gjersdal, S.G., Minde, M.W., Zimmermann, U., Madland, M.V., Hiorth, A., Giske, N.H., Stavland, A. Polymer-injection for IOR purposes at the Norwegian Continental shelf – micro- and nanoanalytical approach for the understanding of phase-formation and its implication for upscaling. *IOR NORWAY 2018*.

Kavli, E., Minde, M.W., Zimmermann, U., Madland, M.V., Korsnes, R.I., Erba, E. The impact of paleontological components on IOR experiments and upscaling from pore to core and larger scales. *IOR NORWAY 2018*.

Minde, M.W., Sachdeva, J.S., Zimmermann, U., Madland, M.V., Korsnes, R.I., Nermoen, A. Mineral alterations in water wet and mixed wet chalk due to flooding of seawater-like brines. *IOR NORWAY 2018*.

Thu, R.S.W.S., Minde, M.W., Zimmermann, U., Madland, M.V., Korsnes, R.I., Kalai, D.Y. Systematic specific surface area analyses on rocks to implement as a necessary, quick and informative method to understand geomechanical parameter in IOR experiments. *IOR NORWAY 2018*.

2017

Zimmermann, U., Madland, M.V., Minde, M.W., Borromeo, L. and Egeland, N. (2017) Tools to Determine and Quantify Mineralogical Changes During EOR Flooding Experiments on Chalk, *Abu Dhabi International Petroleum Exhibition & Conference. Society of Petroleum Engineers*, Abu Dhabi, UAE.

Egeland, N., Minde, M.W., Kobayashi, K., Ota, T., Nakamura, E., Zimmermann, U., Madland, M.V., Korsnes, R.I. Quantification of Mineralogical Changes in Flooded Carbonate under Reservoir Conditions. *2nd Reservoir Characterization Conference*; 2017.

Minde, M.W., Madland, M.V., Zimmermann, U. From Core to Pore to Field. *NFiP annual one day seminar 2017*.

Minde, M.W.., Zimmermann, U., Madland, M.V. Understanding EOR mechanisms. *Lunch and Learn ConocoPhillips*; 2017.

Borromeo, L., Zimmermann, U., Andò, S., Minde, M.W., Egeland, N., Toccafondi, C., Ossikovski, R. Micro-Raman spectroscopy and TERS (Tip Enhanced Raman Spectroscopy) applied to Enhanced Oil Recovery. *Nano Innovation 2017.*

Borromeo, L., Minde, M.W., Zimmermann, U., Andò, S., Toccafondi, C., Ossikovski, R. A new frontier technique for nano-analysis on flooded chalk: TERS (Tip Enhanced Raman Spectroscopy). *EAGE - 19th European Symposium on Improved Oil Recovery/IOR Norway 2017*.

Egeland, N., Minde, M.W., Kobayashi, K., Ota, T., Nakamura, E., Zimmermann, U., Madland, M.V., Korsnes, R.I. Quantification of Mineralogical Changes in Flooded Carbonate under Reservoir Conditions. *EAGE - 19th European Symposium on Improved Oil Recovery/IOR Norway 2017*.

Kallesten, E.I., Zimmermann, U., Minde, M.W., Madland, M.V. Petrological, Mineralogical and Geochemical Constraints on Hydrocarbon Bearing North Sea Reservoir Chalk. *EAGE - 19th European Symposium on Improved Oil Recovery/IOR Norway 2017*.

Minde, M.W., Haser, S., Korsnes, R.I., Zimmermann, U., Madland, M.V. Comparative Studies of Mineralogical Alterations of Three Ultra-long-term Tests of Onshore Chalk at Reservoir Conditions. *EAGE - 19th European Symposium on Improved Oil Recovery/IOR Norway 2017*.

Neuville, A., Renaud, L., Minde, M.W., Vinningland, J.L., Hiorth, A., Dysthe, D.K. Can we get a better knowledge on dissolution processes in chalk by using microfluidic chips? *EGU General Assembly 2017*.

2016

Kjøller, C., Sigalas, L., Christensen, H.F., Minde, M.W. A Fast Method for Homogenous Dissolution of Chalk Specimens for Laboratory Experiments – Documentation by X-ray CT Scanning and Scanning Electron Microscopy. *SCA Annual Symposium; 2016.*

Nermoen, A., Jettestuen, E., Minde, M.W., Madland, M.V. Quantifying the microscopic morphology of SEM images. *Annual IEA-EOR; 2016*.

Egeland, N., Zimmermann, U., Borromeo, L., Andò, S., Madland, M.V., Minde, M.W., Korsnes, R.I. Raman spectroscopy applied to enhanced oil recovery research. *Goldschmidt conference 2016*.

Minde, M.W., Zimmermann, U., Madland, M.V., Korsnes, R.I. Studies of Mineralogical Changes for the Understanding of Enhanced Oil Recovery Mechanisms at Porescale. *Goldschmidt Conference 2016*.

Borromeo, L., Egeland, N., Minde, M.W., Zimmermann, U., Andò, S., Toccafondi, C., Ossikovski, R. Micro- and Nano- Raman analyses of chalk. *IOR NORWAY 2016*.

Minde, M.W., Zimmermann, U., Madland, M.V., Korsnes, R.I. Micron and submicron investigation - what can we learn? *IOR NORWAY 2016*.

Minde, M.W., Zimmermann, U., Madland, M.V., Korsnes, R.I. "Understanding EOR mechanisms at pore-scale". *IOR NORWAY 2016*.

Egeland, N., Madland, M.V., Zimmermann, U., Kobayashi, K., Nakamura, E., Ota, T., Minde, M.W., Korsnes, R.I. Mineralogical and chemical alteration of calcite by $MgCl_2$ injection. *Misasa International Symposium 2016*.

Minde, M.W., Zimmermann, U., Madland, M.V., Korsnes, R.I., Schulz, B., Audinot, J-N. Fluid-flow during EOR experiments in chalk: insights using SEM-MLA, EMPA and nanoSIMS applications. *SCA annual symposium; 2016.*

Nermoen, A., Jettestuen, E., Minde, M.W., Madland, M.V. Quantifying the microscopic morphology of SEM microscopy images. *ENI Workshop; 2016*.

Table of Contents

Table of Figures

Part 1

1 Introduction

On the Norwegian Continental Shelf (NCS) many of the producing hydrocarbon fields are mature with a declining production trend. A large amount of resources cannot be produced with the current technologies or strategies, and the potential is enormous for creating additional values through improving the recovery from these fields. The time is ripe to implement measures which can improve the recovery of oil, as well as providing better solutions to produce hydrocarbons from future reservoirs in an effective way, with regards to recovery rate, produced water, finances and minimizing the environmental footprint.

Carbonate reservoirs hold over 50% of the world's hydrocarbon reserves (Flügel, 2004; Roehl et al., 1985), and research on carbonate mineralogy is therefore important. In the Norwegian, British and Danish sectors of the southern North Sea, one of the major reservoir rocks is the very fine-grained carbonate rock chalk, containing significant hydrocarbon deposits in formations such as the Ekofisk (Danian), Tor (Campanian to Maastrichtian) and Hod (Turonian to Campanian) Formations.

Injection of seawater is a well-proven Improved Oil Recovery (IOR) measure to maintain pore-pressure and production of hydrocarbons from reservoirs. During the 1980's the chalk field at Ekofisk experienced significant compaction accompanied by seabed subsidence due to depletion of the reservoir (Hermansen et al., 2000; Hermansen et al., 1997; Maury et al., 1996; Nagel, 1998; Sulak et al., 1989; Teufel et al., 1991). To reduce compaction and re-pressurize the reservoir, injection of seawater was introduced in 1987. The injection program succeeded to build up pore-pressure, however, reservoir compaction continued even after re-pressurization (Delage et al., 1996). This phenomenon was explained by interactions between ions in the seawater and

the rock itself, and is referred to as "water weakening of chalk". Since this discovery, understanding the interactions between non-equilibrium brines and reservoir rock has been of major interest both in scientific research and to the industry.

Compaction is an important driving mechanism to increase the recovery of oil, and injection of non-equilibrium brines has proven to also affect the wetting state of the rock, thus the possibility to release more of the immobile oil from the rock surface. Injection of fluids with specific compositions is referred to as Enhanced Oil Recovery (EOR), and is concerned with optimizing the injection fluid to produce the immobile oil, thus maximising the recovery of hydrocarbons.

Over the last decades, large amounts of experiments have been carried out to understand how ions in non-equilibrium brines interact with the rock in which it is injected into, in particular with chalk. Spontaneous imbibition experiments have shown that certain ions in e.g. seawater are more active in rock-fluid interaction than others affecting the recovery of oil, and that both temperature and primary mineralogy may be important factors in this interplay (Austad et al., 2008; Fathi et al., 2011; Fernø et al., 2011; Generosi et al., 2017; Milter et al., 1996; Puntervold et al., 2008; Sakuma et al., 2014; Strand et al., 2006; Zhang et al., 2007). Ions in the seawater may alter the mineral surfaces from oil or mixed wet to more water wet, especially at elevated temperatures. Of particular interest are Mg^{2+}, Ca^{2+}, and SO_4^{2-}, and the composition of the pore-fluid and injected water are also found to be important factors in water weakening of chalk e.g. (Andersen et al., 2017; Carles et al., 2005; Delage et al., 1996; Gutierrez et al., 2000; Heggheim et al., 2005; Hellmann et al., 2002; Hiorth et al., 2013; Korsnes et al., 2008a; Korsnes et al., 2008b; Madland et al., 2011; Megawati et al., 2013; Megawati et al., 2015; Nermoen et al., 2015; Nermoen et al., 2018; Newman, 1983; Piau et al., 1994; Rhett et al., 2001;

Risnes et al., 2005; Schroeder et al., 1998; Tucker et al., 1990). There are multiple processes affecting the rock during flooding with reactive brines. This includes changes in surface-complexation, -charge and -potential along with alterations of mineralogy and ion-exchange (e.g. (Andersen et al., 2017; Austad et al., 2008; Borchardt et al., 1989; Flügel, 2004; Heggheim et al., 2005; Hiorth et al., 2010; Hiorth et al., 2013; Jackson et al., 2016; Korsnes et al., 2008b; Madland et al., 2011; Megawati et al., 2013; Nermoen et al., 2015; Sakuma et al., 2014; Strand et al., 2006; Tucker et al., 1990; Zhang et al., 2007; Zimmermann et al., 2015)). Chalk is a rock, which due to its very fine-grained character, has a high specific surface area (often between 1.5 and 7 m^2/g, (Hjuler et al., 2009)), up to 10 times the value of sandstones. The injected seawater therefore interacts with the rock along extended mineral surface areas, which increase the effect of rock-fluid interactions, hence the fluid sensitivity of the rock (Heggheim et al., 2005). Changes in the mineralogic composition affect compaction, specific surface area, mineral surface charges, porosity and permeability of chalk, as well as the wettability of the grain surfaces. Therefore, when the brine composition is optimized for EOR purposes, it is important to study its effect on mechanical properties.

Understanding the underlying mechanisms of water weakening of chalk is important to predict and control hydrocarbon-reservoir behaviour, through modelling and simulation at all scales. Additionally, water weakening also plays a role in carbonate aquifers and erosion of costal carbonate cliff formations (Lawrence et al., 2013; Mortimore et al., 2004).

In this study, the main objective has been to investigate which, how and where mineralogical alterations take place in a rock sample when flooded with specific fluids under specific conditions, and link those mineralogical alterations to the mentioned changes in mechanical properties of the rock. Previous studies have shown that mineralogical alterations first and foremost

take place at micro- and nano-scale (**Paper IV** and **V** (referring to "List of publications", page xiii and part 2 of the thesis) and e.g. (Madland et al., 2011; Minde et al., 2017; Minde et al., 2016; Zimmermann et al., 2015)). Mineralogical alterations or incorporation of ions can even on grain-scale and below change the adsorption energy of the surface, thus altering the wettability (Andersson et al., 2016; Sakuma et al., 2014). The foci of the research in this study are, on one hand, therefore to understand the mineralogical alterations at core- and pore-scale, down to submicron resolution, and, on the other hand, to create a "toolbox" that is equipped with a set of methods that provide informative and effective analyses of mineral replacement reactions in rocks, related to EOR research as discussed in **Paper VI**.

This approach delivers explanations in regard of the which, the how and the where:

1) **Which** mineralogical alterations take place? **Which** shape and structure do the precipitated minerals have?
2) **How** do the mineral replacements take place?
3) **Where** do the changes take place? Is the preferred place related to texture, original mineralogy and distance from the fluid injection site?

Studies of mineral replacements encompass a wide range of disciplines. Research carried out to understand the kinetics and reactions associated with mineral replacements, whether these are linked to metamorphism, metasomatism, diagenesis and/or weathering, is of importance not only as basic knowledge of rock-fluid interactions, but also to "…quantify and predict the response of Earth's surface and crust to the disequilibria caused by the various natural and anthropic input of energy to our planet." (Oelkers et al., 2009). Carbonate sedimentary rocks are common on Earth and limestone and dolomite are two major rock-types found in sedimentary rock successions. Limestones are important contributors in the global carbon and geochemical cycles.

Additionally, carbonate mineral kinetics dictate a wide range of processes in our world like preservation of large monuments and buildings as well as the characteristics of petroleum reservoirs (Morse et al., 2002), and are important for the development of fauna and algae in the marine environments. Understanding carbonate dissolution and precipitation kinetics are therefore paramount for numerous important processes in nature.

In the field of mineral replacements most of the experiments are carried out on single crystals or on powdered material in fluid-suspension. A thorough review of such experiments is given in Putnis et al. (2009), concluding that in fluid-induced mineral replacements, the transition from one mineral to another progresses from the surface and towards the centre of a crystal by the formation of a porous reaction front where the driver is the state of equilibrium at the reaction interface, not the equilibrium state of the bulk fluid. None of the discussed examples show evidence of solid state diffusion through crystal lattices. The alterations are driven by a front of dissolution and precipitation progressing into the crystal with a sharp reaction rim. The alteration products show different scales of pseudomorphism, dictated by the rate-limiting factor being either the dissolution rate, resulting in nanometre-scale pseudomorphism, or being the precipitation rate, resulting in micrometre-scale pseudomorphism (Xia et al., 2009).

Over the years, in the studies of water weakening of chalk and related EOR research, a need to simplify the system has become apparent. Numerous factors, like brine composition, temperature, pressure, and mineralogical aspects are interdependent, hence it is difficult to separate the effects of each parameter. Seawater has been replaced by simpler aqueous brines, such as $MgCl_2$, to study the effects of specific ions, in this case Mg^{2+}, which is very reactive towards calcite even after short periods of flooding. Additionally, even though chalk largely consists of calcite, differences in primary mineralogy and arguably the

depositional environment seem to dictate many of the alterations during mechanical flow-through experiments (**Paper III**), revealing extraordinary complex rock-fluid interactions. Those aspects are central parts of this thesis, including performing EOR experiments on "artificial chalk cores", (see chapter "2.2.2 Calcite powder" and **Paper II** on this topic) and analysing the mineralogical alterations when calcium is replaced by magnesium. The materials that form the basis of this work are different types of chalk sampled in quarries from Denmark, Belgium and USA (see chapter "2.2 Outcrop chalks in this study" for detailed information about the used sample material) and calcite powder, all tested in triaxial cells (see chapter "2.3.1 Triaxial tests" for detailed experiment description) and compared with untested material or sample material flooded with less reactive brines such as NaCl (**Paper IV and V**).

The analytical tools used in this study are on one hand well-known in terms of their application to rocks and partly on chalk and on the other hand this research presented here developed new methodological approaches for the study of mineralogical changes in EOR experiments. The methods used in this project have been:

- Field Emission Gun Scanning Electron Microscopy (FEG-SEM) with Energy Dispersive X-ray Spectroscopy (EDS)
- Mineral Liberation Analyzer (MLA)
- Focused Ion Beam (FIB)-SEM
- Transmission Electron Microscopy (TEM)
- Electron Microprobe Analysis (EMPA)
- X-ray Diffraction (XRD)
- Nano Secondary Ion Mass spectrometry (nanoSIMS)
- Induced Coupled Plasma – Mass spectrometry (ICP-MS)

- Stable isotope analyses
- Analyses of effluent water
- Measurements of Specific Surface Area (SSA) and density by pycnometry
- Additional analyses by Raman spectroscopy and Tip Enhanced Raman Spectroscopy (TERS) combined with Atomic Force Microscopy (AFM)

By combining all of the above mentioned tools, we have been able to extract considerable amount of information from the studied samples by progressively increasing the resolution of the analyses and comparing results from chemical and elemental analyses with mineralogical and crystallographic techniques such as XRD and Raman spectroscopy (e.g. **Paper I, II and VII)**. With this, it is possible to identify, map and quantify the mineralogical alterations, at centimetre, millimetre, micrometre and nanometre-scale. The value of the different methods for EOR-related issues is variable, and some methods have proven to be more suitable than others. However, this process has enabled the selection of which tools should be part of the mentioned toolbox to interpret experiments involving rock-fluid interactions, and which methods are most suitable to answer very specific questions.

The results from this study are therefore important for a wider range of interest groups:

- Mineralogists
- Applied petroleum geologists and engineers
- Technicians to see how far their methods can be stretched on one of the most complicated study material: chalk
- Modellers. The results are basic components for input to models of all scales simulating the effects of EOR fluids and imbibition processes in

porous rocks (Appelo et al., 2009; Aursjø et al., 2017; Evje et al., 2011; Helland et al., 2017; Hiorth et al., 2013; Lichtner, 1996; Pedersen et al., 2016; Pedersen et al., 2014; Vinningland et al., 2017; Wei, 2012). Some of the most important input parameters are primary and secondary mineralogy, and the rate of which the mineralogical changes occurs. Investigation of mineralogical alterations after core-flooding experiments may provide validation for or constrain models and simulations. Continuous interaction between the two disciplines provides information to improve both experimental and modelling work.

Hence, geological and mineralogical understanding together with rock mechanical studies and modelling is an ideal fusion to reveal the most important data for processes for every interest group concerned about commodities in rocks. This research therefore represents a mixture of basic research and applied science.

2 Material and methods

2.1 Material

2.1.1 Chalk

Chalk is by definition a fine-grained, sedimentary rock, belonging to the class of carbonates and mostly a pelagic sediment composed mainly of biogenic and authigenic grains. It is a rather simple rock in terms of its mineralogy, with the major constituent being calcite ($CaCO_3$), and only minor occurrences, varying from a few and up to 15 wt% (weight percent), of other minerals such as dolomite, quartz, opal, apatite, feldspar, pyrite, oxides and different clay minerals, depending on location, age and degree of diagenesis (Hjuler et al., 2009). The colour of chalk is in most cases white to grey or beige, depending on the non-carbonate content. Chalk has commonly a layered structure at centimetre- to metre-scale, due to its low-energy depositional environment and differences in depositional rates. Periods of non-deposition are commonly represented by hardgrounds or thin layers of clay (Brasher et al., 1996). However, in various geographical areas, tectonic movements can destabilize the chalk and allow for movement of large faulted blocks, often towards the deeper basin (Kennedy, 1987), as extensional tectonics were, in a variety of locations, typical for the Cretaceous times. Together with erosion, block faulting also enabled reworking of chalk either as syn- and post-depositional gravitational flows, often producing a more heterogeneous brecciated structure. The rock is composed mainly of skeletal debris of calcareous micro-fossils such as coccolithophores, calcispheres and foraminifera along with fragments of macro-fossils (Scholle et al., 1973; Tucker et al., 1990). Coccolithophores are unicellular algae, belonging to the group of haptophytes, which control intercellular precipitation of calcite into skeletal plates, referred to as coccoliths

(Scholle, 1978; Thiel, 2011). These coccolith plates are transferred to the surface of the algae, forming an exoskeleton of protection. Coccolithophores often dismantle into their individual skeletal plates, coccoliths, as they die and settle to the seafloor. Coccolithophores commonly have a size less than 20 μm (Thiel, 2011), while individual coccolith rings range between 0.3 and 5 μm (Scholle et al., 1973), or even larger (Kennedy, 1987). Each coccolith ring is built up of platelets or grains with sizes of one μm and below (Bjørlykke, 2015), and these platelets are often found in their individual forms in chalk (Figure 1). Coccolithophores have existed from the Mesozoic era, and were extremely abundant during the Cretaceous period. They still exist in oceans today, and play an important part in the global carbon budget (Thiel, 2011).

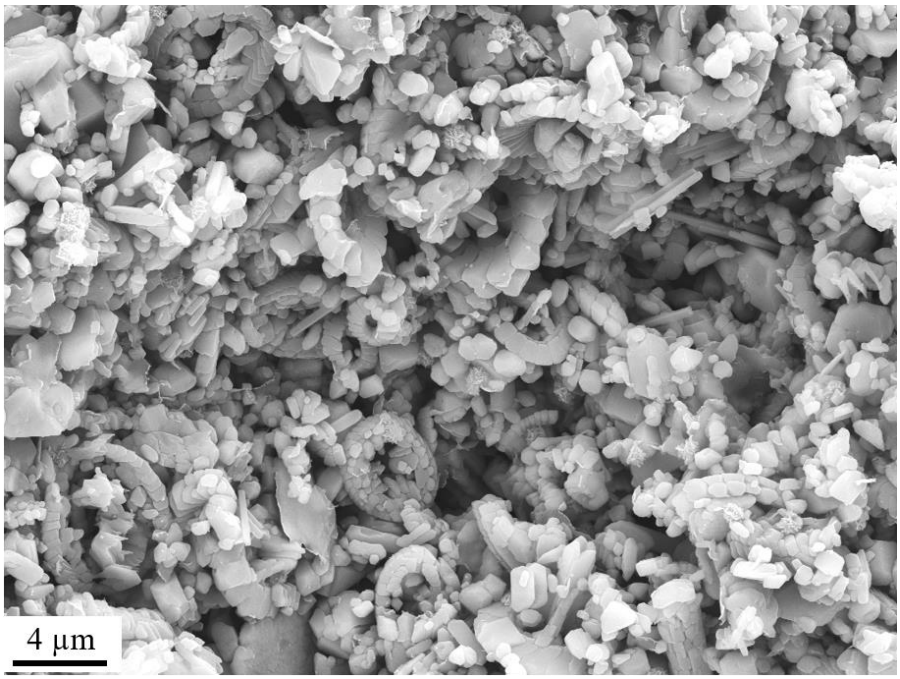

Figure 1: SEM micrograph of Liège chalk showing typical components of chalk; skeletal debris of coccolithophores and other micro-fossils along with minor occurrences of clay minerals.

Foraminifera shells are larger, ranging in size between 20 and 100s of μm, and when preserved, often contribute to larger pore-spaces in chalk (Flügel, 2004;

Scholle, 1978). In addition, shells and fragments from larger fossils like bivalves and gastropods can be observed. As shells and skeletal debris from these organisms fall to the seafloor, they form calcareous ooze. Even though calcareous organisms thrive under warm climatic conditions, oozes accumulates slowly, 1 to 25 cm per thousand year (Garrison, 2010; Tucker et al., 1990), and as such, the over hundreds of metres thick layers of chalk, as found in the North Sea, take millions of years to deposit. The deposition rate is not only related to the accumulation of sediments, but is also affected by dissolution of calcareous material in seawater. Oozes rarely form below the carbon compensation depth (CCD), which is the depth where the dissolution rate is equal to or is higher than the sedimentation rate. This depth usually lies around 4500 meters, depending on e.g. pH, temperature, and CO_2-concentration of the seawater (Garrison, 2010; Hancock, 1975).

Because of the pelagic nature of chalk, the non-carbonate content is generally low. However, clay minerals are often observed, along with other silicates, such as chert and quartz. The origin of these minerals may come from terrigenous inputs in shallow areas or due to depositional lowstands (Brasher et al., 1996), but mainly from volcanic input and diagenesis of siliceous fossils such as sponge spicules, and to a less degree diatoms and radiolarians (Scholle, 1977).

After deposition, burial and de-fluidization lead to compaction and lithification of the ooze. During burial the ooze mechanically compacts, leading to a porosity reduction from 60 – 80% to values commonly between 10 – 50% (Hjuler et al., 2009; Scholle et al., 1973), depending on conditions during burial. Chalk has grainsizes mostly between 1 and 20 µm, with the exception of larger fossils, and permeability is low, often in the range between 1 to 5 mD (Scholle et al., 1973; Sulak et al., 1989). The porosity of reservoir chalk is, however, often surprisingly high for rocks found at such deep burial depth with a fine-grained character, and may be caused by overpressure in the reservoir during

burial or by early oil emplacement (Alam et al., 2012; Brasher et al., 1996; Moore, 2001; Risnes, 2001; Scholle, 1977; Tucker et al., 1990).

During the Late Cretaceous, large areas of Northern Europe were covered by shallow seas, where the Central North Sea Graben formed a deeper marine environment (Molenaar et al., 1997). The sea-floor had structural highs and lows where chalk was commonly deposited in deeper areas.

2.1.2 Fractures in chalk reservoirs

Due to the exceptionally low permeability in high porosity chalk, fractures play an important role during fluid-flow. Matrix permeability in the Ekofisk field, where chalk is the reservoir rock, lies in the range of 1 to 5 mD (Sulak et al., 1989), and can as well be reduced by pore collapse due to increase in effective stress during hydrocarbon depletion of the reservoir during production. Production of oil therefore depends on fractures to increase the effective permeability of the reservoir (Snow et al., 1989) and the effective permeability in the Ekofisk field ranges between 1 to 100 mD (Sulak et al., 1989; Torsaeter, 1984).

Fractures also play an important role during fluid-injection into a reservoir. The fluid-flow mainly follows the fracture system, as well caused by the limited permeability of the matrix. Most of the oil in chalk reservoirs is trapped in the matrix and displacement of oil is mostly related to spontaneous imbibition of water into the matrix (Chen et al., 2001; Cuiec et al., 1994; Milter and Austad, 1996; Morrow and Mason, 2001; Standnes and Austad, 2000; Torsaeter, 1984; Zhang et al., 2007). In a fractured reservoir, where the fluid-flow may be limited to fractures, the contact between injected water and the rock may be limited, thus modifying the effect of EOR fluids (Graue et al., 1999; Gutierrez et al., 2000; Hirasaki and Zhang, 2004; Nielsen et al., 2000). Hence, it is important to understand how injected brines use fractures in conjunction with mobilization

of oil from the matrix and create a more efficient sweep. Scenarios, from a mineralogical aspect, would be clogging of fractures forcing brines to enter the matrix and affecting the production of hydrocarbons.

2.2 Outcrop chalks in this study

Reservoir chalk from the North Sea is difficult to sample due to the expense of extracting it and shortage of core material. Laboratory tests are therefore rarely carried out on reservoir rocks from deposits in the North Sea, but more commonly on onshore chalk analogues. There are several outcrops around the world where analogues to North Sea reservoir chalk may be collected. The various onshore chalks have different composition and mechanical properties (Hjuler et al., 2009), and different chalks are therefore used to test different research questions and to understand different reservoirs. For fundamental studies, the application of outcrop samples gives sufficient information for further research and is paramount for all modelling exercises in this field of research and has been applied with success for decades.

Five types of outcrop chalks have been sampled for this study. They are collected from quarries of Lixhe near Liège and Harmignies in Mons, Belgium, along with two Danish chalks: Stevns Klint sampled near Copenhagen and Rørdal near Aalborg, and chalk from the Niobrara Formation in Kansas (USA).

2.2.1.1 Liège: Gulpen Formation

One of the outcrop chalks used in this study is from the Gulpen Formation, sampled from an outcrop near Liège in Belgium, and is found to match the mechanical behaviour of chalk from the Ekofisk field (Collin et al., 2002). The Gulpen Formation is of Late Campanian to early Maastrichtian age (Molenaar et al., 1997).

The chalk from the Liège outcrop has a high carbonate content. The non-carbonate content is approximately 5 wt% and consists of quartz, smectite/mixed smectite-illite layer, mica and clinoptilolite as well as apatite, feldspar, pyroxene and titanium oxide (Hjuler et al., 2009). The preservation of coccoliths and pore-space is medium and good, respectively. Calcite cementation is commonly not found in studies on this type of chalk (Hjuler et al., 2009), pointing to a low degree of diagenesis. The porosity of chalk from Liège lies in the range of 40 to 43%, with a permeability between 1 and 2 mD (Delage et al., 1996; Korsnes et al., 2006; Madland et al., 2011; Risnes et al., 1994; Schroeder et al., 1998).

2.2.1.2 Mons; Trivières Formation

One of two chalk types with extremely high carbonate content used in this study is collected from Mons, Belgium. The chalk from Mons is taken from the Trivières Formation of Campanian age. The chalk was deposited in the Mons basin, the eastern part of the Paris basin, and the sampled outcrop is found in Harmignies. The Trivières Formation is correlated to the Gulpen Formation sampled in Liège (Dusar et al., 2007). Porosity is in the range of 36 to 44% (Gaviglio et al., 1999) and the non-carbonate content only reach less than 1% (**Paper V**). The chalk from the Trivières Formation has a high degree of intact coccoliths (Richard et al., 2005). Chalk samples from this outcrop have together with chalk from Stevns Klint in Denmark been used as an analogue to both the Valhall, Dan and Ekofisk chalk reservoirs in the North Sea.

2.2.1.3 Stevns Klint: Tor Formation, Sigerslev Member

The chalk from Stevns Klint belongs to the Tor Formation, in particular the Sigerslev Member and is of middle Upper Maastrichtian age (Surlyk et al., 2006). It consists of nearly 99% carbonate minerals, with only scares

occurrences of quartz, clay, feldspar and apatite (Hjuler et al., 2009; Håkansson et al., 1975). The chalk has porosity values between 42 and 50% and permeability of 1-2 mD (Hedegaard et al., 2011; Madland et al., 2011).

2.2.1.4 Aalborg: Tor Formation, Rørdal Member

Aalborg chalk has been studied to understand which effects the abundant opal-CT have on mineralogical and mechanical properties of the rock during rock-fluid interaction (**Paper IV)**. The chalk is taken from the Rørdal quarry near Aalborg, Denmark and is of Lower Upper Maastrichtian age, and contains 90 – 95% carbonate minerals (Håkansson et al., 1975). The remaining impurities consist mainly of clay and quarts, most commonly in the form of opal-CT along with smectite, mica, kaolinite, clinoptilolite, apatite and feldspar. The exposed chalk at the Rørdal quarry belongs to the Tor Formation of the North Sea and the cyclic Rørdal Member, which is approximately 10 m thick. The rather high non-carbonate content, mainly in the form of diagenetic opal-CT, is linked to the early late Maastrichtian cooling event (Surlyk et al., 2010).

2.2.1.5 Kansas: Niobrara Formation

Furthermore, chalk from a different basin has been used, the so-called 'Kansas chalk' sampled from the Niobrara Formation. The samples are taken from the lowermost Fort Hayes Member which is of Early Coniacian age, (Da Gama et al., 2014), deposited as part of the Western Interior Seaway in the Rocky Mountains and Great Plains region, USA. The non-carbonate content is usually less than 5%, and mainly consists of quartz, clay and pyrite and is described as a bioturbated chalk (Hattin et al., 1977; Longman et al., 1998; Runnels et al., 1949). The content of recrystallized, inorganic calcite and calcite cement is higher in the Kansas chalk compared to other outcrop chalks studied in this thesis (Megawati et al., 2015; Scholle, 1977), pointing to deeper burial depth

and a higher degree of diagenesis. Porosity of chalk from the Niobrara Formation is in the range between 37 and 40% and permeability of 2-4 mD (Andersen et al., 2017; Korsnes et al., 2006; Megawati et al., 2013) and has been considered a good analogue to North Sea reservoir chalk with regards to these properties (Tang et al., 2001).

2.2.2 Calcite powder

As an attempt to simplify the experiments further and to be able to study the basic mineral replacement reactions involving Ca^{2+} and Mg^{2+} separately, the mineralogy of the rock itself was simplified by chalk being substituted by cylinders of calcite powder, mimicking the geometry of outcrop chalk core-samples. They consist of 99.95% pure calcite ($CaCO_3$) powder manufactured by Merck®. Minor impurities of other elements such as Fe and Mg occur. However, the total only adds up to ~0.05%. The particle size has an average of ~14 µm, ranging from 3 to 44 µm. The powder was compressed to cylinders (D~37 mm, L~70 mm) and are hereafter referred to as "artificial chalk cores".

2.3 Methods

The main goal for the use of the methods in this thesis is to image and positively identify new-grown crystals and minerals in fine-grained sedimentary rock samples. Some of the methods can image and identify the elemental composition of a sample, while others provide both elemental and mineralogical qualitative analyses. However, the crystallographic mineralogical analyses are only in cases accompanied by a high-resolution images, with the possibility to identify the exact crystal of analysis. Therefore, the amount of methods taken into use is large, providing the possibility to combine methods to gain then useful complementary data from the analyses.

One of the aims of this work is to create a "toolbox" for mineral replacement studies related to EOR experiments. However, not all of the described methods are suitable for an effective and quick analysis to interpret experiments and samples from EOR tests, but may be used as additional tools to study questions of special interest. Research shall attempt a variety of possibilities and this study shows that the approach of challenging methods leads to further knowledge. Last, but not least, we are able to combine analytical data of different scales to describe the properties of grains and the pore-network from nano- to centimetre-scales.

2.3.1 Triaxial tests

Cylindrical cores were drilled from the different outcrop chalks. The cores were shaped to one of two diameters ~ 37.0 or ~ 38.1 mm, with a length of ~ 70.0 mm and used for mechanical flow-through experiments in triaxial cells.

After preparation, the cores were dried for 12 hours in a heating chamber at 100 °C to remove water before the dry mass was determined. The carbonate mineralogy is not affected by the drying conditions (MacDonald, 1956). Thereafter all cores were saturated with distilled water (DW) in a vacuum chamber. Dry and saturated core mass were used for porosity determination. When installing the core inside the triaxial cell, a heat shrinkage sleeve was used to separate the core from the confining oil. After mounting the triaxial cell, the confining pressure was increased to 0.5 MPa. Thereafter all experiments were conducted according to the following stages:

1. The cores were flooded with at least three pore volumes (PVs) of DW overnight at ambient temperature to clean the sample before the flooding test. This flooding procedure does not significantly alter the geochemical properties of the core.

2. Subsequently, a change from flooding with DW to the reactive flooding brine by attaching the piston cell into the flow loop was performed.
3. The confining pressure and pore pressure were increased simultaneously to 1.2 and 0.7 MPa, respectively, before the temperature was raised to the chosen values. The pore pressure and temperature were then kept constant throughout the test.
4. The confining pressure was increased from 1.2 MPa until the rock began to deform plastically, i.e. when the stress - strain behaviour became non-linear. The confining pressure was, if applicable to the test, further increased to the chosen creep stress before the cores were left to compact in the following creep phase (deformation at constant stress).
5. The axial deformation at constant temperature and pressure conditions (termed creep) was monitored during continuous flooding. The pore pressure and confining pressure varied within 0.1 MPa such that the effective stresses were stable throughout the test period.
6. The temperature was kept constant throughout the experiment by a heating jacket, ensuring an accuracy of ±0.1 °C.
7. Before dismantling the core, the samples were cleaned by injection of minimum three PVs of DW to avoid precipitation of any salts.

After testing the cores were divided into six or seven slices for mechanical, chemical and textural analyses and compared to untested material from the same core (Figure 2).

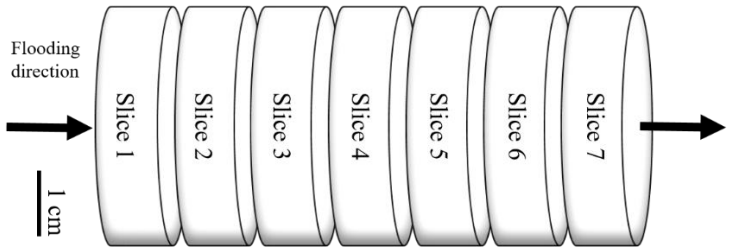

Figure 2: Sketch of a typical core for testing and how it is cut for analyses after ended experiment.

Further details on experimental lay-out and rock mechanical processes can be taken from Madland et al. (2011), Wang et al. (2016) and **Paper IV** and **V** and references therein.

2.3.1.1 Overview over the flooding tests presented in this study

Three long-term tests of injecting $MgCl_2$ into outcrop chalk from Liège were analysed. The cores were flooded for one and a half, two and three years, and named the Long-Term Test (LTT), the Medium-Long-Term Test (MLTT) and the Ultra-Long-Term Test (ULLT), respectively. All cores were flooded at 130 °C, at high effective stresses, with 0.219 M $MgCl_2$ and for the MLTT a period of flooding with 0.219 M $MgCl_2$ + 0,130 M $CaCl_2$ and with changes in pH. For detailed setups and flooding procedures, the reader is referred to **Paper I** and (Minde et al., 2017; Nermoen et al., 2014; Zimmermann et al., 2015).

Chalk from the five described outcrops were flooded for periods of 45-118 days, either with NaCl or $MgCl_2$ at different temperatures. For details, the reader is referred to **Paper IV** and **V**. A chalk core from the Liège outcrop was fractured before flooded with synthetic seawater for 34 days at 130 °C (**Paper III**). Two artificial chalk cores were produced from pure calcite powder and flooded at 130 °C with $MgCl_2$ at close to ambient pressures. The tests lasted for 27 and 289 days. Further description is given in **Paper II**.

2.3.2 Electron microscopy

Electron microscopy offers higher resolution than optical microscopy, in extreme cases up atomic-scale resolution. Unlike with Optical Light Microscopy (OLM), imaging is performed by using an electron beam, with a much smaller wavelength than optical light, thus offering higher resolution than in OLM. Commonly, Scanning Electron Microscopy (SEM) offers also a better depth of field. The interaction of the electron beam with the samples produces different signals, enabling analyses yielding information on topography, texture and composition down to nanometre- and Ångstrøm-scales.

2.3.2.1 Sample preparation

Electron microscopy demands high quality samples. When preparing samples for electron microscopy, it is important that the samples have an electronically conductive surface, to ensure a steady flux of electrons across the sample and avoid charging or build-up of electrons. Sedimentary rocks are, in nearly all cases, non-conductive and have therefore to be coated by a conductive layer, such as carbon, palladium or gold. SEM chambers may take rather large samples, up to tens of cm in diameter, but to ensure good results, the samples should be as small as possible. For chalk, small freshly broken pieces of rock in the size-range of 0.5 x 0.5 x 0.5 cm are often used for analyses. In addition, uncovered, polished thin sections and epoxy impregnated mounts have been used.

For Transmission Electron Microscopy (TEM), sample preparation of the brittle and porous chalk is very challenging. Traditional methods such as mechanical and electrolyte polishing are either difficult or not possible, and the methods found to be most fitted in this study was either deposition of powdered rock on cupper grids coated with carbon films, or sample-preparation by

Focused Ion Beam (FIB)-SEM, discussed in section "2.3.2.4 Focused Ion Beam Scanning Electron Microscopy (FIB-SEM)".

2.3.2.2 Field Emission Gun Scanning Electron Microscope (FEG-SEM)

In Field Emission Gun Scanning Electron Microscopy (FEG-SEM) electrons are accelerated by an electron gun to create a focused electron beam to scan the sample in an evacuated chamber. The FEG-SEM has a field-emission gun, inducing electrons by an electrostatic field. This allows for a much smaller beam-diameter with higher stability and intensity of electrons; hence, the resolution of this type of SEM is higher than when using a filament as source. Through electromagnetic lenses and apertures, the beam is focused and adjusted to produce an as small as possible spot of primary electrons on the sample surface.

When the beam hits the surface of the sample, various energy signals are reflected or produced from the surface which are collected by different detectors. These are, amongst others, Secondary Electrons (SE), Back-Scattered Electrons (BSE), and characteristic X-rays as well as, in cases, visible and fluorescent light. The beam interacts with the sample in three dimension with a spherical emission volume of which diameter will vary with settings of the microscope and the sample-material, but often lie in the range of 1 µm. The emission of secondary electrons will vary as a function of the topography and only partly of the composition of the sample and enables imaging of the surface (Figure 3). As an atom is bombarded with primary electrons, electrons placed in the shells of the atom may be excited and emitted from the sample as secondary electrons. These are in-elastically scattered, and have therefore a lower energy than the primary electrons. The primary electrons penetrate a certain distance into the sample, depending on which type of material is studied

and the settings of the microscope. However, because of the lower energy of secondary electrons, only signals from the upper 5ʎ (ʎ= mean free path of the secondary electrons) will escape the sample (Hjelen et al., 1989). The secondary electrons are gathered by an Everhart-Thornley-detector as the beam scans the surface in a sequence.

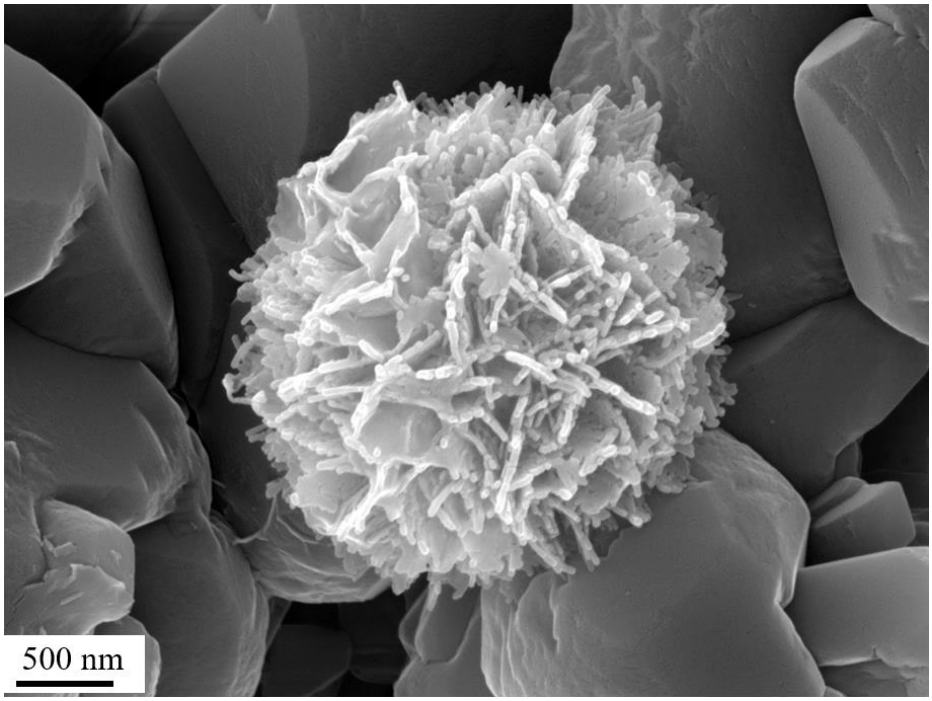

Figure 3: SEM micrograph taken by the use of a SE-detector. The imaged object is an opal-CT lepisphere found in Aalborg chalk.

A BSE detector collects the reflected, or backscattered, primary electrons, which are a result of elastic scattering. The backscattered electrons change direction, while the energy is conserved. The fraction of backscattered electrons produced from the surface is related to the atomic number of the elements in the sample. As such, imaging of different phases in a sample based on composition is possible, returning grey-scale images linked to the Average

Atom Number (AAN) of each phase. A mineral with higher AAN will yield a brighter shade of grey in the image (Figure 4).

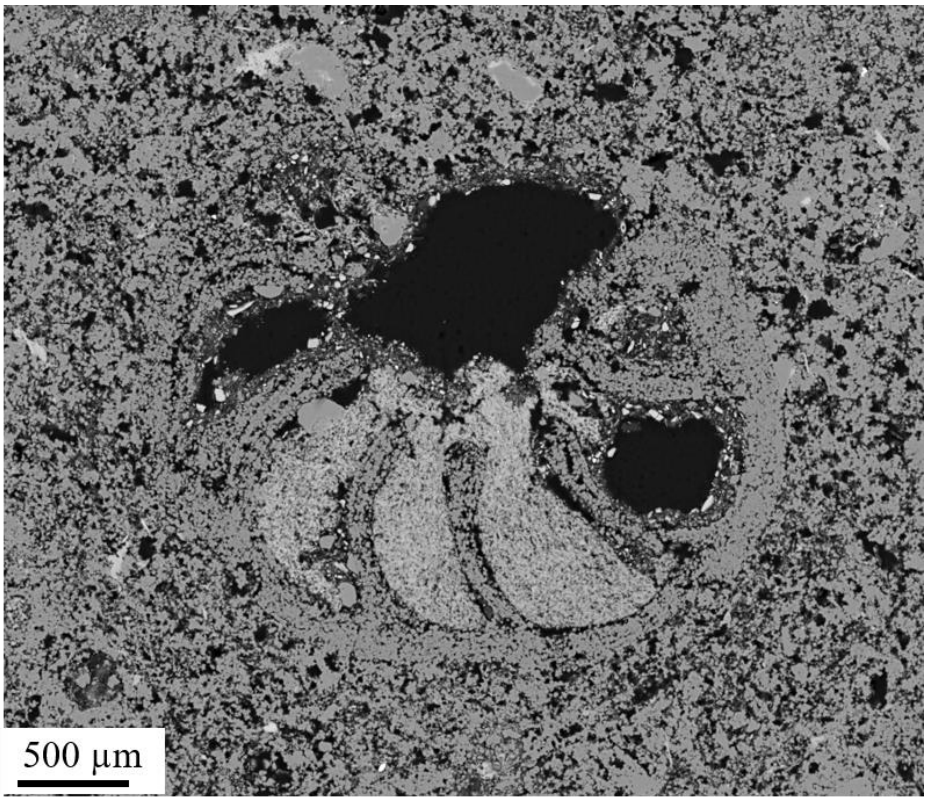

Figure 4: SEM micrograph of a foraminifera fossil found in $MgCl_2$-flooded outcrop chalk from Liège using backscattered electrons (BSE). The difference in grey-scale reflects the average atomic number (AAN) of each phase, thereby separating different mineralogies from each other. Here, clay minerals accumulated inside the fossil walls have a brighter shade of grey than the surrounding magnesite, because of a higher AAN. The black areas are pore-spaces filled with epoxy with a low AAN.

As the backscattered electrons keep their high energy level, the emission-volume of these electrons is larger than for secondary electrons. This means that electrons from deeper into the sample may be emitted and detected.

Energy Dispersive X-ray Spectroscopy (EDS) detects characteristic X-rays which are produced as electrons from the inner shells of atoms are excited by incoming primary electrons and electrons from outer shells jump inward to

replace the excited electrons, thus releasing energy in form of characteristic X-rays. Because of the difference in atomic structure, the energy and the wavelength of the released X-rays from each element will differ. The X-rays are detected by a silicon crystal doped with lithium. Based on the detected X-rays and the energy spectrum, quantification of each element is possible. The accuracy varies based on many factors, and lighter elements such as carbon and oxygen are especially difficult to measure precisely, due to lower energy of the X-rays. However, use of standards allow for quantification, mostly at a semi-quantitative level. X-rays may be detected from single grains, spots or areas. It is also possible to perform EDS analyses in an automated sequence which provides repeated scanning of a line or areas to map the presences of one or several elements in the defined area.

In addition to the signals discussed above, samples bombarded with accelerated electrons also emit light, Auger electrons and continuous X-rays.

For these studies a Zeiss Supra 35VP located at the University of Stavanger (UiS) has been used where the settings were varied as follows: 2 – 25 kV acceleration voltage, apertures between 30 and 60 µm, and a working distance from 3 to 15 mm. The FEG-SEM at UiS is equipped with an EDAX EDS-system and to optimize the results of quantification either an Iceland spar calcite crystal or carbonate standards from Astimex have been used to calibrate the system.

2.3.2.3 Mineral Liberation Analyzer (MLA)

Mineral Liberation Analyzer (MLA) combines imaging by SEM-BSE and X-ray mineral identification by EDS to perform a spatial spectral mapping of polished samples, creating color-coded maps of the mineralogy or chemical composition of the samples. The minerals in the samples are identified and

characterised through comparison of their EDS spectra to a list of reference spectra by a "best match" algorithm.

Before the mapping is started X-ray spectra from the different phases in the samples are classified based on elemental composition as a certain mineral or mix of minerals, assigned a colour, and added to the project database together with a pre-defined basis of common minerals. Each EDS-spectrum is coupled to an average grey-scale value in the BSE images and as the average atomic number of each mineral phase corresponds to the number of backscattered electrons from a sample, the average grey-scale-value will therefore be unique to this mineral (Fandrich et al., 2007). To ensure good measurements of the chalk samples with predominant calcite, the grey-scale is calibrated with a copper standard.

After the BSE-images are scanned, processing of the data is required. The first step is particulation: Removal of background data based on a minimum BSE grey-scale value. Anything below this threshold, in this case, epoxy resin or air bubbles, is removed from the image. Subsequently, segmentation takes place, where grain boundaries and internal structures are defined based on BSE characteristics. After segmentation, classification of minerals or phases is performed in the selected area. The measurement mode used for these projects were GXMAP mode, based on a primary identification of particles through BSE imaging, then mapping of each particle in a pre-defined grid, collecting spectra of characteristic X-rays at each point within this grid. This allows for high spatial resolution and avoids limitation by poorly defined grain boundaries in BSE images caused by similar average atomic number of minerals (Fandrich et al., 2007). The scanned areas are coupled to the database of EDS-spectra for classification of minerals in the sample, and color-coded maps of the mineralogical distribution of the surface are produced, enabling objective evaluation of spatial textural and chemical composition in one process.

To produce a clearer image of the mineral distribution in the sample the different spectra may be grouped into one mineral or mineral-group. The resolution of the MLA scanning depends on the size of the area scanned and the time used, but will, however, always be constrained by the spot-size of the electron beam (one to two µm) and the corresponding excitation volume. In this study, samples were scanned by different settings, with a step-sizes between 1.2 and 12 µm. As the grains in the flooded chalk often have a grainsize below the beam-diameter of the MLA, signals from adjacent grains may in cases affect each other.

MLA analyses used in this thesis were carried out at Technische Universität (TU) Bergakademie Freiberg, Germany. The system was set up with SEM type FEI Quanta 650 FEG-SEM together with two Bruker X-Flash EDS detectors. The software controlling the EDS analyses is "Quantax Esprite 1.8". The mineral liberation analysis software version MLA 2.9 by FEI was used for the automated SEM analyses. Imaging and analyses were performed using 15 kV acceleration voltage and 12 mm working distance. The prepared samples analysed were un-covered thin sections or samples mounted in epoxy, coated with carbon.

2.3.2.4 Focused Ion Beam Scanning Electron Microscopy (FIB-SEM)

Sample preparation of brittle chalk for TEM is a challenging task, because of the demands for extreme thin samples and possible undesired smearing effects if polishing of such small samples is used. The samples were therefore produced by Focused Ion Beam (FIB) milling mounted in a SEM (FIB-SEM) at Saarland University, Germany or at the Institute of Planetary Materials (IPM) at the Okayama University in Misasa, Japan, by the project scientists.

In FIB-SEM sample preparation, predefined samples are placed inside the vacuum chamber of the SEM and tilted at an angle to the ion beam. Lamellas of approximately 20 x 10 µm are cut from the sample by a gallium ion-source gun and transferred by a manipulator to a three mm large cupper grid (Figure 5). The FIB-lamellas are then thinned to approximately 100 - 150 nm thickness by the same ion source.

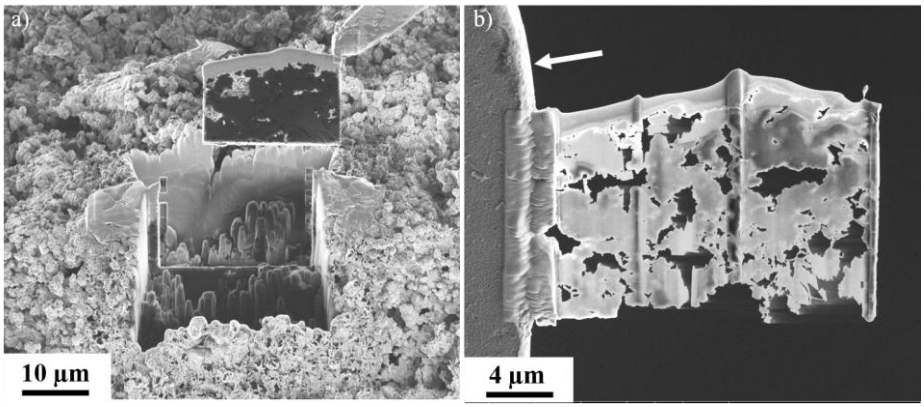

Figure 5: Production of FIB-lamella of $MgCl_2$-flooded chalk. a) cut-out of lamella from the sample surface. b) Thinned lamella welded to the cupper grid (white arrow).

As it can be observed in Figure 5, the chalk samples produced by FIB-SEM may be fragile due to their high porosity and low degree of cementation and compaction.

2.3.2.5 Transmission Electron Microscopy (TEM)

In Transmission Electron Microscopy (TEM) the electron beam is transmitted through the sample as opposed to reflected off the surface in SEM analyses. This requires higher acceleration voltage, often in the range between 100 and 200 kV, and extremely thin samples. For this study, the samples were prepared by FIB-SEM. The samples are brittle, and may be affected by the electron beam, i.e. burning holes in the samples or creating mineralogical changes due

to beam damage (Hjuler, 2007). Hence, microscope set-up and bombardment times need to be calculated well.

The advantage of studying samples in TEM compared to SEM, is the possibility to obtain higher resolution. The higher acceleration voltage used in TEM produces an electron beam with shorter wavelengths. Therefore, the resolution may reach below 1 nm. In Scanning Transmission Electron Microscopy (STEM) mode, a convergent beam is used and mapping of the elemental distribution at nano-scale is possible. A TEM combined with an EDS detector provides imaging and elemental analyses at high resolution and offers also analyses by electron diffraction, enabling identification of mineral phases based on the lattice parameters in addition to the elemental identification by EDS. In electron diffraction, electrons from the incoming beam are scattered elastically (Bragg scattering) and the direction of the scattering is a result of the periodic positioning of atoms in the crystal structure (Solberg et al., 2007).

A JEOL JEM-2100 TEM at UiS was used with acceleration voltage of 200 kV for bright field imaging (use of the direct beam), together with STEM mode mapping. For X-ray elemental identification, an EDS detector (EDAX) was applied to create color-coded maps of the elemental composition of the samples. Additional analyses were performed at the Institute of Planetary Materials (IPM) at the Okayama University, Misasa, Japan. A field emission JEOL JEM-2100F TEM was used with an accelerating voltage of 200 kV, beam current of 2.6 nA, dwell time of 0.2 ms. The high magnification and small beam-size of TEM enables imaging and EDS-mapping below grainsize-resolution of chalk, in this study at a resolution between 5 and 20 nm.

2.3.2.6 Electron Microprobe Analyses (EMPA)

An electron microprobe is a SEM equipped with Wavelength Dispersive X-ray Spectroscopy (WDS) instead of EDS. This method has the advantage of better

quantitative measurements compared to EDS analyses as it analyses the individual wavelength of the X-rays and does not have to identify each element from a partly overlapping energy spectrum, as in EDS. In this study, a JEOL JXA-8900RL was used with 15 kV acceleration voltage, 20 nA current and 2 μm beam at Technische Universität (TU) Bergakademie Freiberg, Germany. The measurements were set up with five separate detectors tuned to detect the wavelengths of specific elements. To test more than five elements, repetitive analyses were performed on the same area on polished thin sections, using standards for the investigated minerals.

2.3.3 Nano Secondary Ion Mass spectrometry (NanoSIMS)

Secondary Ion Mass Spectrometry (SIMS) is based on a primary ion beam striking the sample surface, releasing secondary ions which may provide information about chemical composition and structures of the surface (Hirata et al., 2011). Chalk is very fine-grained and the particle size is often too small to be sufficiently recognized by MLA or EMPA. Therefore, the need for further sub-micron studies is present and one possibility, besides TEM, is nanoSIMS. Using nanoSIMS, the surface is scanned with a focused Cs^+ ion beam. The beam is expected to be less than 100 nm in diameter (lateral resolution) (Zimmermann et al., 2015). For this project, the area that was scanned varied between 55 and 10 μm and as the images have 256 x 256 pixels, this results in a resolution between approximately 200 and 40 nm per pixel.

The impact of the primary beam produces a secondary ion beam, known as "sputtering". The particles produced from the surface may be positively, negatively, or neutrally charged, depending on the primary ions identity (Griffiths, 2008). The ion-yield varies with respect to the type of beam used, e.g. caesium or oxygen, and the ionization energy of the elements and sample matrix (Handley, 2002) To be able to detect neutral particles, a laser ionizes the

secondary beam and the ions are accelerated and directed into a mass spectrometer by an electric field. Using a Time-Of-Flight (TOF) detector, the amount of ejected ion may be measured for several ions or groups, referred to as masses, at one time. As such, multiple scanning of a fragile surface is avoided (Griffiths, 2008). In this way, identification of which elements are present in one certain grain or crystal down to a resolution of 40 nm is possible.

NanoSIMS scanning provides an intensity-map for each ion, oxide or mass, depicting the relative intensity of ions produced from an area. The intensity-values between two images of e.g. calcium and magnesium is not directly comparable, meaning that the method is not quantitative as such, it is rather a tool to identify whether a certain element is present or not in a grain and evaluate the relative concentrations within one scanned area.

Another application of nanoSIMS is the possibility to make depth profiles and to create 3D-images, scanning an e.g. 10 x 10 μm area repeatedly to measure the composition of a specific area, grain, or crystal, to a depth of approximately 1μm.

To navigate to the areas of interest in a sample, the nanoSIMS is coupled to an optical camera. Navigation on polished surfaces of chalk is challenging because of the lack of topography and colours and can therefore be very time consuming. Another important issue is that the nanoSIMS needs an extreme high vacuum during measurements and this can be very time-consuming to reach when studying high-porosity chalks.

The samples in this study were analysed with a Cameca NanoSIMS50 application at the "Centre de Recherche Public Gabriel Lippmann" in Luxembourg (now Luxembourg Institute of Science and Technology, LIST).

2.3.4 Carbon and Oxygen Isotopes

Stable isotope analyses of carbon and oxygen isotopes are used as a tool to understand paleo-climate and post-depositional alterations of rocks. The relative abundance of the stable isotopes of an element in a mineral depends upon fractionation by mass, temperature and/or biological processes that underlie mineralization. Formation temperatures, i.e. the temperature when minerals form, can be used as a chemo-stratigraphic tool and to constrain the degree of rock-fluid interactions during e.g. diagenesis or flooding experiments. Based on $\delta^{18}O$, the formation temperature (T) can be estimated according to the empirical relation described in (Anderson et al., 1983) and (Gòmez et al., 2008):

$$T = 16.0 - 4.14(\delta_c - \delta_w) + 0.13(\delta_c - \delta_w)^2 \qquad (1)$$

where δ_c attains the values of the oxygen isotope ($\delta^{18}O$), $\delta_w = -1‰$ according to the assumption Standard Mean Ocean Water (SMOW) of the ambient Cretaceous seawater (Wright, 1987) ('normal' salinity). The estimated temperature is given in centigrade (℃). $\delta^{18}O$ isotopes fractionate due to kinetic processes reflecting the paleo-climate.

Temperature estimates of untested material and expected values of Upper Cretaceous chalk (Hjuler et al., 2009; Jørgensen, 1987; Surlyk et al., 2010; Tucker et al., 1990) are compared to tested core material.

For each sample, a fresh surface was drilled to produce samples of fine powder. Oxygen and carbon stable isotope analyses were performed on crushed 1.0 - 3.0 mg sub-samples. The carbonate powder was dissolved in 100% orthophosphoric acid at 90 °C in an ISOCARB automatic carbonate preparation system. The resulting CO_2 was then analysed on a VG Isogas PRISM III stable isotope ratio mass spectrometer at the University of Edinburgh. The standard

deviation was measured on a powdered coral laboratory standard (COR1D, $\delta^{13}C$= -0.648, $\delta^{18}O$= -4.920), run as a sample on the same days as the studied samples. All carbonate isotopic values are quoted relative to the Vienna Pee Dee Belemnite (VPDB).

2.3.5 Whole-rock geochemistry (Inductive Coupled Plasma Mass Spectrometry, ICP-MS)

Using Inductive Coupled Plasma Mass Spectrometry (ICP-MS) the concentrations of oxides and elements in a sample can be studied. For each analysed sample, ideally, material of at least 5 grams is needed. The material is milled and the results will therefore yield an overview of the relative distribution of each element or oxide in the bulk sample material. Representative material was retrieved from all samples. The material was analysed at Bureau Veritas Minerals' laboratories in Canada using a porcelain beaker to avoid any contamination. The process is shortly described here, but detailed information of the analytical method and processing can be found currently at http://acmelab.com. The samples are ground in an agate mill and mixed with $LiBO_2/Li_2B_4O_7$ flux in crucibles and fused in a furnace. After cooling, the bead is dissolved in American Chemical Society (ACS) grade nitric acid and analysed by ICP-MS. Loss on ignition (LOI) is determined by igniting a sample split and then measuring the weight loss. A 1g sample is weighed into a tarred crucible and ignited at 1000°C for one hour, and then cooled to be weighed again. The loss in weight represents the LOI of the sample. Total carbon and sulphur are determined by the LECO® method. Here, induction flux is added to the prepared sample then ignited in an induction furnace. During the process a carrier gas sweeps up released carbon or sulphur to be measured by adsorption in an infrared spectrometric cell. The results are total concentrations and attributed to the presence of carbon or sulphur in all components. The

prepared sample is digested with a modified Aqua Regia solution of equal parts concentrated HCl, HNO_3, and Di-H_2O for one hour in a heating block or hot water bath. The sample volume is increased with dilute HCl-solutions and splits of 0.5 g are analysed. None of the measured concentrations were too far above the possible detection limit, but in standard range, and accuracy and precision are between 1-2%.

2.3.6 Analyses of effluent water

Effluents, or waste-water, from the triaxial flow experiments were collected at regular intervals during the test period to compare effluent composition over time, both with the injected brine and similar experiments, which assist in the understanding of any changes in mineralogical composition of the cores during flooding. The ionic concentrations were analysed with a Dionex Ion Chromatography System (ICS)-3000 or 5000+ ion-exchange chromatograph at UiS. The analyses were performed with IonPac AS16 and IonPac CS12A or IonPac AS20 and IonPac CS19 used as anion and cation exchange columns, respectively. The sampled effluents were diluted by a dilution-pump (Gilson, GX-271) to stay in the linear region of the calibration curve and ionic concentrations were calculated based on an external standard method. The following ion concentrations were quantified: Mg^{2+}, Na^{+}, Cl^{-} and Ca^{2+}.

Si^{4+}-concentrations were quantified at UiS by using an Optima 4300 DV Inductively Coupled Plasma Optical Emission Spectrometry (ICP-OES) detector from Perkin Elmer. The samples were prepared by separating approximately 1 mL of the fluid before dilution. The method detection limit (MDL) for the analysis of Si^{4+} is 0.3 mg/L.

2.3.7 X-ray Diffraction (XRD)

X-ray Diffraction (XRD) is based on elastic scattering of the incoming X-rays on the sample. The angle of the incoming X-rays, θ, yields a reflections pattern after Bragg's law:

$$2dsin\theta = n\lambda \qquad (2)$$

The pattern is related to the lattice parameters of the crystals, where d is the distance between lattice planes, n is a positive integer and λ is the wavelength of the incoming X-rays. Constructive interference of the X-rays diffracted in the crystal lattice produces peaks as the angle of the incoming X-rays is stepwise increased. Based on the yielded pattern, the minerals present in the sample may be identified. The better the orientation of the minerals, the more precise are the peak positions to interpret the minerals. XRD has limitations in detecting low quantities of minerals, often if the occurrence is below 5 wt%. The intensities of the peaks also vary with the crystal structure, thus some minerals are easier to interpret than others. Carbonates are mostly easy to identify, while others, such as clay minerals often need additional analyses by e.g. SEM to be positively identified.

In this study, XRD patterns were obtained from grinded bulk samples and performed by using a Bruker D5005 diffractometer (Cu-Kα radiation, 40 kV, 40 mA, 0.02 ° step, at 1 s per step), at the Institute of Earth Sciences Jaume Almera (Barcelona, Spain), together with a Philips X´Pert PRO PW 3040/60 diffractometer (Cu-Kα x-ray radiation, Si monochromator, 40kV and 30mA, step scan at ~1.5º/minute, step size of 0.02º 2θ) at the Facultad de Ciencias Químicas (Universidad Nacional de Córdoba, Argentina). Additional analyses were performed with a Bruker D8 ADVANCE ECO diffractometer with a Lynxeye detector (Cu-Kα radiation 1.5406 Kα1, 40 kV 25 mA, 0.6 mm

receiving slit, 0.01 ° step, at 0.2 s per step) at UiS. The measurements were repeated in certain samples to evaluate the reproducibility of the results; particularly for cases involving newly formed trace minerals. The amount of material used for measurements was approximately 1 g.

2.3.8 Specific Surface Area (SSA), Brunauer–Emmett–Teller (BET) theory

The Specific Surface Area (SSA) is a measure of how extended the surface of grains or crystals is per gram sample, commonly given in m^2/g. This is measured by the amount of gas which can adsorb as a monolayer on the sample. When injecting e.g. N_2 gas, the change in relative pressure is monitored, producing a measure of how much gas is adsorbed on the surface. Given the sample weight as input, one may calculate the SSA of the sample by the Brunauer–Emmett–Teller (BET) theory (Brunauer et al., 1938). The surface area of a sample will vary as a function of several factors such as grain size and shape, as well as porosity and permeability of a sample and can therefore be used as a tool to interpret the amount of dissolution and precipitation of a sample through changes in grain-size distribution.

SSA on grinded bulk samples was measured by Micromeritics' TriStar II surface area and porosity analyser and the data was calculated by TriStar II 3020 Software. Before inserted into the sample tube, each sample was weighed. The sample tube was connected to a vacuum pump and when the pressure reached 20–30 mTorr, nitrogen gas was introduced into the tube and the change in pressure was logged. The sample tube was submerged in liquid nitrogen (N_2) to cool the sample during the measurement. At increased partial pressures, nitrogen gas fills a greater area of the micro-pores adsorbing as a monolayer on the surface of the grains. The change in pressure is a measure of the amount of

gas adsorbed, thus the surface area of the sample. The SSA was measured on both powdered rock and on small ~0.5 x 0.5 x 0.5 cm sized cubes.

2.3.9 Pycnometry

The solid volume of selected samples was measured with an AccuPyc II 1340 gas pycnometer that measures the amount of displaced helium gas by a porous rock sample in an enclosed chamber. This enables calculation of the average density of a sample, based on the sample-weight, and calculation of the porosity, if also the bulk volume is given.

During measurement, a dry sample is placed into a chamber where helium gas molecules rapidly fills the chamber. A chamber of 35 cm^3 was selected to provide the best fit with the samples. The pressure in the chamber is measured and the change in volume is calculated by Boyle's law:

$$P_1V_1 = P_2V_2 \qquad (3)$$

where P is the pressure and V is the volume of the chamber.

2.3.10 Raman spectroscopy

To broaden grounds for analyses, Raman spectroscopy was tested for this research. Raman is an analytical technique which uses a monochromatic laser beam focused on the sample. In the scattered light, or secondary radiation, most photons scatter with no energy change, however a number of photons exchange a small amount of energy which causes the molecules in the sample to vibrate, called Raman scattering, discovered in 1928 (Raman, 1928). The vibrational frequency causes a shift in the frequency of the scattered light, hence a shift in wavelength. This shift is referred to as the Raman shift and is linked to lattice parameters of the crystal phase, the atomic weight and strength of the atomic bonds. Identification of mineralogy is therefore possible through analyses of

the Raman spectra. The advantage is that the method is quick and rather cheap, and uses the crystallography instead of the chemical composition and can therefore differentiate polymorphs.

However, when using micro-Raman, the beam-size is approximately 1 µm. The positioning of the laser beam is done through an optical microscope, and it is challenging to identify and analyse one specific chalk grain by the use of this method.

Recently, Tip Enhanced Raman Spectroscopy coupled with Atomic Force Microscopy (TERS-AFM) has been tested as a method to perform Raman analyses at higher resolution with spot-sizes of 20 nm, and to produce topography maps of the analysed areas. However, this method sets extreme demands on sample-preparation, especially the surface-roughness of the sample. This is to avoid the tip of the AFM to crash into topographic features of the surface. Samples for TERS-AFM were prepared by using an ultrasonic drill to cut out small circular disks (3 mm in diameter) from polished thin sections. In regard of chalk, sample preparation is still a major challenge. Principally this method is, together with TEM-EDS and electron diffraction, the only method in this study which can image and identify minerals on nano-scale.

3 Main results and discussion

The research carried out in this project has yielded results on scales from centimetres to Ångstrøm. The different techniques offer results based on imaging and chemical analyses of specific crystals, grains or areas as well as on powdered bulk samples. Some methods provide elemental and textural results, while others reveal the mineralogy based on crystallographic analyses. Combining the results from several methods may therefore provide additional understanding that each method may not provide on its own.

When chalk is flooded with reactive brines in mechanical flow-through experiments, the composition of the flooding brine affects the strength and the stiffness of the chalk plug. Systematic tests have shown that injection of SO_4^{2-} has an effect on yield and bulk modulus during hydrostatic loading (Megawati, 2015), while Mg^{2+} significantly increases the strain rate during the following creep phase (e.g. (Andersen et al., 2017; Korsnes et al., 2008a; Madland et al., 2011)). To be able to understand rock-fluid interactions along with being able to predict and simulate mechanical behaviour during flooding, the exact changes in mineralogy must be understood. Analyses show that changes in creep strain are, in addition to the applied stress, also dependent on time. A series of long-term tests on chalk cores flooded with simplified brines have therefore been performed (LTT, MLTT and ULTT) to observe chemical effects over time. The main results of the textural, chemical and mineralogical analyses of these long-term experiments are presented and discussed here, together with results from tests flooded for shorter time, tests on fractured chalk and on simplified artificial chalk cores made from calcite powder. In general, very few alterations are observed when flooding with NaCl. Only minor alterations in the silicate distribution are observed along with slight dissolution of calcite. In cores flooded with $MgCl_2$ changes are pronounced.

3.1 Core-scale alterations

3.1.1 Two fronts of alterations

Core-scale mapping of the three long-term test, LTT, MLTT and ULTT (see chapter "2.3.1.1 Overview over the flooding tests presented in this study"), using MLA shows that there are seemingly two fronts of alteration progressing through the cores during long-term flooding of chalk with $MgCl_2$. In **Paper I**, chemical mapping of thin sections covering the radius of each core along the flooding axis was performed.

The two fronts of alteration seem to progress at different velocities through the cores during flooding. The first front is observed towards the outlet of the long-term tests. This induces only minor mineralogical alterations, where most of the original calcite is preserved, and individual idiomorphic crystals of magnesite, commonly 1 to 10 µm in size, are precipitated together with polycrystalline clusters of smaller sized magnesite crystals and clay minerals, mainly in open pore-spaces (**Paper I**). Magnesite is visible as small blue pixels inside the red calcite in the MLA-scans of the LTT and the MLTT (the two centre samples, Figure 6). Such occurrences of magnesite is not observed in unflooded chalk (Figure 6, left), but are commonly found in short-term chalk experiments (**Paper IV and V**).

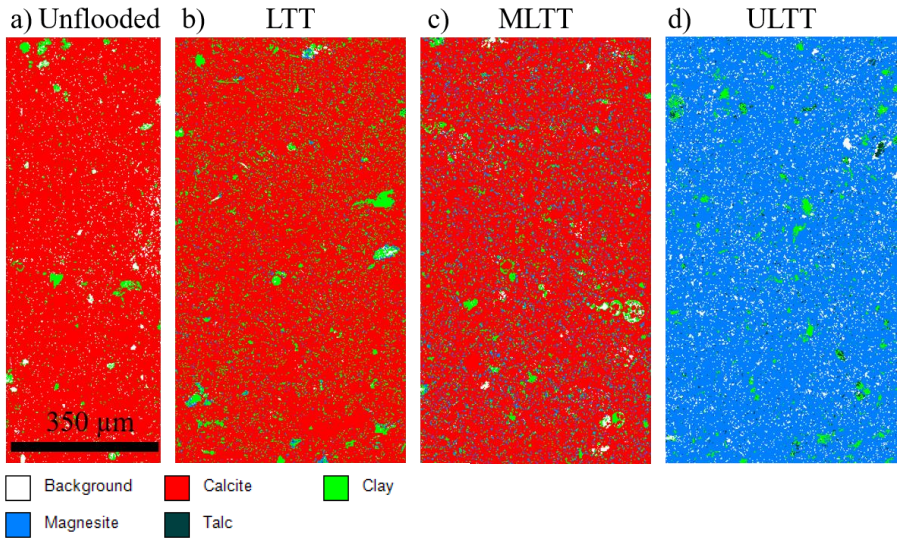

Figure 6: MLA scans of a) unflooded material b), the LTT, slice 4, c) MLTT, Slice 4 and d) the ULTT (slice 5). Legend below. The LTT and MLTT show small abundances of precipitated magnesite (blue) inside the original calcite (red), not observed in unflooded material (a). The ULTT consist only of magnesite (blue) and clay minerals (green).

The abundance of precipitated magnesite is higher in the MLTT, slice 4, compared to the LTT, slice 4, which seems reasonable with the increased flooding time.

The observations in MLA scans are also confirmed by FEG-SEM. No magnesite crystals are observed in unflooded chalk (Figure 7).

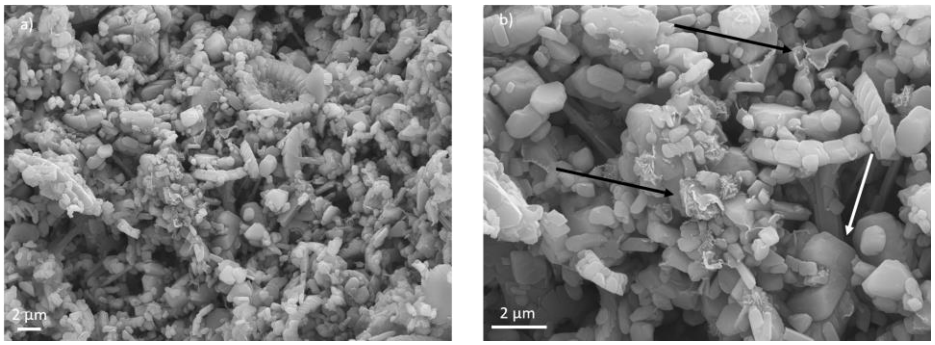

Figure 7: FEG-SEM micrographs of unflooded Liège chalk. a) Recognizable rings (coccoliths) from coccolithophores along with fragments and decoupled grains from micro- and nano-fossils. b) Occurrences of clay minerals (black arrows) and authigenic calcite crystals (white arrow).

Inside the first front of alteration, the occurrence of single magnesite crystals is common (up to ~10 µm), preferentially in larger pore-spaces where the crystals have space to grow and the rock-fluid equilibrium may be altered due to differences in original composition of grains or fossils and in tortuosity of the flow (**Paper I, III, IV and V**). Magnesite is observed as smaller crystals or polycrystalline aggregates further towards the outlet (Figure 8). These observations of scattered magnesite precipitation, which is linked to dissolution of calcite; the provider of CO_3^{2-} in these experiments, are also found in short-term experiments, typically after 30 to 90 days of flooding (**Paper IV and V**). Together with the occurrences of magnesite, observations of original and newly formed silicates are made.

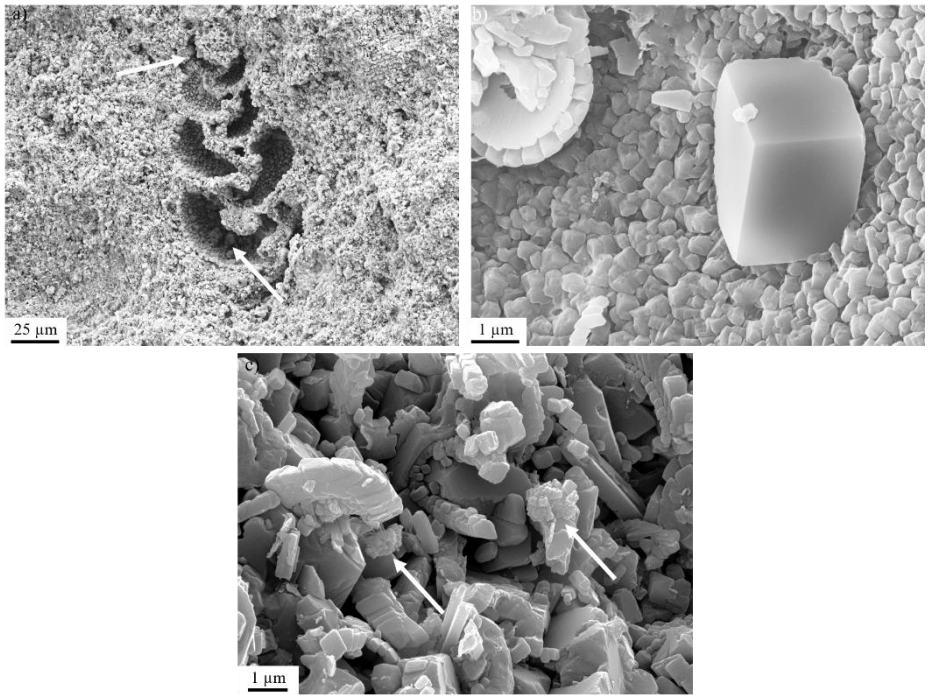

Figure 8: Examples of precipitation of magnesite in a) inside a foraminifera in the LTT (white arrows), b) Close-up of magnesite crystal found at the inlet of outcrop chalk from Stevns Klint flooded with $MgCl_2$ for 61 days. c) Polycrystalline aggregates of magnesite (white arrows) found in chalk from Kansas flooded for 75 days with $MgCl_2$.

The primary mineralogy and diagenetic history of outcrop chalks also affect the mineralogical alterations during flooding. In e.g. outcrop chalk from Kansas, many of the larger pore-spaces of foraminifera are filled with authigenic inorganic calcite, presumably formed during diagenesis (Figure 9). Observations of newly precipitated magnesite crystals of large size in this type of chalk are not so common, compared to other outcrop chalks. There is simply not enough space to grow.

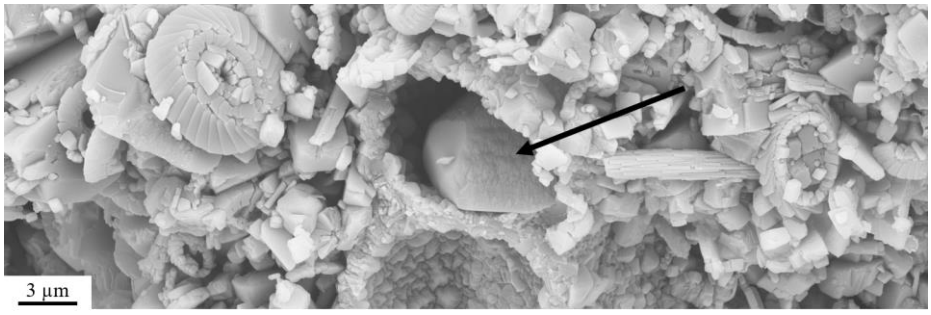

Figure 9: Example of authigenic inorganic calcite (black arrow) found inside a foraminifera shell in unflooded outcrop chalk from Kansas.

The second front progressing through the cores is only observed in the long-term experiments, after more than 500 days of flooding. The alterations are characterized by a complete transformation from calcite and original non-carbonate minerals to magnesite and clay minerals. Minor occurrences of un-altered non-carbonate minerals are also found after flooding. The clay minerals present after flooding seem to be both unaltered original clay minerals together with newly formed phases. The front has a piston shape, and the transition between the two areas of the cores is sharp, and covers only less than 2 mm (**Paper I**).

When imaged by FEG-SEM (Figure 10), both the composition and texture of this completely altered areas are different from unflooded chalk (Figure 7).

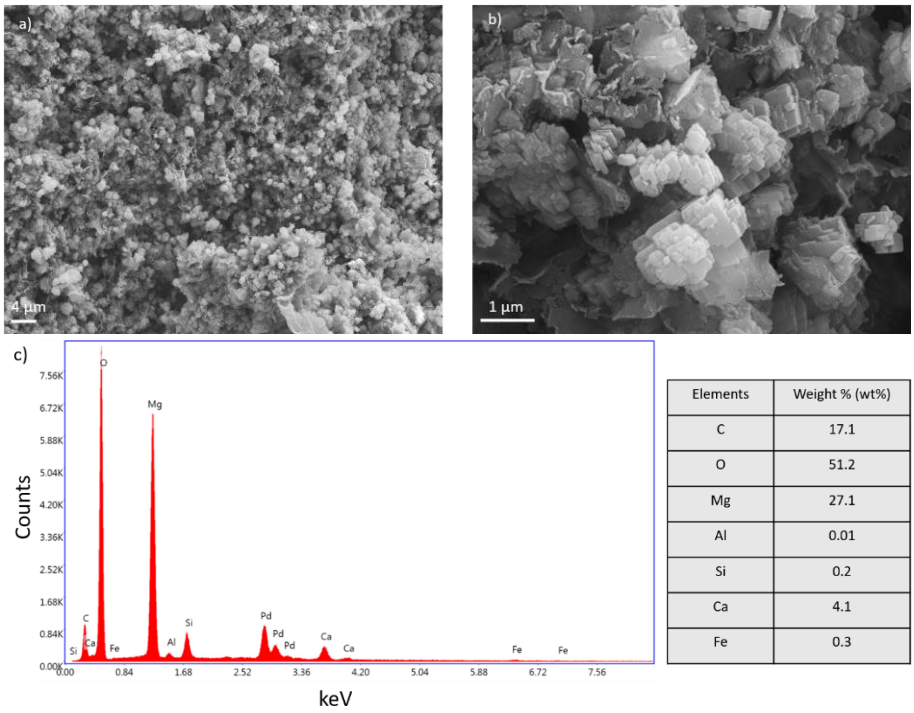

Elements	Weight % (wt%)
C	17.1
O	51.2
Mg	27.1
Al	0.01
Si	0.2
Ca	4.1
Fe	0.3

Figure 10: Material from completely altered area in the ULTT. a) Typical texture of the newly formed crystals with rhombic shape and sizes mostly between 100 nm and 2 µm. b) Close-up of crystals in a). c) Spectrum and semi-quantitative analyses of the elemental composition of the area in a). The sample is coated with palladium (Pd), hence the Pd-peak in the spectrum.

The composition after flooding is dominated by magnesite, composed of Mg, C and O, with minor impurities of Ca. The crystals commonly have a grainsize up to 2 µm, and are more angular than in unflooded chalk.

The same type of precipitates is observed in flooded calcite powder (artificial chalk cores, **Paper II**). Unflooded material has grainsizes in the range of the calcite observed in outcrop chalk, between 4 and 33 µm (Figure 11).

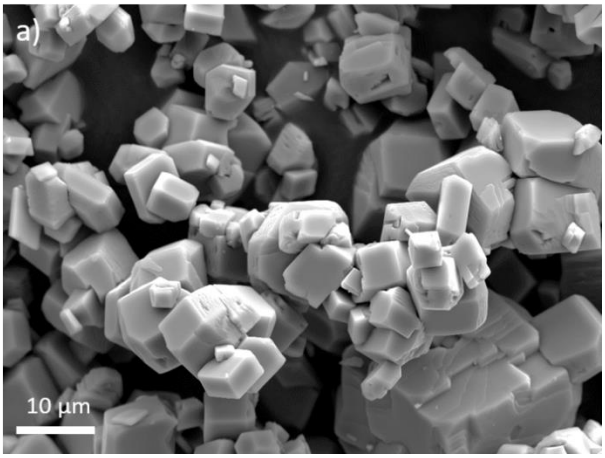

Figure 11: FEG-SEM micrograph of unflooded calcite powder. Grainsize varies between ~4 and 33 µm, with partially interlocking grains.

After short periods of flooding, 27 days, angular grains with trigonal crystal shape varying in size from only tens of nm to ~2 µm are observed, growing on top of existing calcite grains (Figure 12). EDS analyses show a significant content of magnesium (not shown here). These are similar to single crystals of magnesite found in flooded outcrop chalk (Figure 8).

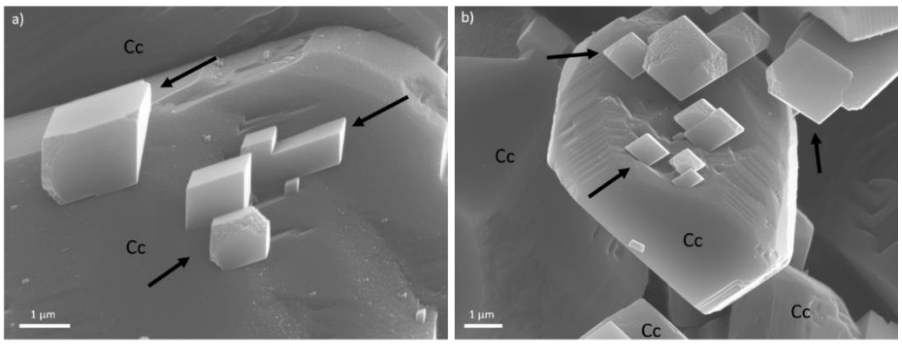

Figure 12: FEG-SEM micrographs of crystals with high magnesium content growing on existing calcite grains at the inlet of an artificial chalk core after 27 days of flooding, marked with black arrows. Original calcite grains are marked with Cc.

In the artificial chalk core flooded for 289 days, polycrystalline aggregates with high magnesium content are found between larger calcite crystals (Figure 13). The clusters comprise of idiomorphic crystals with a trigonal crystal shape and

sizes varying between 100 and 200 nm. The clusters themselves vary in size, most often between 1 and 5 µm, and display a framboidal shape, similar to what can be found for pyrite (Ohfuji et al., 2005). These clusters match the form and composition found in samples of flooded outcrop chalk. In both cases, the aggregates are found from approximately halfway along the flooding axis of the cores and until the outlet.

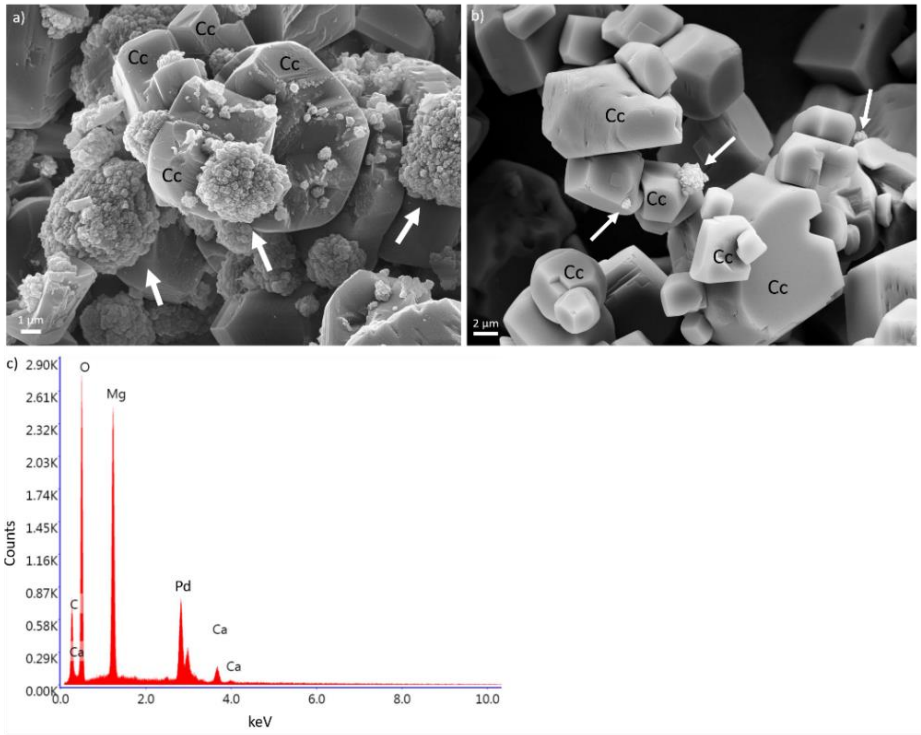

Figure 13: FEG-SEM micrographs of polycrystalline aggregates of new-grown crystals with high magnesium content found after 289 days of flooding with $MgCl_2$. Original calcite grains are marked with Cc. a) Observations are made halfway along the flooding-axis and at the outlet (b) Similar observations made at the outlet of the same core, but with smaller aggregates of magnesite. c) EDS spectrum of new-grown minerals with main contents of C, O and Mg and only minor content of Ca, corresponding to clusters in a).

Severe signs of dissolution are observed on calcite grains (Figure 14). The dissolution can be observed as defects on the crystal faces, where layers in the crystals are partly absent (white boxes in Figure 14).

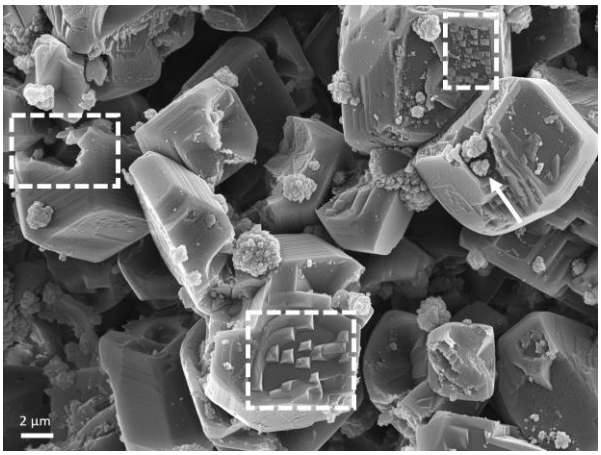

Figure 14: Severe defects on crystal faces found in long-term flooded calcite powder, halfway between the inlet and the outlet of the cylinder. White boxes show partly dissolved surfaces, while the white arrow points to polycrystalline magnesium aggregates inside one of the defects.

At the inlet of the long-term flooded artificial chalk core, most of crystals contain a high amount of magnesium (Figure 15). The crystals are in different sizes and shapes, mainly with a bimodal distribution:

- Smaller angular crystals with a size below 2 µm
- Larger crystals in the size-range between 10 and 15 µm with irregular shapes, partly rounded.

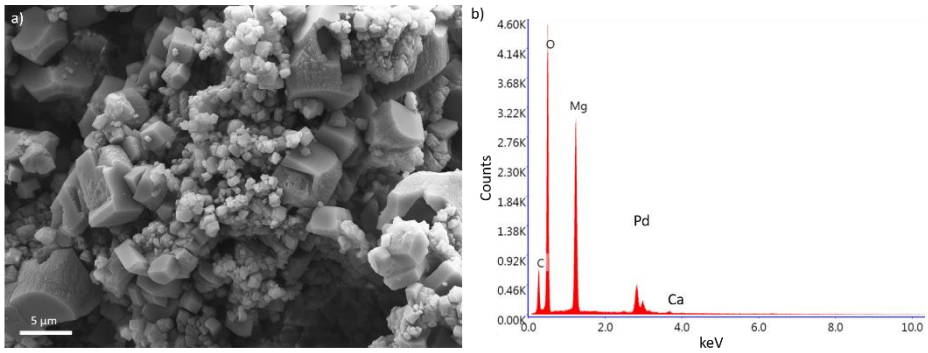

Figure 15: FEG-SEM micrograph of the strongest mineralogical alteration in flooded calcite powder. a) A distribution of crystals of different sizes and shapes is observed. All grains show minimal content of Ca, b) typical EDS spectrum for the crystals. Samples coated with palladium (Pd).

In FEG-SEM analyses no calcite nor dolomite were observed, similar to outcrop chalk. It seems that this area at the inlet of the core flooded for the longest period, mostly consists of magnesite, as also observed in the LTT and the MLTT; two of the long-term flooded outcrop chalk cores. As such, it is reasonable to assume that the artificial chalk cores behave over time much like outcrop chalk, with two fronts of alterations progressing through the cores over time, and that the here observed alterations are part of the secondary front of complete alteration.

Core-scale alterations are also observed by other measurements of the three long-term tests on outcrop chalk (LTT, MLTT and the ULTT) matching the observations made by MLA and FEG-SEM (**Paper I**). As seen in Figure 16, bulk analyses by ICP-MS, show values of CaO (red graph), MgO (black graph), and $\delta^{18}O$ isotopes (green graph) that follow the same trends as the MLA maps. In the inlet of the two shorter tests, LTT and MLTT, the MgO concentrations are high, while CaO values are low. This adhere to the area which is mapped as blue in the MLA maps, corresponding to magnesite. (For slice 2 in the LTT, there was not enough material to be analysed by ICP-MS, and is in the graph indicated by dashed lines). The crossover between MgO and CaO is shifted towards the outlet in the MLTT, compared to the LTT, which is to be expected with longer flooding time and matches the progression of the secondary magnesite front. At the outlet of the LTT and MLTT, where the mineralogy still is calcite-dominated, CaO values are high, MgO values are low, and they are close to the concentrations of unflooded rock. In the ULTT, the whole core is completely altered after three years of flooding with $MgCl_2$ and the same high MgO- and low CaO-values are found throughout the core.

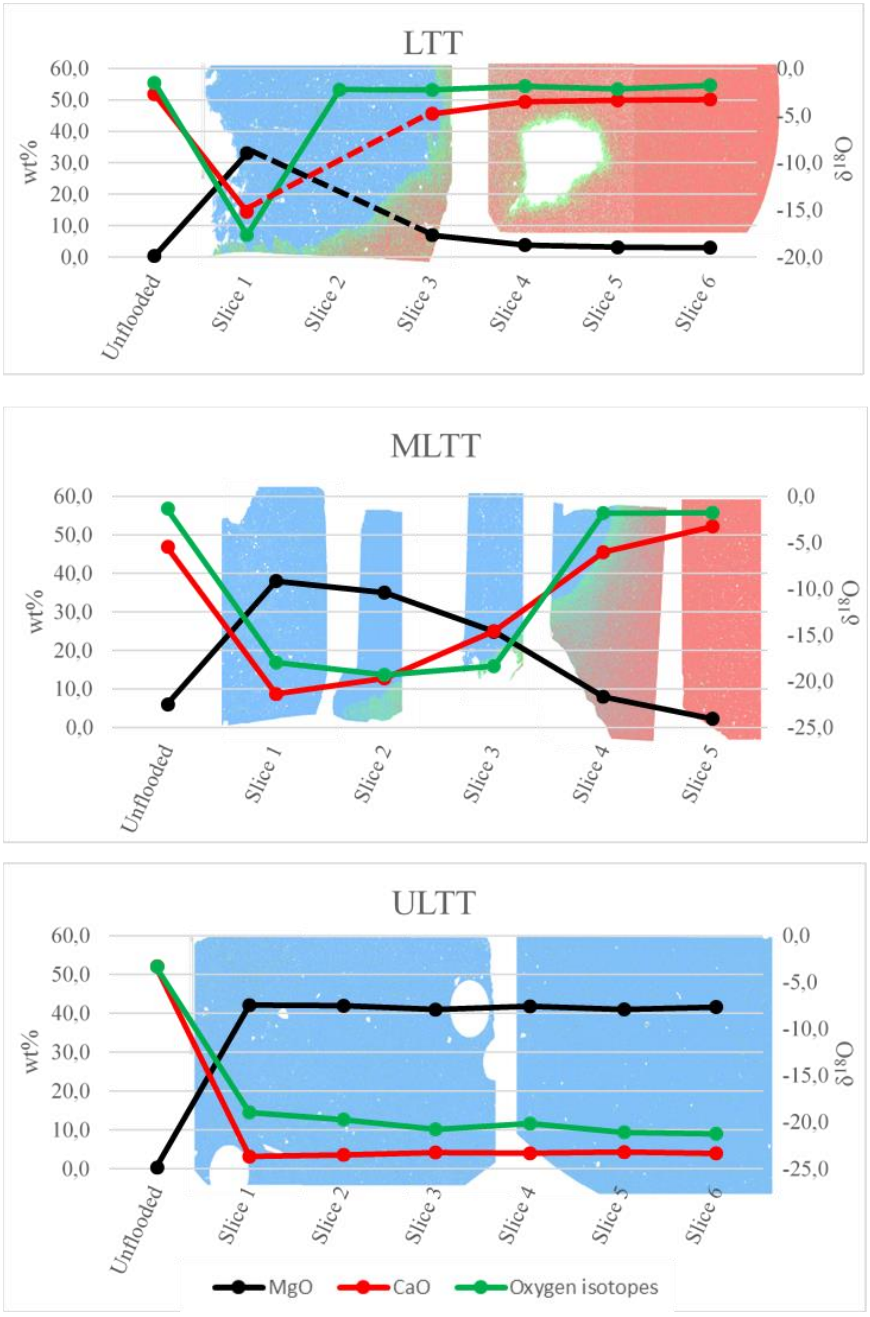

Figure 16: Combination of MLA mapping, ICP-MS analyses and oxygen isotopes measured along the centre of the flooding axis of the three long-term tests. CaO, MgO and $\delta^{18}O$ isotopes vary along the flooding axis, and match the MLA maps. MLA legend in Figure 6.

$\delta^{18}O$ isotopes fractionate due to temperature, yielding a more negative value, corresponding to an enrichment of lighter isotopes, in warmer formation conditions. In the completely altered areas of the three cores, $\delta^{18}O$ isotopes are severely disturbed compared to unflooded material.

Although calculations for paleo-temperature from oxygen isotopes are based on fractionation in open ocean seawater and may not necessarily be directly applicable to laboratory experiments such as the ones presented here, it is interesting to estimate the formation temperature of the newly formed minerals in the flooded cores. Based on the equation given in section "2.3.4 Carbon and Oxygen Isotopes", the calculated precipitation temperature of the magnesite lies in the range of the experiment temperatures (130 °C). The values decrease towards temperatures of unflooded material and the expected values of Cretaceous chalk in the region (Surlyk et al., 2010) towards the outlet of the LTT and MLTT. For chalk cores flooded for shorter periods of time, between 2 and 4 months, an increase in $\delta^{18}O$ and calculated higher fluid temperatures can be observed at the inlet of the flooded cores, interpreted as a result of newly formed magnesite.

Given information on how oxygen isotopes fractionate due to changes in the global climate with differences in evaporation and precipitation (Appelo et al., 2009), it is clear that this is not the mechanism at play in these laboratory tests. However, the results indicate a considerable enrichment of the lighter ^{16}O isotope on the expense of ^{18}O. This exchange has to be related either to fractionation processes during re-precipitation of minerals, a signature of the isotope composition of the injected brine or even both. The isotope exchange may take place in the fluid when the dissolved species are in solution or through solid-state diffusion. The extent of alteration of isotope ratios is much higher when the process takes place through dissolution and precipitation (Hoefs, 2015). As such, the deviation from normal values of unflooded Cretaceous

outcrop chalk, points to precipitation of carbonate minerals under elevated temperatures and the extent of this deviation can be used as a measure of the amount of newly formed carbonates, in this case magnesite. Carbon isotope ratios, $\delta^{13}C$, (see **Papers I, IV** and **V**) are, as expected under the given laboratory conditions, not disturbed and reflect expected values for Late Cretaceous chalk (Jørgensen, 1987; Tucker et al., 1990), hence containing their primary signature.

The same geochemical trends are observed in the artificial chalk cores, made of calcite powder, flooded with 0.219 M $MgCl_2$ (Figure 17) (**Paper II)**. ICP-MS analyses were performed on bulk samples of each slice, and the distribution of MgO compared to the distribution CaO, match observations made in outcrop-chalk, both for short-term (**Paper V**) and long-term tests (Figure 16) (**Paper I**). MgO concentrations are high at the inlet, and are reduced towards the outlet. Longer flooding periods, correspond to higher levels of MgO.

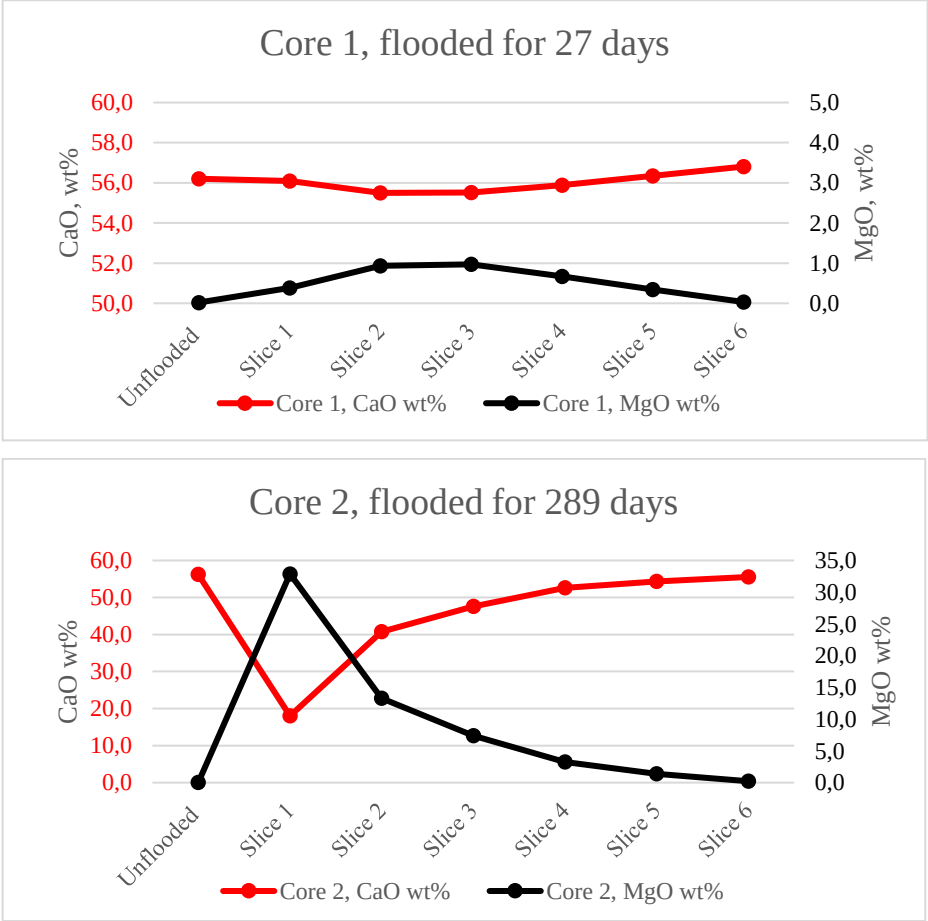

Figure 17: Results of ICP-MS analyses of the two flooded artificial chalk cores, along with the values for unflooded powder. Only the wt% for MgO and CaO are presented. MgO is higher in the inlet of the two cores, and generally higher after longer flooding period (Core 2). Please observe differences in scale of CaO and MgO wt% for the two graphs, Core 1 has been adjusted to show the minor changes in composition.

ICP-MS analyses of both the here presented calcite powder and outcrop chalk yield higher concentration of MgO in all flooded slices compared to unflooded material. It is difficult to observe any newly precipitated mineral phases in all areas of the flooded cores. However, certain replacements between Mg and Ca has to have taken place. This could be through precipitation of minute grains or

crystals of magnesite or other magnesium bearing minerals, or through ion-exchange processes on the surface of the grains inside the cores.

In general, density values change accordingly to variations in MgO and CaO concentrations along the flooding axis of the chalk cores, as discussed in e.g. **Paper IV** and **V** and (Nermoen et al., 2015; Zimmermann et al., 2015). Magnesite has a higher density than calcite and a shift of calcite to magnesite, via the complex processes described above, matches the increases in density observed in flooded chalk along with changes in other mineral phases such as silicates. Correspondingly, SSA measurements on flooded material are significantly altered, reflecting dissolution, precipitation or transportation of mineral phases within the cores (**Paper IV** and **V**). When flooding with NaCl, SSA values are in general lowered at the inlet, and slightly increased towards the outlet of the cores. This indicates small amount of dissolution and re-precipitation of fine-grained minerals, such as clay minerals, or transport of those from the inlet towards the outlet. In silica-rich chalk, as from Aalborg, partly dissolved opal-CT is observed at the inlet, together with newly formed clay minerals when flooding $MgCl_2$ at temperatures from 25-130 °C, also corresponding to the measured SSA values (**Paper IV**). This, however, complicates the interpretation as opal-CT lepispheres have a high SSA-values, as have clay minerals. For the other chalk types studied in this project, the SSA corresponds to the increase in magnesium content implying the precipitation of new phases, e.g. magnesite and clay, characterized by smaller crystal sizes.

3.1.2 A porous transition zone with sharp boundaries

Possibly, the most compelling observation made when studying the long-term tests is not only the presence of the mm-sized sharp transition between the two mineral regimes in the two shorter tests (LTT and MLTT), but also that this transition zone seems to have higher porosity than the rest of the rock material

in the cores. In MLA-scans of prepared thin-sections (Figure 16 and **Paper I**), this was firstly interpreted as a zone with higher density of clay minerals because of its high values of silicon (Si) and oxygen (O). However, after complementary analyses by FEG-SEM, the areas in question look rather like a high-porosity zones (Figure 18). The detection of Si and O may be affected by the glass slides the thin-sections were prepared on, more visible where the porosity is increased (discussed in **Paper I**).

Figure 18: FEG-SEM micrograph of the transition-zone in the LTT with increased porosity, below the white dashed line, compared to the area still dominated by the original calcite mineralogy to the top of the image.

Additionally, high-magnification FEG-SEM images of the high-porous zones show that clay minerals found distributed in the flooded cores are more visible inside the transition zone (Figure 19), than in other areas inside the secondary front. ICP-MS analyses of two cores (details in **Paper I**), do not show any

increase in Si and Al, elements often associated with clay minerals, in the slices corresponding to the transition zones. It is therefore likely that the reason for the increased visibility of clay minerals in this area is the higher porosity, not a net increase in silicates or clay minerals.

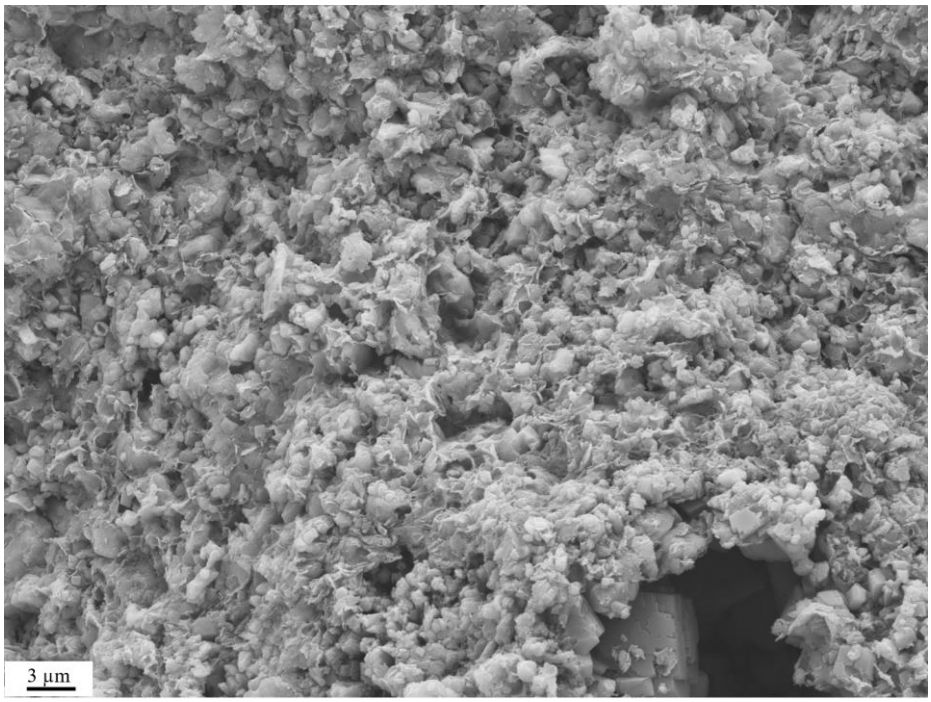

Figure 19: High magnification FEG-SEM micrograph of clay minerals found inside the transition zone of the LTT.

The formation of a high-porosity zone is in agreement of what is observed by e.g. Putnis et al. (2009) when studying mineral replacement reactions in single crystals. The formation of such a zone is the driving mechanism enabling mineral replacement to take place and progress through the crystals. In addition, observations made on outcrop chalk from Mons, St. Vaast Formation, also suggest the presence of such a porous transition zone. Cores drilled with longitudinal holes along the flooding axis were flooded with different brines (Abubeker, 2013; Geitle, 2013). One of the cores were flooded with $MgCl_2$,

prepared as a thin-section and then mapped by FEG-SEM-EDS. Magnesite (red pixels) seems to be precipitated inside the hole, and mimics cementation, reducing porosity and permeability in the hole (Figure 20). A gap, or porous reaction front, towards the calcite (blue pixels) can be observed in slice 5, near the outlet of the core. The interpretation of precipitated magnesite was confirmed by XRD analyses (Bredal, 2018).

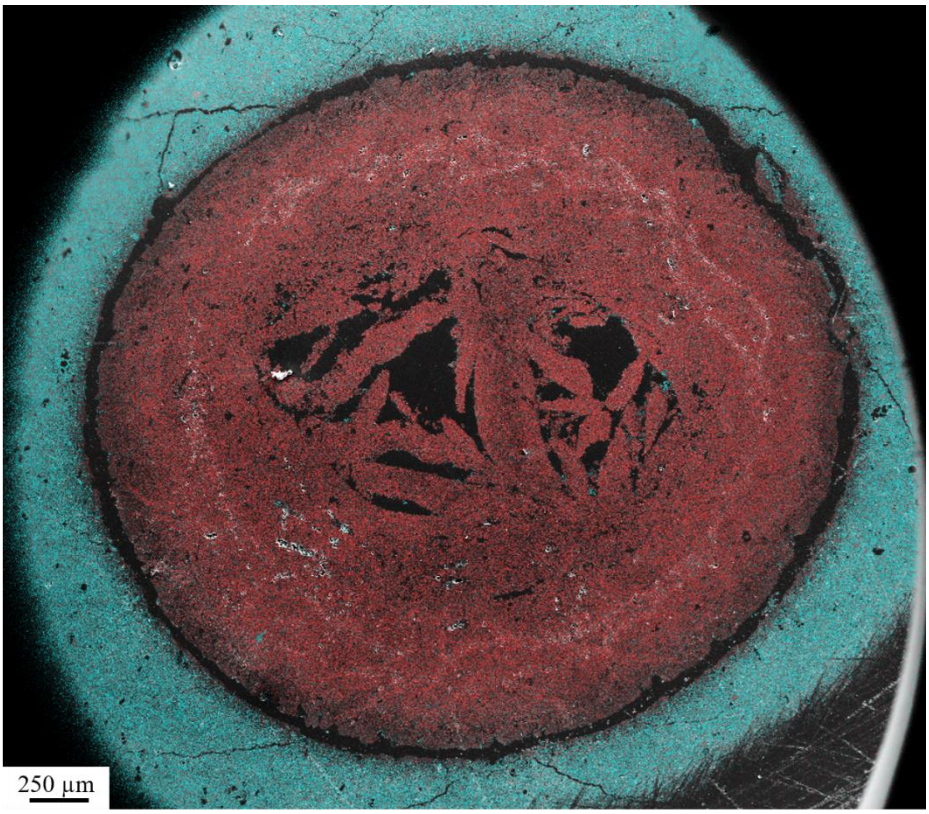

Figure 20: FEG-SEM-EDS mapping of newly grown magnesite in a hollow cylinder chalk core flooded with $MgCl_2$. Red pixels = magnesium, blue pixels = calcium. Cortesey of Tine Vigdel Bredal.

Detailed MLA-scans of the transition zones in the long-term tests show that there is an increasing amount of calcite (red) from the inlet side (left) of the zone towards the outlet (right) here visualized in the LTT (Figure 21).

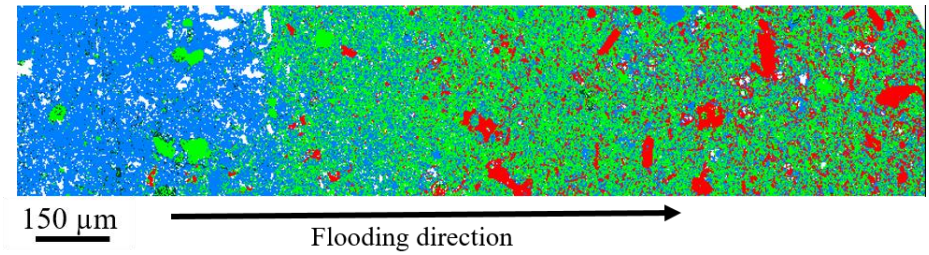

Figure 21: MLA scan of the transition zone in LTT. Legend in Figure 6. Blue pixels = magnesite, red = calcite and green = clay minerals.

The occurrence of calcite, a heavier mineral phase compared to magnesite, yields more backscattered electrons in FEG-SEM-BSE and appears as brighter shade of grey in the SEM-BSE micrograph. The occurrence of calcite inside the front seems to be linked to larger fossils in the chalk, such as foraminifera shells (Figure 22). This is in accordance with what was observed in **Paper III**.

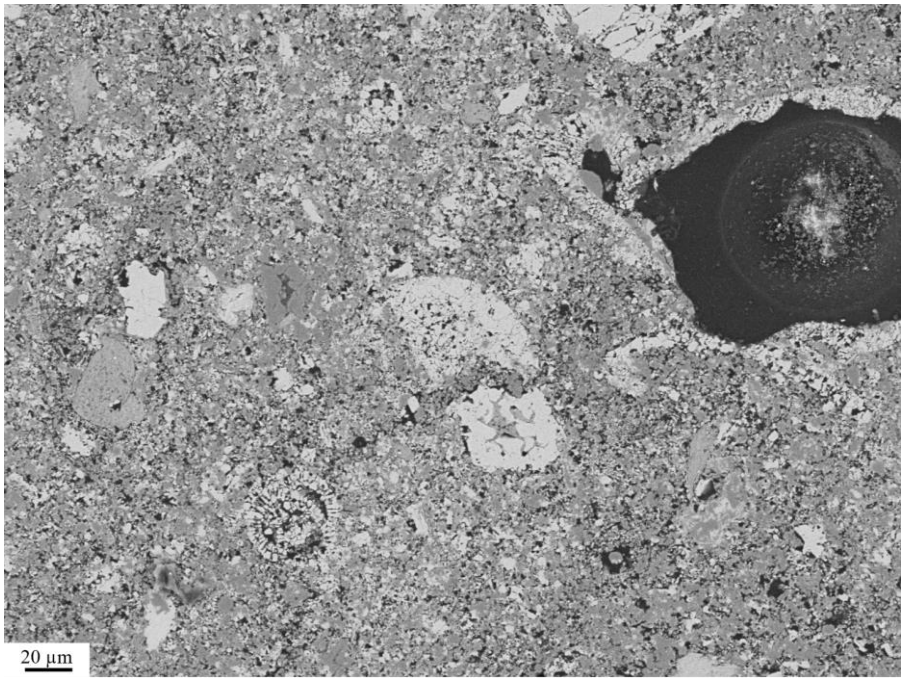

Figure 22: FEG-SEM-BSE micrograph from inside the transition zone of LTT. Lighter mineral phases with lower AAN yield less electrons and are therefore darker in the image.

When preliminary EDS analyses of the transition zones were performed, the results implied that the area had a dolomitic composition, with comparable amounts of Ca and Mg (Minde et al., 2016) (Figure 23).

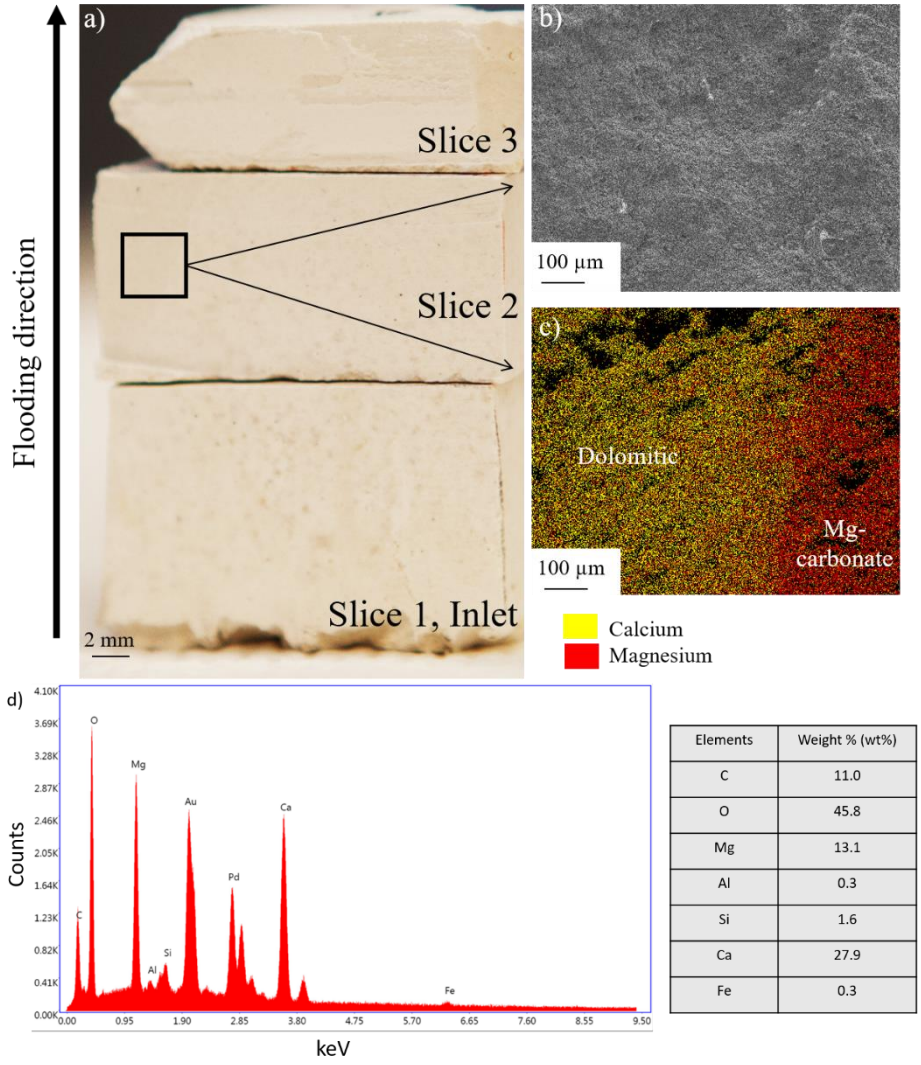

Elements	Weight % (wt%)
C	11.0
O	45.8
Mg	13.1
Al	0.3
Si	1.6
Ca	27.9
Fe	0.3

Figure 23: SEM-EDS mapping and analysis of the transition zone in MLTT. a) The three slices closest to the inlet of the core. Black box indicates mapped area b) FEG-SEM micrograph of the mapped area. c) EDS map showing the distribution of calcium (yellow) and magnesium (red) in the area of interest. d) EDS spectrum and quantification from the "dolomitic" part of the sample. The sample was coated with Au and Pd, hence the peaks.

Because of the fine-grained character of chalk and the even smaller sized new-formed minerals which precipitated due to flooding with non-equilibrium brines, limitations of methods such as FEG-SEM in terms of resolution may require the results to be controlled by complementary methods.

Material from the transition zone in slice 2 in the MLTT was analysed by XRD, and show the absence of dolomite or any Mg-carbonate at core-scale, but magnesite (Figure 24).

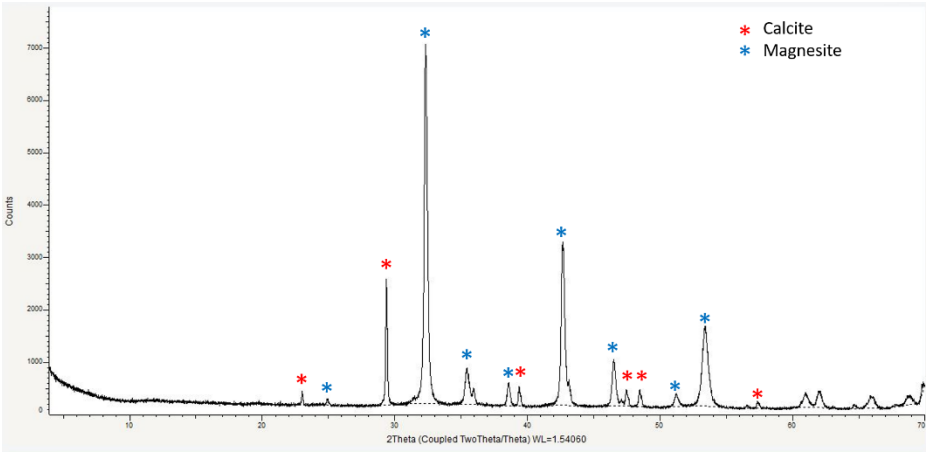

Figure 24: XRD analyses of the transition zone in slice 2 of MLTT, marked with major peaks. Only calcite (red asterisks) and magnesite (blue asterisk) were observed together with possible observations of clay minerals. No dolomite could be observed.

Complementary XRD analyses were also conducted on the artificial chalk cores, confirming the existence of only calcite and magnesite in the cores after flooding (Figure 25). Dolomite was not found.

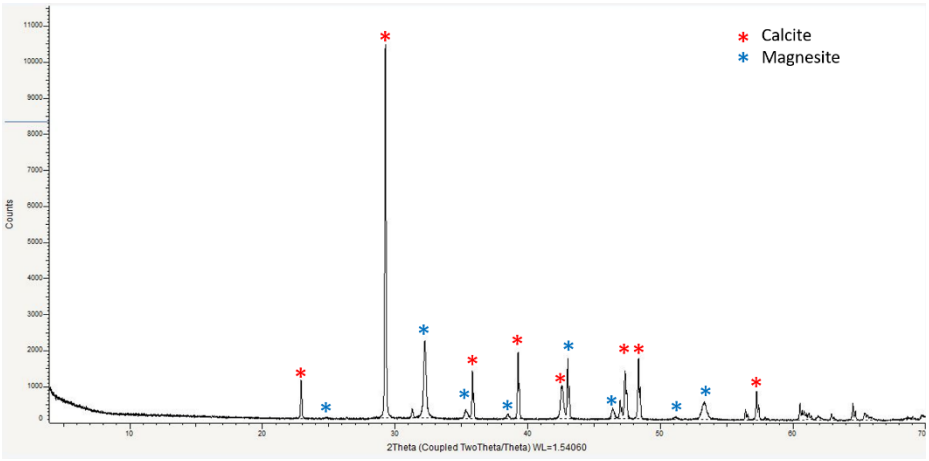

Figure 25: XRD analysis of slice 2 in the artificial chalk core flooded for 289 days with $MgCl_2$, marked with major peaks. Only calcite (red asterisks) and magnesite (blue asterisk) were observed together with possible observations of clay minerals. No dolomite could be observed.

As such, the similar results in XRD-analyses for outcrop chalk and the flooded calcite powder, support observations by FEG-SEM and ICP-MS analyses. Results from all methods suggest a similarity in mineralogical alterations between outcrop and artificial chalk.

Analyses of the three long-term tests by micro-Raman spectroscopy confirmed the results from the XRD, with positive identification of the abundant minerals as magnesite and calcite (**Paper VII**). Again, dolomite could not be detected (Figure 26).

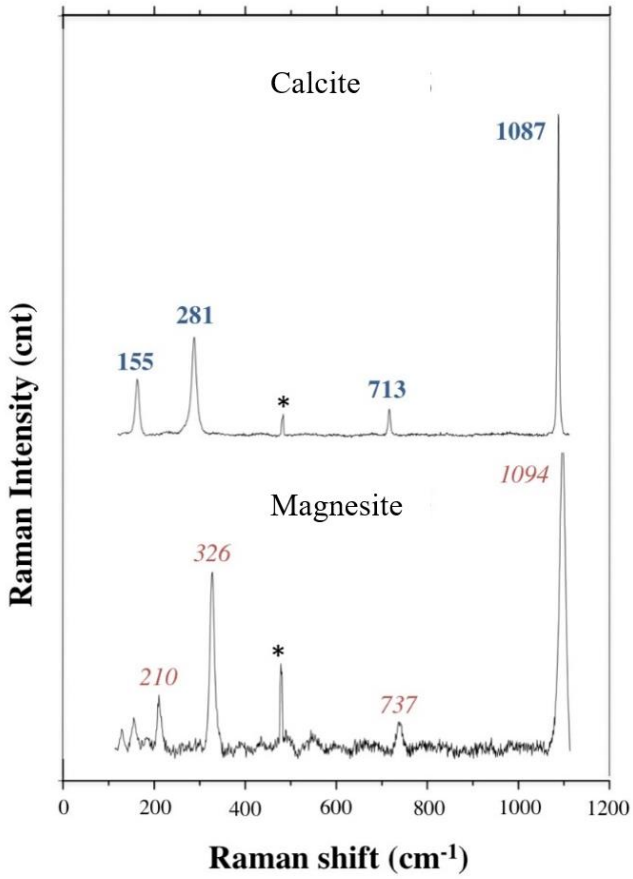

Figure 26: Raman spectra collected on the first slice of the LTT showing the presence of calcite and the presence of recrystallized magnesite. Calcite peaks are reported in blue/bold, magnesite peaks in red/italic. * represent the neon lamp emission line at 476.8 cm_1 used for calibration with the Horiba XploRA spectrometer. Peak positions are reported without decimals.

Limitation in detection limits for XRD in these type of experiments (Zimmermann et al., 2015) and lack of resolution for micron to sub-micron minerals in micro-Raman analyses (**Paper VII**) may be the reason for the absence of observed dolomite, however, the contradictive results from the three methods demonstrated a need to investigate the mineralogy further with even higher resolution at pore-scale.

3.2 Pore-scale alterations

Chalk is a very fine-grained rock with grainsizes often below one µm. This causes single-grain analyses to be challenging. Additionally, the rock is very soft and brittle, a factor which makes sample preparation more difficult. Despite of this, several interesting observations on pore-scale have been made, especially by using TEM.

As discussed in section "3.1.2 A porous transition zone with sharp boundaries", the composition of flooded chalk can in cases seem to be dolomitic when analysed by EDS at scales of tens of micrometres and above. Samples from the transition zone in the MLTT (Figure 23), were cut from the sample surface and prepared by FIB-SEM, and then analysed by STEM-EDS at UiS. In total, seven samples were taken from the three long-term tests. This is undoubtedly not enough to describe the mineralogy of the entire cores, but can aid in identifying the true changes in mineralogy in these fine-grained rocks.

STEM-EDS analyses from all studied samples show similar results. Inside the transition zone, two types of elemental compositions of the carbonate crystals or grains can be found. Here, newly precipitated magnesite grains containing 1-4 wt% Ca are present (red, Figure 27), together with calcite grains (blue, Figure 27). The calcite grains are more rounded (white arrows, Figure 27), compared to the angular magnesite crystals. The size of these rounded calcite grains is commonly between one and two µm and the grains appear in cases to be partly dissolved, with etch marks at the edges of crystal planes (black arrow, Figure 27). They are often arranged in circular structures, resembling the original coccolithophore ring-type textures of chalk.

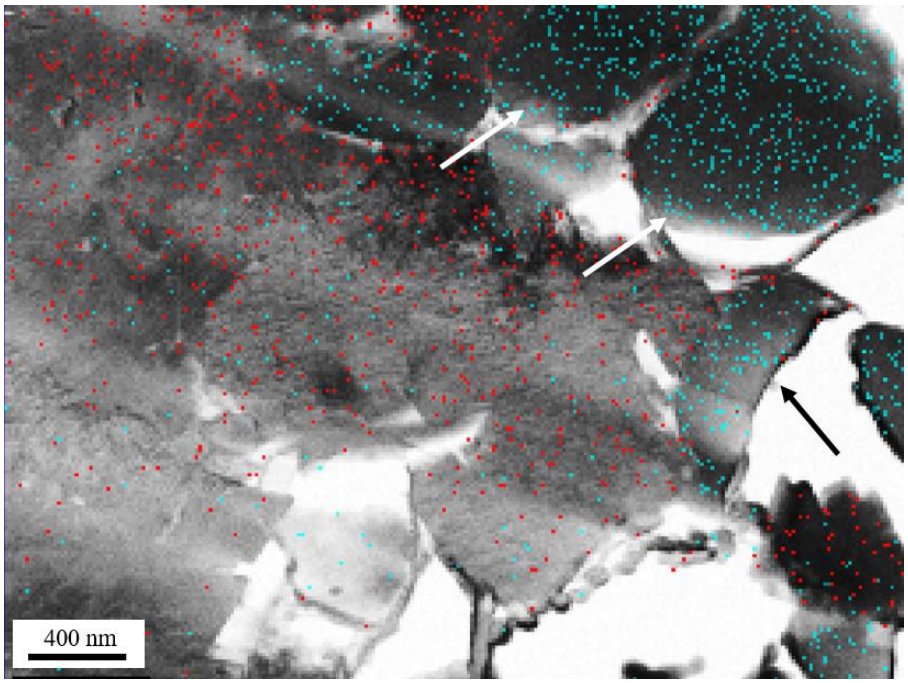

Figure 27: Bright field-STEM image of the primary front in the MLTT, slice 2. Original calcite grains (blue) are rounded (white arrows) and the structure resembles the form of coccolithophore rings. To the right of the image, partly dissolved grains are observed (black arrow). Newly precipitated magnesite grains (red) have a more angular shape and contain small impurities of calcium.

No dolomite was observed in these grain-scale studies and the TEM results support the findings using XRD and micro-Raman.

The areas which were strongest affected by chemical changes, inside the secondary front, are in the three tests characterised by a complete alteration from calcite to magnesite (Figure 28) and all analysed grains (images from the MLTT are shown here) display comparatively the same composition, similar to the magnesite grains found inside the transition zone (Figure 27). The calcium is homogenously distributed within the imaged crystals, and does not appear as separate grains or crystals. The crystals were precipitated out of a fluid with high Ca-concentration after dissolution of calcite, and the mentioned impurities

are therefore not unlikely. The newly formed Mg-rich crystals have an angular shape, and appear in varying sizes, from approximately 100 nm to one µm.

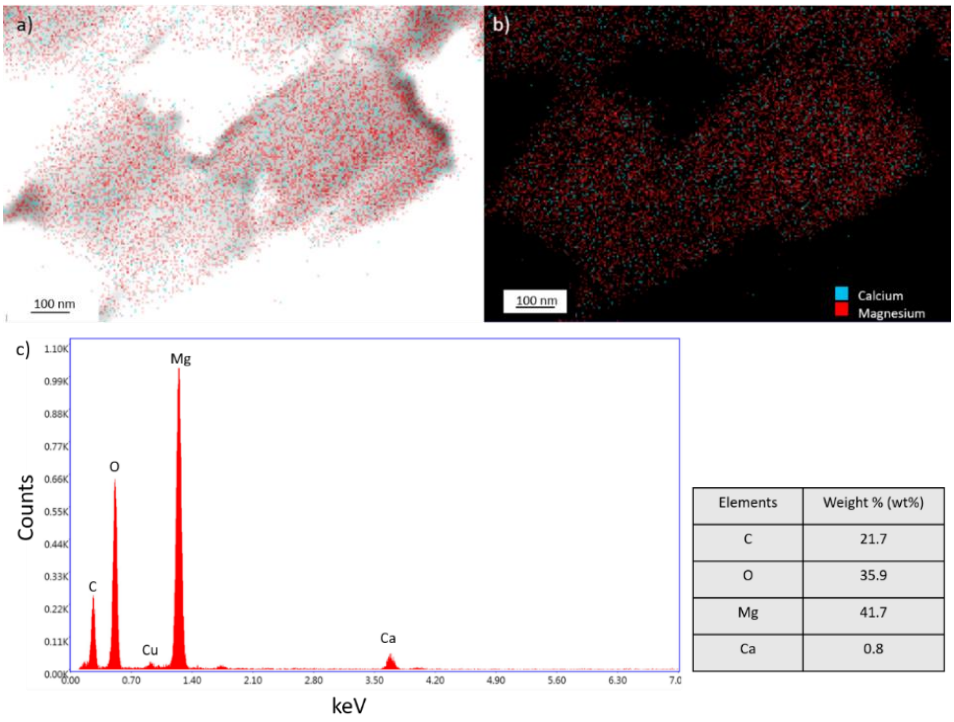

Elements	Weight % (wt%)
C	21.7
O	35.9
Mg	41.7
Ca	0.8

Figure 28: a) Bright field-STEM-EDS image inside the secondary front in the MLTT, slice 2. Newly precipitated magnesite grains (red) with an angular shape, containing small impurities of calcium (blue). b) The distribution of magnesium (red) and calcium (blue) in the crystals c) Typical spectrum and non-standard quantification of the magnesite found in the three long-term flooded cores. The FIB-lamellas are welded to a cupper grid (Cu), hence the peak.

To verify the results of TEM-EDS and test out a new analytical method, TERS-AFM was applied to small 3 mm diameter disks drilled from the thin-sections of the three long-term tests (Borromeo, 2018). Even though there were difficulties both in finding suitable sample preparation methods and achieving good high resolution maps by this method, the mineralogy combination of calcite and magnesite was confirmed on pore-scale (Figure 29), as it was with Micro-Raman on core-scale.

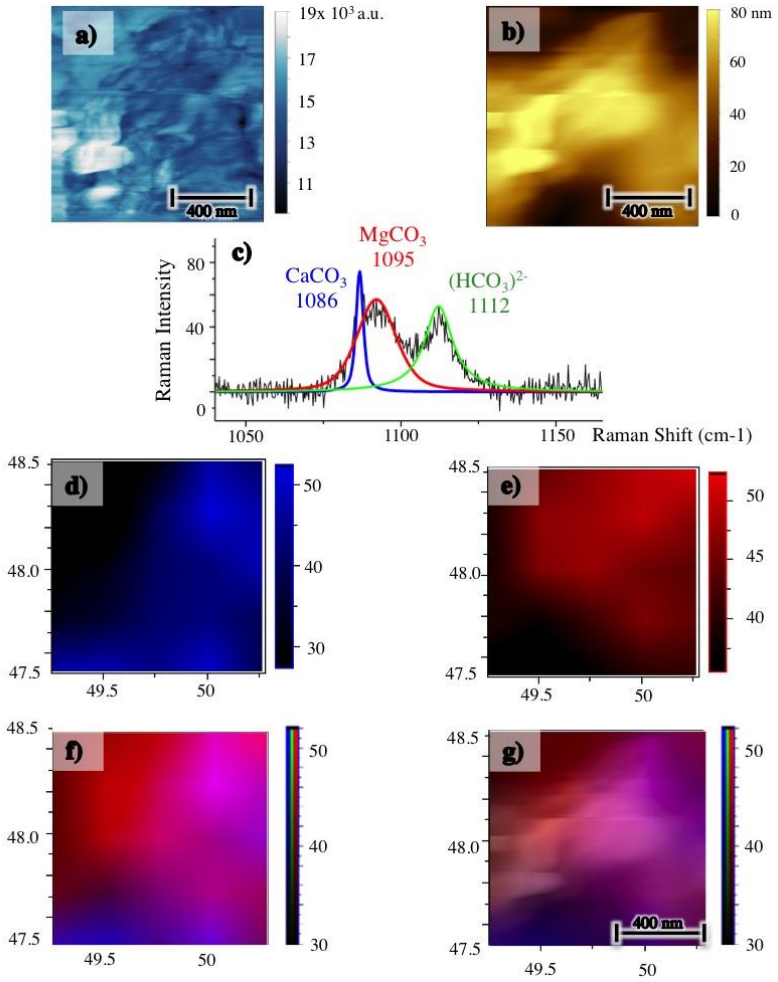

Figure 29: TERS mapping acquired on the MLTT. a) 1 µm x 1 µm topography acquired with tuning-fork based AFM. b) Magnitude signal acquired in the same 1 µm x 1 µm area. c) typical TERS spectrum obtained on a single point, showing peaks at 1086 cm^{-1} (calcite), 1094 cm^{-1} (magnesite) and 1112 cm^{-1} (bicarbonate ion). d) TERS mapping showing the distribution of the 1086 cm^{-1} calcite ν_1 peak. e) TERS mapping showing the distribution of the 1094 cm^{-1} magnesite ν_1 peak. f) Superimposition of the TERS mappings of calcite and magnesite, following the colour code used in the previous panels; g) superimposition of the TERS mappings of calcite and magnesite and of the topography image in a).

As described on core-scale, observations in flooded outcrop chalk are matched by observations in the artificial chalk also on pore-scale. FIB-slices of the flooded calcite powder were analysed by STEM-EDS (**Paper II**). Figure 30a and b show a bright field image of a magnesite crystal precipitated on top of a

calcite crystal along with STEM-mapping of calcium- and magnesium-distribution in the two crystals. The transition between the two adjacent crystals is sharp. The Ca- and Mg-concentrations in both crystals were scanned over a cross-section in Figure 30c and d. The distribution of Mg and Ca is uniform within the two crystals in the line-scan, and the transition between the two phases is nearly instantaneous, only minor impurities of calcium can be found homogenously distributed within the magnesite crystal.

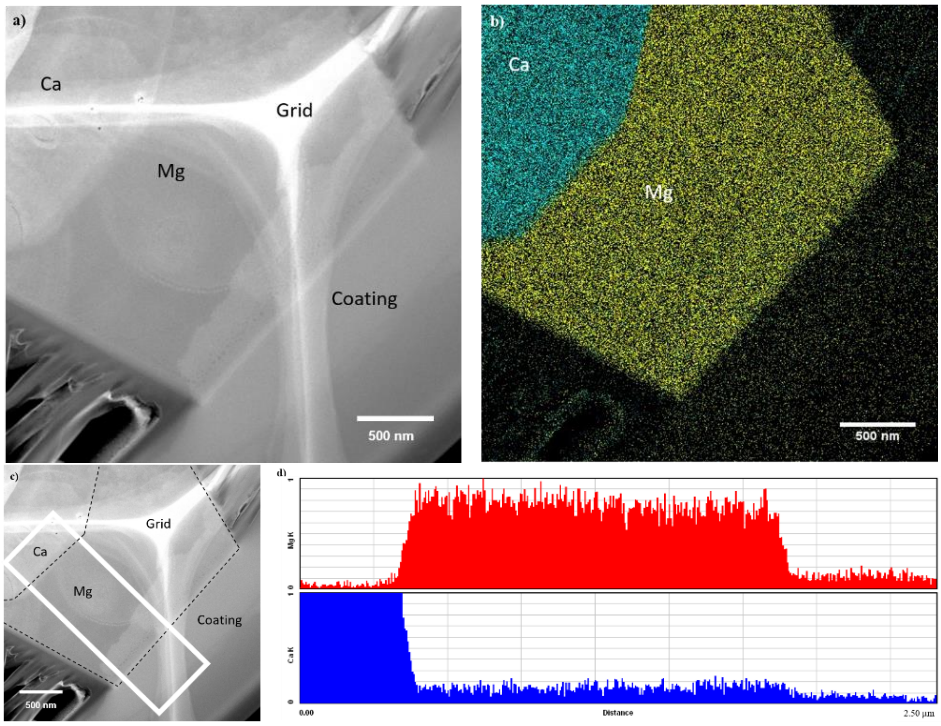

Figure 30: a) Bright field image of adjacent crystals. b) STEM mapping of crystal growing on top of original calcite crystal. Ca = calcium = blue, Mg = magnesium = yellow. c) The position of the line-scan profiles for the crystals in a). d) Chemical analysis along the line scan in c) with X-ray intensities for Mg and Ca. Ca = calcium = blue, Mg = magnesium = red. The white pattern behind the crystals is the copper grid the slice is attached to.

TEM studies (Figure 30) suggests that the processes of alteration are linked to dissolution and precipitation, and not to solid-state molecular diffusion, as the transitions between the Ca- and Mg-phases are rather abrupt. This is also

supported by severe signs of dissolution observed at core-scale in the flooded artificial chalk cores (Figure 14) and indications of minerals precipitated under elevated experiment temperatures measured by $\delta^{18}O$ isotopes (Figure 16) in flooded onshore chalk. Dolomite was not observed. As such, it is most probable that in $MgCl_2$-flooding of outcrop chalk and of calcite powder, the only carbonate mineral phases involved are calcite and magnesite, and that the process of alteration is through dissolution and precipitation.

3.3 Scales of pseudomorphism

By studying the mineralogy at several scales, including nano-scale, the scale of pseudomorphism may also be determined. Pseudomorphism is not uncommon in geological aspect, and involves a change in mineralogy while the original shape is preserved. This is described by several authors based on inorganic-crystal experiments in still-standing fluids, e.g. Jonas et al. (2015), Putnis et al. (2007) and Putnis et al. (2009). The experiments in this study were carried out under continuous fluid-flow and can therefore not directly be compared to the results from these authors.

In the long-term tests, inside the first front, observed at the outlet of the LTT and MLTT, it seems that the diffusion and transport rates are sufficiently high to limit a local process of coupled dissolution and precipitation. In this part of the two cores the accumulation of larger magnesite crystal and polycrystalline aggregates in sizable pore-spaces seem to be the primary alterations, as also observed in flooding-experiments of shorter periods of time (**Paper IV** and **V**). Much of the original calcite is still present in these areas.

In the secondary front, observed at the inlet of the LTT and MLTT along with the entire ULTT, the processes of alteration seem to be different from the primary front. Micro- and macro-fossils have, together with the rest of the rock material, an altered mineralogy while the fossil-structures are preserved, much

like the results described by (Putnis et al., 2007) as pseudomorphism. In Figure 31, a foraminifera shell is easily recognized in a), while in b) a circular structure of magnesite crystals may resemble the shape and size of a coccolith ring. Both these observations indicate pseudomorphism at µm-scale and above. It may therefore be possible that this second alteration front behaves more like the alteration processes in beaker experiments, without fluid-flow.

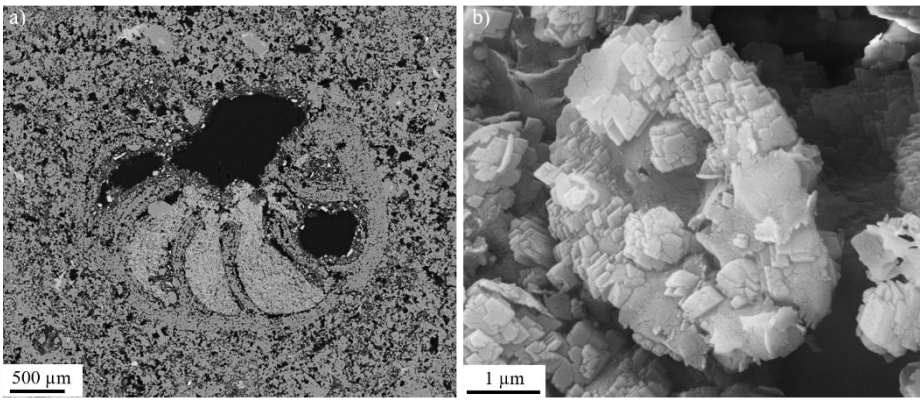

Figure 31: SEM-BSE micrograph of a shell of a foraminifera preserved in the ULTT, ~0.5 cm from the outlet (see Figure 2). The shape of the fossil is preserved, but the mineralogy consists of magnesite with calcium impurities. b) Newly formed crystals of magnesite observed in slice 2 of the ULTT, resembling the shape and size of a coccolithophore ring.

Xia et al. (2009) have given an accurate explanation of this phenomenon: As long as the dissolution rate of the primary mineral is the limiting factor, nanometre-scale pseudomorphism is possible, enabling precipitation of the secondary mineral as soon as there is dissolution. If the precipitation rate of the secondary mineral is the limiting factor, pseudomorphism is only visible at a larger scale, typically around 10 µm, which is also the case in the three long-term flooded cores. A complete understanding of these alteration-mechanisms by analysing the cores after flooding is difficult, and further experiments where in-situ observations are possible would greatly contribute to a complete understanding. This could e.g. be performed by high resolution 3D X-ray

microscopy, micro-Computer Tomography (CT), Magnetic Resonance Imaging (MRI) or Positron Emission Tomography (PET).

In flooded calcite powder, there is after 289 days of flooding an area at the inlet of the core where the distribution of crystal-sizes is bi-modal, with the larger crystals being in the size-range of the original calcite grains. Because of the lack of easily recognizable shapes and features as seen in fossils, it is hard to confirm, however, it could be speculated that this is also a result of micrometre-scale pseudomorphism formed during the progression of the second alteration front.

3.4 Fractures and texture

In chalk reservoirs with low matrix permeability, fluid-flow is significantly affected by fractures and the texture of the rock. Understanding how such features in the chalk affect the mineralogical alteration during flooding of non-equilibrium brines is important to anticipate how the fluid-flow could be altered during injection.

A chalk core from the Liège outcrop was fractured along the flooding direction in a Brazilian test (For more details see **Paper III**). Figure 32 shows part of the fracture after flooding with synthetic seawater (SSW) for 34 days. It was imaged by FEG-SEM-BSE after set in epoxy and polished. The fracture seems to have healed during flooding and only traces of the original fracture are visible as denser areas and as an increase in lighter mineral phases, observed as brighter shades of grey in the BSE micrograph.

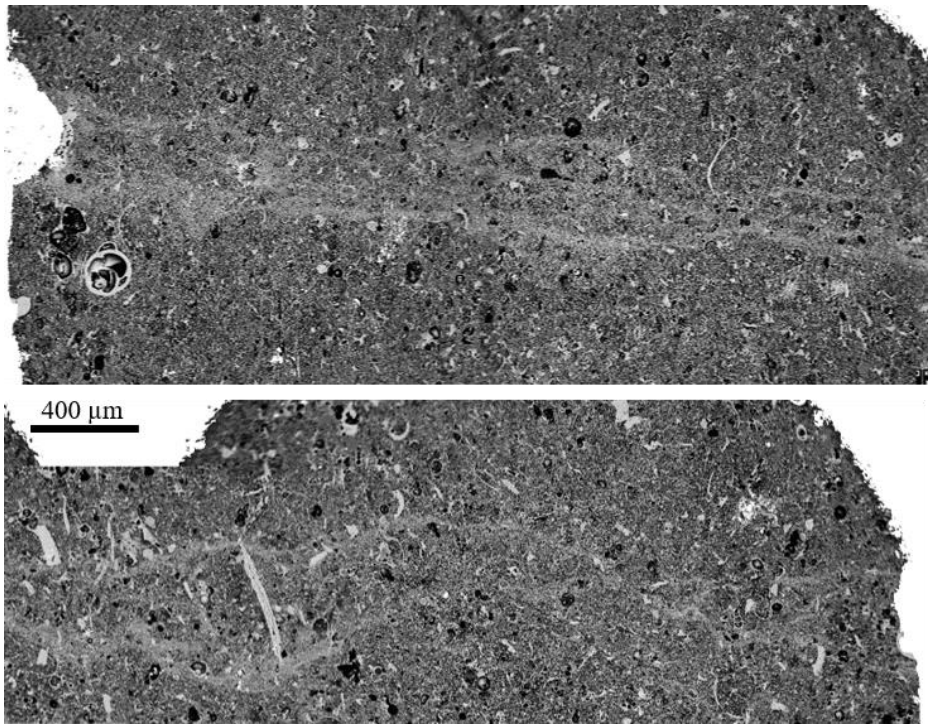

Figure 32. FEG-SEM-BSE micrograph of the fracture after flooding with SSW for 34 days. The flooding direction was horizontally in the images that show approximately one cm of the fracture, split into two images. The lighter phases in the SEM-BSE image are remnants of the fracture, seem denser and have an increase in lighter mineral phases.

Possible healing of fractures during fluid injection in reservoirs is of high importance when studying the effects of EOR-fluids. However, this effect should be further studied at larger scales to investigate how significant this effect is on reservoir-scale.

MLA-images of the same fractured chalk core flooded with SSW, show that inside fractures there is in general a higher concentration of magnesium (Mg), silicon (Si) and aluminium (Al). Shells of micro- and macrofossils stand out to have very low Mg content compared to the matrix. A shell from a macrofossil is embedded perpendicular to the fracture (Figure 33). This texture provokes a significant difference in Mg content between the concave side of the shell, with

higher Mg concentrations, and the area of the convex side of the obstruction, with lower concentrations. This trend is confirmed by EMPA data along the profile A-A' in Figure 33, showing higher values for MgO, SiO_2 and Al_2O_3 on the concave side of the shell (Figure 34).

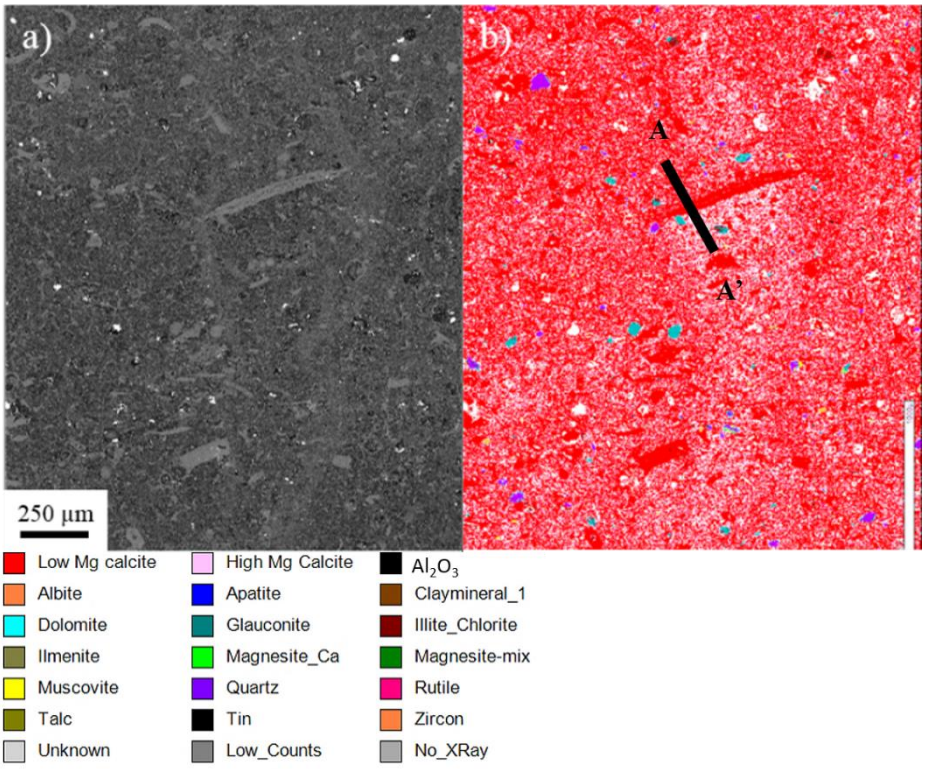

Figure 33: SEM-BSE micrograph (a) and MLA scan (b) of the same area of the fracture. The Mg-content is higher on the concave side (below) of the shell than on the convex side (above). Legend below. White areas relate to pore space. Flooding direction is vertical in the images.

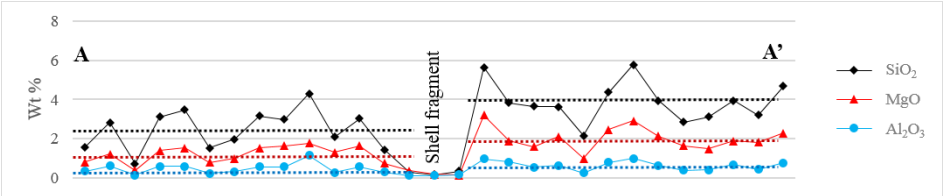

Figure 34: Oxide values measured by EMPA along the profile A - A' in Figure 33. Dotted lines are average values.

Analyses of the fractured core by nanoSIMS show another fragment of a shell embedded in the matrix. The fragment exhibits different alteration behaviour than the surrounding particles (Figure 35), as also observed by FEG-SEM-EDS (Figure 22) and MLA (Figure 21 and Figure 33). The shell fragment does not seem altered by flooding of SSW and shows a clear depletion of Si, Mg, Fe, S, Al and P and, compared to the matrix, it seems to have kept its original calcitic composition.

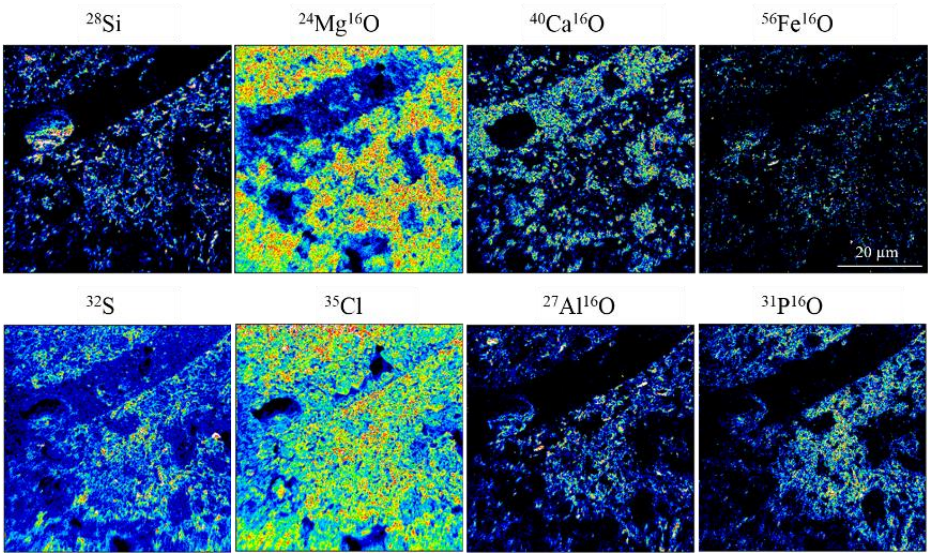

Figure 35: NanoSIMS images showing relative concentrations of elements between a shell-fragment and the surrounding matrix in fractured Liège chalk flooded with synthetic seawater (SSW). Notice the enrichment of Mg in the surrounding matrix compared to the concentration of Mg in the shell-fragment and the opposite pattern for Ca.

The flow is clearly obstructed by the shell-fragments, and the ions in the SSW have not infiltrated the shell during the flooding period. Although most of the surrounding matrix seems affected by the flooding of SSW, the shells and microfossils seem inert to the flooding agent and show to much less degree, if any, mineralogical changes as partly observed in the transition zones in the long-term tests flooded with $MgCl_2$ (Figure 21). There may be several reasons for this differentiation: 1) The size of the carbonaceous particle matters for the

chemical stability of the grain. Smaller particles may be more prone to alteration and mineralogical changes than larger ones (Oswald ripening). 2) The initial composition of the fossils differs from the finer-grained matrix, such as Mg/Ca ratio depending on e.g. age, seawater composition and temperature at formation. 3) Curvature and surface properties affect the dissolution rates of the initial grains and fossils (Levenson et al., 2013). 4) The increase in other elements in the matrix may be due to precipitation of smaller crystals/grains in the pore-spaces or in the fractures where there is more free space and the stress state is different. All these points could be deciding factors, and the mineralogical composition and texture of the rock itself is therefore paramount for the fluid flow in chalks. From these images and elemental analyses, it seems clear that the larger fossils have a higher resistance to mineralogical alterations than the smaller coccolithophores and fragments in the matrix.

Without the knowledge of the micro-facies, fluid-flow is barely predictable even on core-scale for the length of the experiment here. It is possible that these criteria are of less significance when massive fluid flow affects entire rocks over a longer time. However, they definitely should be acknowledged in simulation and modelling at pore- and core-scale.

3.5 Effects of primary mineralogy

Most of the results presented in this study involve minerals replacement reactions involving Ca^{2+} and Mg^{2+} only. However, in the flooding of outcrop chalk, there is always a presence of clay minerals and other non-carbonate minerals which affect the equilibrium state and the dissolution – precipitation processes in the cores. In **Paper V**, five different outcrop chalks have been studied and compared, and the strength and stiffness of the cores, correspond to the amount and type of non-carbonate minerals which is present. This also affects changes in porosity, and to large extent permeability, especially studied

in **Paper IV**. When flooding e.g. chalk from Aalborg, which has a high content of silica in the form of opal-CT, at different temperatures (25-130 °C), large amounts of clay minerals containing Mg and Si are precipitated in pores, severely reducing permeability (Figure 36) with up to 98% (including compaction effects).

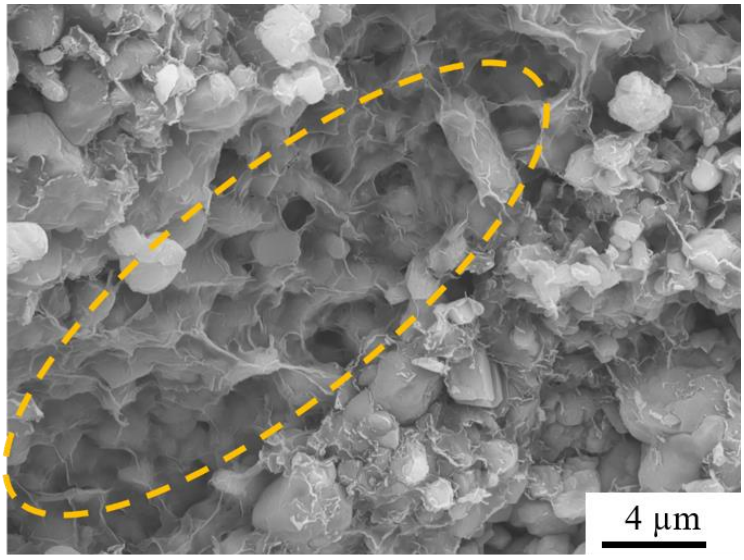

Figure 36: FEG-SEM image of outcrop chalk from Aalborg flooded at 130 °C for 115 days with $MgCl_2$ (slice 6, near the outlet), showing pore surfaces and throats covered by newly formed Si-Mg-bearing minerals (orange dashed circle). Courtesy of Tania Hildebrand-Habel.

The amount of permeability-reducing clay minerals which precipitate during flooding with $MgCl_2$ vary in correlation with the temperature of the flooding fluid for the chalks: The higher the temperature, the larger the amount of precipitated minerals. The presence of clay minerals along the flooding axis of the cores can also be correlated with the changes in SSA as described in "3.1.1 Two fronts of alterations".

In chalks with low non-carbonate content, e.g. from Stevns Klint, no clay minerals are observed precipitating during flooding, and the mineral exchange from calcite to magnesite may rather increase porosity and permeability, if one

does not consider compaction effects. This is also observed in two of the three long-term experiments, were all three cores underwent severe compaction (10 to 18%). However, for the cores flooded for approximately two and three years, the permeability, and the calculated porosity, started to increase after a primary phase of compaction-reduced permeability and porosity. As magnesite precipitates at the expense of calcite, the density is increased, thus filling less space in the core. This enhances porosity and permeability if bulk volume is kept constant.

As discussed in "3.4 Fractures and texture", the non-carbonate content may also significantly disturb fluid-flow in fractures. The diagenetic history of the rock and the amount of available pore-space may affect fluid-flow, and in turn the distribution of newly formed mineral phases. The knowledge of primary mineralogy and texture of the rock is therefore important parameters to acknowledge if one want to predict and possibly control the effects an EOR-fluid would have in a chalk core or even in a reservoir.

3.6 Mechanisms controlling crystal shape and distribution of new-grown minerals

In this thesis, analyses of experiments performed on different outcrop chalk and pure calcite powder have been presented. In chalk, the non-carbonate minerals dictate some of the mineral replacement reactions taking place during flooding with non-equilibrium brines, especially when the content of silicate minerals is high. This is e.g. observed in experiments on Aalborg chalk flooded with $MgCl_2$, where massive amounts of Si-Mg bearing clay phases fill up pore-spaces and significantly reduce the permeability (Figure 36). However, alongside the precipitation of non-carbonate minerals, there is also observed a process of dissolution of calcite and precipitation of magnesite, with calcium impurities, in all experiments where $MgCl_2$ is the flooding brine. The

distribution of newly formed magnesite along the flooding axis of the cores, is as expected, with most pronounced alterations at the inlet of the cores. Similar single crystals and polycrystalline aggregates of magnesite can be found in all experiments. Polycrystalline aggregates are observed downstream of larger single crystals found at the inlet of the cores. As discussed in **Paper II**, the saturation indices in $MgCl_2$ flooded chalk cores (Andersen et al., 2012) do not match the distribution of the shape and size of crystals and aggregates found in the cores after the experiments. Aggregates of smaller crystals are more likely to precipitate at the inlet of the cores, where the saturation index, i.e. the degree of super-saturation, is the highest. Such a state of equilibrium produces high nucleation rates and low growth rates, which favour the formation of abundant small crystals. At states closer to equilibrium, growth rates are higher, favouring the formation of larger single crystals (Myerson et al., 2002). For the calcite powder experiment, the saturation index along the core was modelled by IORCoreSim and show changes over time (Figure 37). The highest values, i.e. where the degree of super-saturation is highest, is found near the inlet of the core, both after 10, 50 and 289 days, where there is a constant supply of Mg^{2+}. Over time, the amount of calcite present at the inlet is reduced meanwhile the amount of magnesite increase. This also affects the saturation index, thus the formation of new crystals. After 289 days, magnesite does not precipitate at the first mm of the core, most likely because all of the calcite is dissolved in this area.

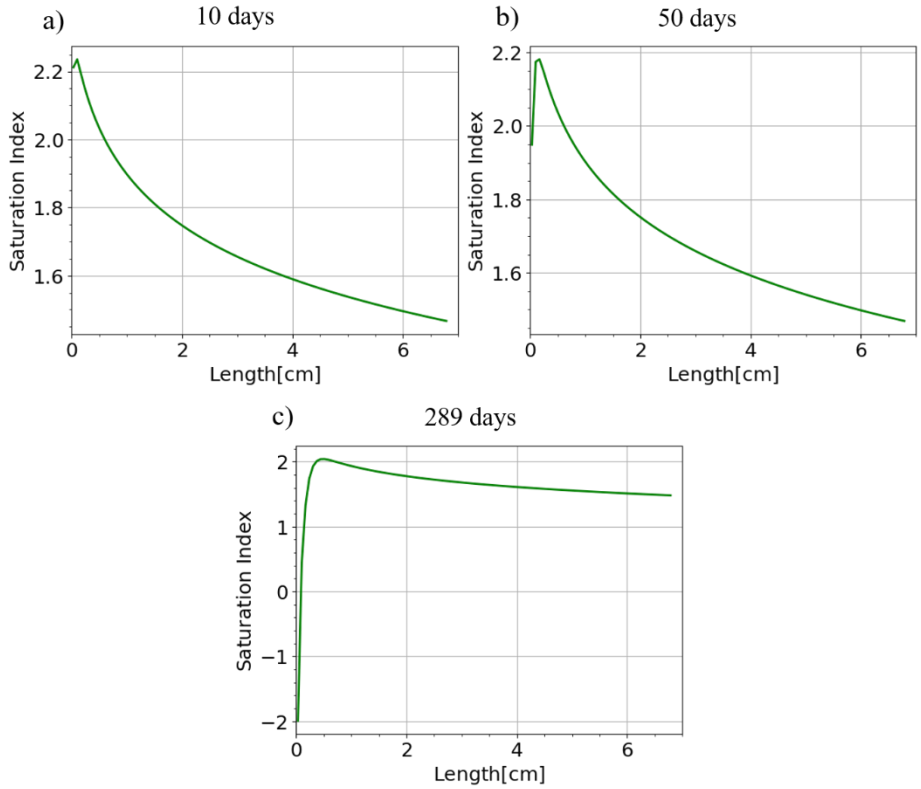

Figure 37: Saturation index of magnesite in the flooded calcite powder after a) 10 days b) 50 days and c) 289 days. After 289 days, magnesite no longer precipitates at the inlet, and may possibly even dissolve, due to changes in e.g. pH. Courtesy of Aksel Hiorth.

The most probable explanation for this miss-match is that small crystals of magnesite precipitate in the fluid phase at the inlet of the cores, where saturation indices are high, aggregate and settle further along the flooding axis of the core. This trend is observed already after months of flooding, but as seen in Figure 37, saturation indices are different towards the end of the flooding periods, and the processes of precipitation may also change. Even though this phenomenon was most easily observed in the artificial chalk cores, the same type of crystals and aggregates are found in experiments on outcrop chalk. It is therefore likely, as observed with other methodologies, that the same mechanisms are at play in outcrop and in reservoir chalk.

The abundance of magnesite and calcite at any given time and point in the core will influence the dissolution or precipitation rate accordingly, along with the surface properties of grains and crystals. As such, a combination of nucleation rate, growth rate and advection controls the distribution and population of magnesite precipitated during flooding. As there seem to be two fronts of alterations in both flooded chalk and possibly in flooded calcite powder (artificial chalk cores), one may presume that the different rates vary relative to each other and therefore impact the alteration processes in different ways with time of flooding and most likely the amount of material already altered. This could be linked to a threshold value of magnesite being precipitated in an area, as observed in the artificial chalk cores, where the level of measured MgO by ICP-MS had to be at least above 0.97 wt% for the core to consolidate (**Paper II**). All "slices" that had an MgO concentration below this value, was still in powdered form after flooding.

As discussed in chapter "3.1.2 A porous transition zone with sharp boundaries" the transition between the two alteration fronts has two features that were not expected before analyses. It is sharp, on mm-scale, and seems to be more porous than the remaining parts of the cores. This opens for discussion if the transformation from one mineralogy in a porous chalk core follows the same laws as the single crystal experiments observed by e.g. (Putnis et al., 2009), where the transformation is described to progress due to the formation of a porous zone. Such a zone is even more visible in the hollow cylinder experiment (Figure 20) described in section "3.1.2 A porous transition zone with sharp boundaries". Based on this, one may say that the mineral replacement reactions in a porous multi-grain system, behave much like in a single crystal experiments. However, because of the porous nature of the system, occurrences of newly precipitated crystals, clusters or grains, appear downstream of the transition zone, with distribution dependent on saturation

index, the amount of other minerals present and advection of the injected fluid through the system. These factors affect nucleation and growth rates, and therefore the appearance of the precipitated mineral. Additionally, differences in texture, structure and composition affect the rate of dissolution of existing minerals, but also the fluid-flow, or tortuosity, in the core. These factors will also influence the equilibrium-states such that they may differ throughout the system, hence again nucleation and growth rates are affected. It is therefore important to acknowledge the change over time in these factors when interpreting and modelling such experiments.

Special focus has been given to the reactive Mg^{2+}-ion in this work, as in several other research projects in EOR research e.g. (Korsnes et al., 2008a; Korsnes et al., 2008b; Madland et al., 2011; Megawati et al., 2011; Megawati et al., 2015; Nermoen et al., 2015; Wang et al., 2016; Zimmermann et al., 2015). This is because it is found that interactions between calcite and magnesium weaken the chalk. This may be due to differences in density (volume) of newly precipitated minerals. In addition, other processes or phenomena resulting from injection of Mg^{2+}, such as changes in surface charge and electrostatic forces between grains (Nermoen et al., 2018) or changes in non-carbonate content (Megawati et al., 2011) may affect the strength of the chalk. Even though many processes may be at play at one time during flooding, it is important to understand where and when these alterations take place and which minerals do precipitate. These observations are one of the tools used to constrain and validate models at both pore- and core-scale.

3.7 The effect of wettability

All of the presented experiments in this project have been performed on water wet cores, i.e. without oil present in the cores. It is also paramount to understand if the described mineralogical alterations also take place when oil is present in

chalk cores. FEG-SEM-EDS analyses have therefore been carried out on both water wet and mixed wet cores of Kansas chalk, flooded with $MgCl_2$, to compare the results. Micrographs show similar alterations in both cores, with smaller grains of precipitated magnesite along with scarce occurrences of larger crystals at the inlet of the cores (Figure 38a and b). Further away from the inlet, approximately at the middle of the cores along the flooding direction, polycrystalline aggregates of magnesite (Figure 38c and d), matching the aggregates found in both calcite powder and other outcrop chalks, are observed.

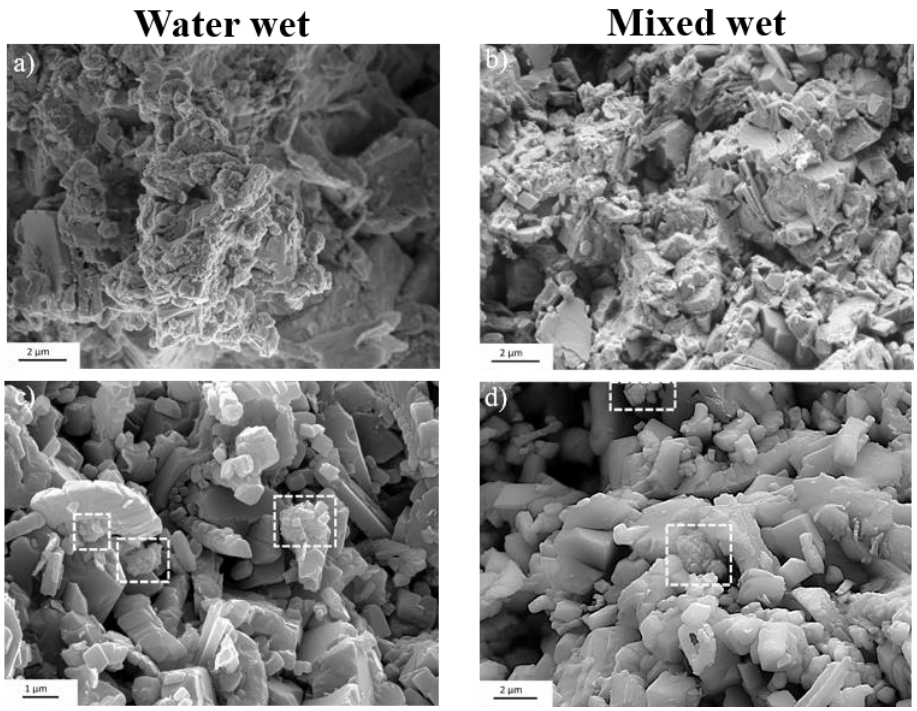

Figure 38: FEG-SEM micrographs of water wet and mixed wet Kansas chalk. At the inlet (a and b), small grains or crystals of magnesite precipitate on top of original calcite grains, while further into the core (c and d), polycrystalline magnesite aggregates precipitate.

Towards the outlet of the cores, no newly formed minerals could be observed by FEG-SEM. Given that also the geomechanical behaviour seems to be similar during creep in water wet and mixed wet chalk during flooding with $MgCl_2$

(Sachdeva, 2018), the preliminary conclusions of these studies indicate that the results on mineralogical alterations from test performed on water wet chalk, seem also be valid for mixed wet chalk.

3.8 A toolbox to analyse EOR experiments

Part of the objective for this project has been to design a toolbox that hold the capability to sufficiently resolve mineralogical questions related to EOR experiments (**Paper VI**). Not all of the described methods in this project are suitable to use as routine tools for studying the effect on mineralogical alterations due to different EOR-fluids. Several of the methods are challenging both with regards to time, expenses and sample preparation and should therefore only be used in cases when it is necessary to perform high-resolution analyses of e.g. nm-sized single grains, grain-contacts or pore-walls. TEM analyses are in themselves not especially time-consuming or expensive, but sample-preparation of brittle fine-grained rocks is challenging and should be performed with care. One of the methods taken into use is ion milling by FIB-SEM, which could be expensive. In addition, samples prepared by FIB-SEM are only ~100 nm thick, and are therefore easy to damage during measurements. Sample-preparation is also an issue with TERS-AFM, where good results are dependent on a very smooth surface to avoid too large differences in topography, which hampers the analyses. TERS-AFM is also a new technique to EOR research, and needs further tests to be optimized if to be used in this setting. Methods such as TERS-AFM, FIB-SEM and nanoSIMS can therefore not be part of a routine analyses toolbox.

Methods such as FEG-SEM, stable isotope and whole-rock geochemistry along with XRD can provide the user with enough information at a high enough resolution to identify and quantify mineralogical alterations in fine-grained rocks due to flooding with EOR fluids. These are methods, which are not too

expensive and do not take too much time. Complementary methods such as density and SSA measurements are also useful tools to measure the degree of alterations in flooded chalk, along with preliminary identification of mineralogy by Raman spectroscopy, depending on grain-size (**Paper VII**). For mapping of mineralogy on core-scale and down to micrometre-scale, MLA or equivalent methods may be used. The focus of in this thesis has been on fine-grained sedimentary rocks, which demands high-resolution analyses. The methods discussed here can therefore easily be taken into use for other types of rock, where grainsizes are larger and the rock samples are harder.

Last, but not least, it is important to see the huge advantages of using several methods that complement each other. Techniques such as FEG-SEM provides imaging and semi-quantitative results on the "which" and "where" of chemical alterations. This may be complemented by whole-rock and stable isotope geochemistry for more exact quantification in bulk samples and XRD to identify the exact mineralogy before and after flooding. Also, FEG-SEM can identify areas of special interest where one may want to take other methods into use, such as TEM, to gain more detailed information.

3.9 Implications for the industry

Large parts of the research process presented in this thesis can be considered basic research and cannot be directly applied for the oil industry. Directly applicable is the demonstration of which methods are ideally useful to gain quick data for an evaluation of laboratory experiments, and the mentioned 'toolbox' provides access to a set of tools ready to aid in interpretation of e.g. pilot tests or field-testing to understand the effects EOR-fluids and induced mineralogical alterations may have on mechanical parameters of the rock.

A deeper understanding of processes within the texture and the relation between primary and secondary mineralogy of the rock during flooding plays an

important part for all EOR efforts. This understanding is valuable as input to models and simulators, especially at pore- and core-scale, but also in the aspect of choosing the correct test material when performing experiments on EOR-effects in the laboratory. And, this study provides an understanding of that more detailed datasets on a nanoscale are necessary, in chalk for instance. Methods to gain those data are tested, although some are work intensive.

The importance of the role of non-carbonate minerals in the rock-fluid interaction cannot be underestimated. In chalk, this component is complex as the abundance is often minute, but can be of high significance during flooding of non-equilibrium brines. Silicates may also be affected by inert fluid-injection, and, when flooded with reactive brines, have significant impact on permeability of the matrix and fractures in the rock due to precipitation of clay minerals or other silicates. However, flooding with the same type of reactive brine in chalks with very low non-carbonate content may instead increase the permeability during the time of flooding. The effects of an EOR-fluid may therefore vary both with the composition of the brine as well as temperature and the primary mineralogy. This is e.g. observed in one of the long-term tests. For the core flooded for approximately two years, the compaction during creep was stopped and the production of calcium in the effluent were insignificant for a period of 63 days, when 0.130 M $CaCl_2$ was added to the $MgCl_2$ injection brine (**Paper I** and (Megawati et al., 2011)). This provides evidence that changing the composition of the injected brine, may directly impact the strain evolution of the rock.

Another interesting finding is how inhomogeneous alterations within a core are, with respect to changes in mineralogy, porosity and permeability (Figure 16 and Figure 18, and **Paper I)**. This may also be important at larger scales. The geomechanical and mineralogical alterations are also dependent on temperature (**Paper IV**), along with formation fluids, which need to be considered when

injecting fluids with different temperatures into a reservoir formation. The study clarifies that the depositional environment of the rocks, and in turn the paleoecology (including grain size, shape, organism-type, etc.) affect the fluid flow and the dissolution and precipitation. How much this is of importance when up-scaling, needs to be tested at larger scales.

The preliminary tests done in this project comparing water wet and mixed wet rock indicate that many of the results from the vast amount of experiments performed studying the effect of EOR-fluids in water wet rock, seem also to be valid for rocks containing oil, and may be used to understand reservoir behaviour. However, the studies performed here needs to be continued to validate this hypothesis.

4 Conclusion and future work

4.1 Conclusions

When searching for an optimized brine for EOR purposes, it is important to study the interactions between the brine and the rock, and the consequences for geomechanical parameters of the rock. In chalk, many of these interactions involve mineral replacement reactions. Therefore, the overall aim of this project has been to identify the minerals replacement reactions at play during mechanical flow-through experiments using various outcrop chalks and artificial chalk cores made of pure calcite powder. A thorough investigation has been conducted at core- pore- and nano-scale, and the results from all scales match, and, in cases, the combination of scales supplement each other to an improved understanding of the data. Most of the experiments presented in this thesis used reactive $MgCl_2$-brine as flooding agent, and some valuable conclusions can be drawn from the combination of their results.

The **which**: Besides silicate mineral phases such as talc, chlorite or possibly saponite, the main replacement of minerals involve dissolution of calcite and precipitation of magnesite with ~1–4 wt% calcium impurities, even after years of flooding (Figure 10). The clay minerals and magnesite vary in their distribution, shape and size, depending on flooding time and the type of chalk which is flooded. Differences in primary mineralogy, texture and diagenetic history affect precipitation of new mineral phases with respect to types of minerals, size, shape and abundance at any point in the core. However, certain similarities are observed. Within the original calcite mineralogy, magnesite is found as single crystals in the size-range from a few nm up to 10 µm, depending on available space and flooding time (Figure 8). Polycrystalline aggregates of the same type of magnesite also precipitate. The aggregates mostly comprise of

idiomorphic crystals of 100-200 nm, and the clusters themselves typically vary in size from 1 to 5 µm. These alterations are interpreted to take place as a primary mineralization front. After longer flooding periods, more than 500 days, a complete alteration of the mineralogy from calcite to magnesite is observed in parts of the chalk cores, the secondary front. Similar observations are found in flooded calcite powder (Figure 12, Figure 13 and Figure 15).

The **how**: The mineralogical transformations in long-term flooded chalk can be described to take place in two stages, identified by the primary and secondary mineralization fronts progressing through the cores, separated by a more porous transition zone with a sharp boundary (Figure 18). This process may also take place for tests flooded for shorter periods of time, but be difficult to observe.

Three interesting observations have been made on how these processes of alterations take place. 1) SEM and TEM-studies confirm that the contact-planes between adjacent calcite and magnesite crystals are sharp (Figure 30). The alterations are therefore considered to take place through dissolution and precipitation, and not molecular solid state diffusion through the crystal lattice. Severe dissolution defects observed on original calcite crystals support this result. 2) Crystal shapes and sizes vary with where in the core magnesite precipitate. During precipitation, shape and size of a crystal vary depending on the degree of super-saturation at any given point in the core, and the resulting nucleation and growth rates. In the studied experiments, the shapes and sizes of magnesite crystals, are not necessarily matched to the calculated saturation indices, where clusters of smaller crystals are found further along the flooding axis than expected. This may be explained by nanometre-sized crystals precipitating in the fluid-phase at the inlet of cores, where the saturation index are highest, for so to be transported further into the core by advection. The distribution of saturation indices can also be more complex and do, as seen when modelled by IORCoreSim, change over the time of the flooding

experiment (Figure 37). 3) The transition between the two alteration-regimes seems to be a sharp, highly porous zone. This observation matches what is observed by others on single crystal experiments, where the transformation process is driven by the formation of a porous zone between the old and the new mineralogy and is controlled by the equilibrium state within this zone, not of the saturation index of the bulk fluid (Putnis et al., 2009).

The **where**: The amount of newly formed magnesium-bearing minerals is highest at the inlet. The distribution of silicates after flooding vary with primary mineralogy and temperature. The crystal shapes and sizes are dictated by a combination of nucleation, growth and advection rates. Nucleation and growth rates are linked to the degree of super-saturation in the fluid with regards to magnesite. A miss-match in calculated saturation indices and the observed crystal shapes and sized in the core suggest that magnesite can be formed in one part of the core and transported to other places by the fluid-flow.

Another factor which affect crystal growth is the available space to grow in and available ions in the pore-fluid. Larger crystals are observed in larger pore-spaces and the concentration of precipitated clay minerals are enriched in pores and fractures.

A couple of other conclusions can also be drawn from this work. When flooding fine-grained chalk, commonly with low permeability, the texture of the rock, hence, the depositional environment and diagenetic history, seem to affect the fluid-flow and subsequently the degree of alteration due to rock-fluid interactions. Certain fossils are less prone to dissolution (Figure 22 and Figure 35) and may also block fluid-flow or locally alter the tortuosity of the flow, creating differences in the equilibrium state. Similar observations have been made with regards to fractures in chalk flooded with synthetic seawater (Figure 33). Accumulation of new-grown minerals are observed in the fractures, causing alterations of the fluid-flow and healing of fractures on centimetre-

scale (Figure 32). Thus, flooding with reactive brines may lead to altered permeability, blocking of existing fractures and re-direction of fluid-flow pathways, both at core-scale and possibly at reservoir-scale. Healing of fractures seems to, in these experiments, mainly involve precipitation of clay minerals, which are also observed to greatly reduce permeability during flooding of silicate rich chalk (Figure 36). The primary mineralogy affects the strength of the rock and which minerals precipitate during flooding as observed when comparing the results of flooding different outcrop chalks (**Paper V**) and the amount of non-carbonate content in chalk contribute to dictate which mineral replacement reactions take place.

A much discussed topic in the studies of mineral replacement reactions is the process of pseudomorphism. In the here presented experiments, pseudomorphism may be observed at several scales. In the ULTT, the whole core is transformed from calcite to magnesite, while keeping its cylindrical form. This may be considered pseudomorphism at centimetre-scale. However, more interesting is the pseudomorphism observed at micrometre-scale, where the shapes of macro-and micro-fossils are preserved, while the mineralogy is altered (Figure 31). As pseudomorphism is not observed on nanometre-scale, it may be concluded that the overall limiting factor is the precipitation rate of magnesite, not the dissolution rate of calcite (Xia et al., 2009).

Even though not directly applicable to a hydrocarbon reservoir, the results from this study show that mineralogical alterations in chalk due to flooding with reactive brines can be linked to certain observed changes in geomechanical parameters. As magnesite precipitates on the expense of calcite, measurements show that both the density and specific surface area increase after flooding with $MgCl_2$. This fits well with an increase in porosity and permeability and changes in mineralogy over the time of flooding, as observed in the MLTT and the ULTT after longer periods. Additionally, the process of dissolution and

precipitation may directly impact the strength of the chalk together with changes in surface-charge and electrostatic forces (Nermoen et al., 2018). Manipulating the composition of the injection-fluid may directly affect the changes that occur in geomechanical parameters of chalk (**Paper I** and (Megawati et al., 2011)). Insights into the "which, how and where" of these mechanisms are paramount input information to simulators used to model and predict the effects of EOR fluids at all scales. The true mineralogical data and their distribution are important to constrain and validate models.

FEG-SEM analyses conducted in this study can lead to preliminary conclusion that the mineralogical alterations observed in flooded chalk are the same whether the rock is water wet or mixed wet (Figure 38).

A toolbox which may be used to study mineralogical alterations from pore- to core-scale on effects of EOR-fluids has been put together. Analyses by FEG-SEM, XRD and whole-rock and stable isotope analyses can, along with analyses by SEM-based mapping techniques, provide enough data to assess the mineralogical alterations in most EOR-related experiments, or in pilot test and field-scale testing. When higher resolution is needed, tools like TEM and nanoSIMS may complement the results further.

4.2 Future work

In the future, core- and pore-scale research on EOR-fluids needs to be continued together with experiments to understand the effects such brines have on the rock. Several different EOR strategies are suggested, e.g. polymer and low salinity injection. Even though a lot of knowledge in this field already is in place, the impacts these fluids have on mineralogy should to be fully understood, down to nano-scale.

As mentioned, the amount and character of non-carbonate material are affecting several rock parameters during flooding. Clay minerals are, however, difficult

to positively identify based on elemental compositions alone and not possible to identify with Raman spectroscopy. The combination of textural analyses by SEM-EDS often aids in identification, along with crystallographic analyses such as XRD. Most clay minerals have similar dimensions in two directions, and only differ in the Z-dimension. Producing XRD signals that yield detailed enough patterns to separate clay minerals from each other is therefore challenging. TERS or sub-micron Raman studies are not favourable for chalk because of the softness of the material (Borromeo, 2018), but AFM and measurements of surface charges would be a method to identify distribution of clay minerals (Skovbjerg et al., 2012), but not feasible for a larger (> 5 micron) area of study. The best way would be to separate clay minerals from the chalk to be able to gain more accurate results in identifying these in the future.

With regards to the two stages of alterations observed during long-term testing of chalk, further experiments should be performed to investigate the timing and propagation of the front of complete transformation from calcite to magnesite. The onset of this alteration process may explain phenomena observed during flooding such as delayed creep for certain chalk types and the in-homogenous alteration processes in chalk may also be essential also at reservoir-scale. In-situ studies during flooding may be performed by using e.g. high resolution 3D X-ray microscopy, micro-Computer Tomography (CT), Magnetic Resonance Imaging (MRI) or Positron Emission Tomography (PET), and could contribute to the full understanding of this phenomena. Similarly, the possible healing effect of fractures and the distribution of silicate in chalk during flooding should be further studied, both in-situ on smaller scales, but also on larger scales to understand the effect of possible healing of fractures by flooding with reactive brines of different ionic compositions, inducing precipitation of e.g. clay minerals, anhydrite or gypsum.

An important point is to intensify the mineralogical analyses of mechanical flow-through experiments on mixed wet or oil wet systems. Our preliminary studies suggests that the results from water systems may be used to understand rock-fluid interactions in mixed wet systems and in a hydrocarbon reservoir. However, these analyses should be continued to understand the exact similarities and differences with regards to the wetting state of the rock when injecting EOR fluids at all scales.

One of the major challenges in EOR research is up-scaling of EOR-effects to reservoir-scale. This thesis describes processes that are important at pore- and core-scale, but the effect at field-scale (kilometre-scale) is not sufficiently studied. Injection of brines should therefore also be tested at scales of meter, or tens of meters to bridge the gap between centimetre- and kilometre-scale. Tests on larger blocks and cores have been performed (e.g. (Graue, 1994; Graue et al., 2000)), however, even larger facilities are needed to be able to understand which parameters and effects are important at reservoir-scale. Reservoir-scale testing has shown to be useful in studies of e.g. CO_2-foam e.g. (Sharma, 2019). This study, however, gave several inputs to possible consequences and factors which need to be acknowledged when studying the effect of EOR-fluids. These factors may be combined at shortest with the expression ‘depositional environment’. To determine this parameter in chalk is difficult and a meticulous effort, but the impact this has in up-scaling may be observed when tests are monitored on larger scales. On a pore- and core-scale this certainly plays an important role.

References

Abubeker, E. (2013) Water weakening of chalks - comparsion of intact and fractured cores. University of Stavanger, Norway.

Alam, M.M., Fabricius, I.L. and Christensen, H.F. (2012) Static and dynamic effective stress coefficient of chalk. *Geophysics* 77, L1-L11.

Andersen, P.Ø., Evje, S., Madland, M.V. and Hiorth, A. (2012) A geochemical model for interpretation of chalk core flooding experiments. *Chemical Engineering Science* 84, 218-241.

Andersen, P.Ø., Wang, W., Madland, M.V., Zimmermann, U., Korsnes, R.I., Bertolino, S.R.A., Minde, M., Schulz, B. and Gilbricht, S. (2017) Comparative Study of Five Outcrop Chalks Flooded at Reservoir Conditions: Chemo-mechanical Behaviour and Profiles of Compositional Alteration. *Transport in Porous Media* 121, 135–181.

Anderson, T. and Arthur, M. (1983) Stable isotopes of oxygen and carbon and their application to sedimentologic and paleoenvironmental problems. *Stable Isotopes in Sedimentary Geology, SEPM Short Course* 10, 1-151.

Andersson, M.P., Dideriksen, K., Sakuma, H. and Stipp, S.L.S. (2016) Modelling how incorporation of divalent cations affects calcite wettability–implications for biomineralisation and oil recovery. *Scientific Reports* 6.

Appelo, C.A.J. and Postma, D. (2009) *Geochemistry, groundwater and pollution*, 2 ed. CRC Press, New York.

Aursjø, O., Jettestuen, E., Vinningland, J.L. and Hiorth, A. (2017) An improved lattice Boltzmann method for simulating advective–diffusive processes in fluids. *J. Comput. Phys.* 332, 363-375.

Austad, T., Strand, S., Madland, M.V., Puntervold, T. and Korsnes, R.I. (2008) Seawater in chalk: An EOR and compaction fluid. *SPE Reservoir Evaluation and Engineering* 11, 648-654.

Bjørlykke, K. (2015) *Introduction to sedimentology: Sediment transport and sedimentary environments*. Springer Internation Publishing Berlin

Borchardt, J.K., Yen, T.F. and Chemical Congress of North, A. (1989) *Oil-field chemistry : enhanced recovery and production stimulation*. American Chemical Society, Washington, DC.

Borromeo, L. (2018) Raman spectroscopy applied to the mineralogical analysis of flooded chalk. University of Stavanger, Faculty of Science and Technology, Department of Energy Resources, Stavanger.

Brasher, J.E. and Vagle, K.R. (1996) Influence of lithofacies and diagenesis on Norwegian North Sea chalk reservoirs. *AAPG Bulletin* 80, 746-769.

Bredal, T.V. (2018) Micro- and nano-analyses of fracture-filling after flooding on-shore chalk with different IOR fluids. University of Stavanger.

Brunauer, S., Emmett, P.H. and Teller, E. (1938) Adsorption of Gases in Multimolecular Layers. *Journal of the American Chemical Society* 60, 309-319.

Carles, P. and Lapointe, P. (2005) Water-Weakening of Carbonates under Stress: New Insights into Pore-Volume Compressibility Measurements. *PETROPHYSICS* 46.

Collin, F., Cui, Y.J., Schroeder, C. and Charlier, R. (2002) Mechanical behaviour of Lixhe chalk partly saturated by oil and water: experiment and modelling. *International Journal for Numerical and Analytical Methods in Geomechanics* 26, 897-924.

Da Gama, R.O.B.P., Lutz, B., Desjardins, P., Thompson, M., Prince, I. and Espejo, I. (2014) Integrated paleoenvironmental analysis of the Niobrara Formation: Cretaceous Western Interior Seaway, northern Colorado. *Palaeogeography, Palaeoclimatology, Palaeoecology* 413, 66-80.

Delage, P., Cui, Y.J. and Schroeder, C. (1996) Subsidence And Capillary Effects In Chalks, *ISRM International Symposium - EUROCK 96. International Society for Rock Mechanics and Rock Engineering, Turin - Italy*.

Dusar, M. and Lagrou, D. (2007) Cretaceous flooding of the Brabant Massif and the lithostratigraphic characteristics of its chalk cover in northern Belgium. *Geologica Belgica*.

Evje, S. and Hiorth, A. (2011) A model for interpretation of brine-dependent spontaneous imbibition experiments. *Advances in Water Resources* 34, 1627-1642.

Fandrich, R., Gu, Y., Burrows, D. and Moeller, K. (2007) Modern SEM-based mineral liberation analysis. *International Journal of Mineral Processing* 84, 310-320.

Fathi, S.J., Austad, T. and Strand, S. (2011) Water-based enhanced oil recovery (EOR) by "Smart Water": optimal ionic composition for EOR in carbonates. *Energy and Fuels* 25.

Fernø, M.A., Grønsdal, R., Åsheim, J., Nyheim, A., Berge, M. and Graue, A. (2011) Use of sulfate for water based enhanced oil recovery during spontaneous imbibition in chalk. *Energy and Fuels* 25, 1697-1706.

Flügel, E. (2004) *Microfacies of carbonate rocks : analysis, interpretation and application*. Springer, Berlin.

Garrison, T. (2010) *Oceanography : an invitation to marine science*, 7th ed. ed. Brooks/Cole Cengage Learning, Belmont, Calif.

Gaviglio, P., Vandycke, S., Schroeder, C., Coulon, M., Bergerat, F., Dubois, C. and Pointeau, I. (1999) Matrix strains along normal fault planes in the Campanian White Chalk of Belgium: structural consequences. *Tectonophysics* 309, 41-56.

Geitle, K. (2013) Chemically induced compaction in fractured and intact chalk cores. University of Stavanger, Norway.

Generosi, J., Ceccato, M., Andersson, M.P., Hassenkam, T., Dobberschütz, S., Bovet, N. and Stipp, S.L.S. (2017) Calcite wettability in the presence of dissolved Mg 2+ and SO 4 2. *Energy and Fuels* 31, 1005-1014.

Gòmez, J., Goy, A. and Canales, M. (2008) Seawater temperature and carbon isotope variations in belemnites linked to mass extinction during the Toarcian (Early Jurassic) in Central and Northern Spain. *Palaeogeography, Palaeoclimatology, and Palaeoecology* 258, 28-58.

Graue, A. (1994) Imaging the Effect of Capillary Heterogeneites on Local Saturation Development in Long-Core Floods. *SPEDC* 9.

Graue, A., Moe, R.W. and Bognø, T. (2000) Oil Recovery in Fractured Reservoirs, 6th Nordic Symposium on Petrophysics, Trondheim.

Griffiths, J. (2008) Secondary Ion Mass Spectrometry. *Analytical Chemistry* 80, 7194-7197.

Gutierrez, M., Øino, L.E. and Høeg, K. (2000) The Effect of Fluid Content on the Mechanical Behaviour of Fractures in Chalk. *Rock Mechanics and Rock Engineering* 33, 93-117.

Hancock, J.M. (1975) The petrology of the Chalk. *Proceedings of the Geologists Association* 86, 499-535.

Handley, J. (2002) Product Review: Secondary Ion Mass Spectrometry. *Analytical Chemistry* 74, 335 A-341 A.

Hattin, D.E. and Cobban, W.A. (1977) Fourth and Fifth Days Upper Cretaceous Stratigraphy, Paleontology and Paleecology of Western Kansas. *The Mountain Geologist*.

Hedegaard, K. and Graue, A. (2011) Does Wettability Affect the Strength of Chalk?, *45th U.S. Rock Mechanics / Geomechanics Symposium. American Rock Mechanics Association*, San Francisco, California.

Heggheim, T., Madland, M.V., Risnes, R. and Austad, T. (2005) A chemical induced enhanced weakening of chalk by seawater. *Journal of Petroleum Science and Engineering* 46, 171 - 184.

Helland, J.O., Friis, H.A., Jettestuen, E. and Skjæveland, S.M. (2017) Footprints of spontaneous fluid redistribution on capillary pressure in porous rock. *Geophysical Research Letters* 44.

Hellmann, R., J N Renders, P., Gratier, J.-P. and Robert Guiguet, A. (2002) *Experimental pressure solution compaction of chalk in aqueous solutions Part 1. Deformation behavior and chemistry*.

Hermansen, H., Landa, G.H., Sylte, J.E. and Thomas, L.K. (2000) Experiences after 10 years of waterflooding the Ekofisk Field, Norway. *Journal of Petroleum Science and Engineering* 26, 11-18.

Hermansen, H., Thomas, L.K., Sylte, J.E. and Aasboe, B.T. (1997) Twenty Five Years of Ekofisk Reservoir Management. *Society of Petroleum Engineers*.

Hiorth, A., Cathles, L.M. and Madland, M.V. (2010) The Impact of Pore Water Chemistry on Carbonate Surface Charge and Oil Wettability. *Transport in Porous Media* 85, 1-21.

Hiorth, A., Jettestuen, E., Cathles, L.M. and Madland, M.V. (2013) Precipitation, dissolution, and ion exchange processes coupled with a lattice Boltzmann advection diffusion solver. *Geochim. Cosmochim. Acta* 104, 99-110.

Hirata, K., Saitoh, Y., Chiba, A., Yamada, K., Takahashi, Y. and Narumi, K. (2011) Secondary ion counting for surface-sensitive chemical analysis of organic compounds using time-of-flight secondary ion mass spectroscopy with cluster ion impact ionization. *Review of Scientific Instruments* 82.

Hjelen, J. and Sintef (1989) *Scanning elektron-mikroskopi*. SINTEF, Trondheim.

Hjuler, M.L. (2007) Diagenesis of Upper Cretaceous onshore and offshore chalk from the North Sea area, Institute of Environment & Resources. Technical University of Denmark.

Hjuler, M.L. and Fabricius, I.L. (2009) Engineering properties of chalk related to diagenetic variations of Upper Cretaceous onshore and offshore chalk in the North Sea area. *Journal of Petroleum Science and Engineering* 68, 151-170.

Hoefs, J. (2015) *Stable Isotope Geochemistry*, 7th ed. 2015. ed. Springer International Publishing, Berlin.

Håkansson, E., Bromley, R. and Perch-Nielsen, K. (1975) Maastrichtian chalk of north-west Europe—a pelagic shelf sediment. *Pelagic Sediments: on Land and under the Sea*, 211-233.

Jackson, M., Al-Mahrouqi, D. and Vinogradov, J. (2016) Zeta potential in oil-water-carbonate systems and its impact on oil recovery during controlled salinity water-flooding. *Scientific Reports (Nature Publisher Group)* 6, 37363.

Jonas, L., Mueller, T., Dohmen, R., Baumgartner, L. and Putlitz, B. (2015) Transport-controlled hydrothermal replacement of calcite by Mg-carbonates. *Geology (Boulder)* 43, 779-782.

Jørgensen, N.O. (1987) Oxygen and carbon isotope compositions of Upper Cretaceous chalk from the Danish sub-basin and the North Sea Central Graben. *Sedimentology* 34, 559-570.

Kennedy, W.J. (1987) *Late Cretaceous and early Palaeocene Chalk Group sedimentation in the Greater Ekofisk area, North Sea central graben*.

Korsnes, R.I., Hiorth, A. and Madland, M.V. (2008a) Detection of chemical processes affecting chalk mechanical strength with the use of different flooding brines at elevated temperatures, *33rd International Geological Congress*, Oslo.

Korsnes, R.I., Madland, M.V., Austad, T., Haver, S. and Røsland, G. (2008b) The effects of temperature on the water weakening of chalk by seawater. *Journal of Petroleum Science and Engineering* 60, 183-193.

Korsnes, R.I., Risnes, R., Faldaas, I. and Norland, T. (2006) End effects on stress dependent permeability measurements. *Tectonophysics* 426, 239-251.

Lawrence, J.A., Mortimore, R.N., Stone, K.J. and Busby, J.P. (2013) Sea saltwater weakening of chalk and the impact on cliff instability. *Geomorphology* 191, 14-22.

Levenson, Y. and Emmanuel, S. (2013) Pore-scale heterogeneous reaction rates on a dissolving. *Geochimica et Cosmochimica Acta* 119, 188 - 197.

Lichtner, P.C., Steefel, C. I., Oelkers, E. H. (1996) *Reactive Transport in Porous Media*. Mineralogical Society of America, Washington D.C., USA.

Longman, M., Luneau, B.A. and Landon, S.M. (1998) *Nature and distribution of Niobrara lithologies in the Cretaceous Western Interior Seaway of the Rocky Mountain region*.

MacDonald, G.J.F. (1956) Experimental determination of calcite-aragonite equilibrium relations at elevated temperatures and pressures. *American Mineralogist* 41, 744-756.

Madland, M., Hiorth, A., Omdal, E., Megawati, M., Hildebrand-Habel, T., Korsnes, R., Evje, S. and Cathles, L. (2011) Chemical Alterations Induced by Rock–Fluid Interactions When Injecting Brines in High Porosity Chalks. *Transport in Porous Media* 87, 679-702.

Maury, V., Piau, J.M. and Halle, G. (1996) Subsidence induced by water injection in water sensitive reservoir rocks: The example of Ekofisk, *SPE European Petroleum Conference*, Milan, Italy, pp. 153-170.

Megawati, M. (2015) Geochemical aspects of water-induced compaction in high-porosity chalks, Institutt for petroleumsteknologi. University of Stavanger, Faculty of Science and Technology, Department of Petroleum Engineering, Stavanger.

Megawati, M., Andersen, P.Ø., Korsnes, R.I., Evje, S., Hiorth, A. and Madland, M.V. (2011) The effect of aqueous chemistry pH on the time dependent deformation behaviour of chalk - experimental and modeling studies, *Flows and and mechanics in natural porous media from pore to field scale. Pore2Field*, Paris.

Megawati, M., Hiorth, A. and Madland, M.V. (2013) The Impact of Surface Charge on the Mechanical Behavior of High-Porosity Chalk. *Rock Mechanics and Rock Engineering* 46, 1073-1090.

Megawati, M., Madland, M.V. and Hiorth, A. (2015) Mechanical and physical behavior of high-porosity chalks exposed to chemical perturbation. *Journal of Petroleum Science and Engineering* 133, 313-327.

Milter, J. and Øxnevad, I.E.I. (1996) Spontaneous imbibition in two different chalk facies. *Petroleum Geoscience* 2, 231-240.

Minde, M.W., Haser, S., Korsnes, R.I., Zimmermann, U. and Madland, M.V. (2017) Comparative Studies of Mineralogical Alterations of Three Ultra-long-term Tests of Onshore Chalk at Reservoir Conditions, *EAGE - 19th European Symposium on Improved Oil Recovery/IOR NORWAY 2017*, Stavanger.

Minde, M.W., Zimmermann, U., Madland, M.V. and Korsnes, R.I. (2016) Micron and submicron investigation - what can we learn?, *IOR NORWAY 2016*, Stavanger.

Molenaar, N. and Zijlstra, J.J.P. (1997) Differential early diagenetic low-Mg calcite cementation and rhythmic hardground development in Campanian-Maastrichtian chalk. *Sedimentary Geology* 109, 261-281.

Moore, C.H. (2001) *Carbonate reservoirs : porosity evolution and diagenesis in a sequence stratigraphic framework*. Elsevier, Amsterdam.

Morse, J.W. and Arvidson, R.S. (2002) The dissolution kinetics of major sedimentary carbonate minerals. *Earth Science Reviews* 58, 51-84.

Mortimore, R.N., Stone, K.J., Lawrence, J. and Duperret, A. (2004) Chalk physical properties and cliff instability. *Geological Society, London, Engineering Geology Special Publications* 20, 75-88.

Myerson, A. and Myerson, A.S. (2002) *Handbook of industrial crystallization*, 2nd ed. ed. Butterworth-Heinemann, Boston.

Nagel, N.B. (1998) Ekofisk Field Overburden Modelling. *Society of Petroleum Engineers.*

Nermoen, A., Korsnes, R.I., Hiorth, A. and Madland, M.V. (2014) Insights from long term experiments of compaction and non-equilibrium water flooding of chalks, *Geological Society of London*, 2014, London.

Nermoen, A., Korsnes, R.I., Hiorth, A. and Madland, M.V. (2015) Porosity and permeability development in compacting chalks during flooding of nonequilibrium brines: Insights from long-term experiment. *Journal of Geophysical Research: Solid Earth* 120, 2935-2960.

Nermoen, A., Korsnes, R.I., Storm, E.V., Stødle, T., Madland, M.V. and Fabricius, I.L. (2018) Incorporating electrostatic effects into the effective stress relation — Insights from chalk experiments. *Geophysics* 33 (3).

Newman, G.H. (1983) The Effect of Water Chemistry on the Laboratory Compression and Permeability Characteristics of Some North Sea Chalks. *Journal of Petroleum Technology* 35(05). 976-980.

Oelkers, E.H. and Schott, J. (2009) *Thermodynamics and Kinetics of Water-Rock Interaction*. Mineralogical Society of America, Cantilly, Virginia, USA.

Ohfuji, H. and Rickard, D. (2005) Experimental syntheses of framboids—a review. *Earth Science Reviews* 71, 147-170.

Pedersen, J., Jettestuen, E., Madland, M.V., Hildebrand-Habel, T., Korsnes, R.I., Vinningland, J.L. and Hiorth, A. (2016) A dissolution model that accounts for coverage of mineral surfaces by precipitation in core floods. *Advances in Water Resources* 87, 68-79.

Pedersen, J., Jettestuen, E., Vinningland, J.L. and Hiorth, A. (2014) Improved Lattice Boltzmann Models for Precipitation and Dissolution. *Transport in Porous Media* 104, 593-605.

Piau, J.M. and Maury, V. (1994) Mechanical effects of water injection on chalk reservoirs, *Rock Mechanics in Petroleum Engineering. Society of Petroleum Engineers*, Delft, Netherlands.

Puntervold, T. and Austad, T. (2008) Injection of seawater and mixtures with produced water into North Sea chalk formation: Impact of fluid-rock interactions on wettability and scale formation. *J. Pet. Sci. Eng.* 63, 23-33.

Putnis, A., Oelkers, E.H. and Schott, J. (2009) Mineral replacement reactions. *Reviews in Mineralogy and Geochemistry* 70, 87-124.

Putnis, A. and Putnis, C.V. (2007) The mechanism of reequilibration of solids in the presence of a fluid phase. *Journal of Solid State Chemistry* 180, 1783-1786.

Raman, C.V. (1928) A new radiation*. *Indian Journal of Physics* 2, 387-398.

Rhett, D.W. and Lord, C.J. (2001) Water weakening in sedimentary rocks, DC Rocks 2001, *The 38th U.S. Symposium on Rock Mechanics (USRMS). American Rock Mechanics Association*, Washington, D.C.

Richard, J., Sizun, J.P. and Machhour, L. (2005) Environmental and diagenetic records from a new reference section for the Boreal realm: The Campanian chalk of the Mons basin (Belgium). *Sedimentary Geology* 178, 99-111.

Risnes, M.V., Madland, M.V., Hole, M.V. and Kwabiah, M.V. (2005) Water weakening of chalk - Mechanical effects of water-glycol mixtures. *Journal of Petroleum Science and Engineering* 48, 21-36.

Risnes, R. (2001) Deformation and yield in high porosity outcrop chalk. *Phys. Chem. Earth Pt. A-Solid Earth Geod.* 26, 53-57.

Risnes, R., Gjesdal, S.A., Landaas, T.L. and Madland, I. (1994) Changes in mechanical properties of chalk caused by deformation and by pore pressure, *Rock Mechanics in Petroleum Engineering. Society of Petroleum Engineers*, Delft, Netherlands.

Roehl, P.O. and Choquette, P.W. (1985) *Carbonate petroleum reservoirs*. Springer, New York.

Runnels, R.T. and Dubins, I.M. (1949) Chemical and petrographic studies of the Fort Hays Chalk in Kansas. *Kansas Geological Survey Bulletin* 82, 1-36.

Sachdeva, J.S., Nermoen, Anders, Korsnes, Reidar I., Madland, Merete V., (2018) Effect of presence of oil and water on chalk mechanics, *IOR NORWAY 2018*. Stavanger, Norway.

Sakuma, H., Andersson, M.P., Bechgaard, K., Stipp, S.L.S. and Sakuma, S.L.S. (2014) Surface tension alteration on calcite, induced by ion substitution. *Journal of Physical Chemistry C* 118, 3078-3087.

Scholle, P.A. (1977) Chalk diagenesis and its relation to petroleum exploration; oil from chalks, a modern miracle? *AAPG Bulletin* 61, 982-1009.

Scholle, P.A. (1978) *A color illustrated guide to carbonate rock constituents, textures, cements, and porosities*. American Ass. of Petroleum geologists, Tulsa.

Scholle, P.A. and Kinsman, D.J.J. (1973) Diagenesis of upper Cretaceous chalks from North Sea, England and Northern Ireland. *The American Association of Petroleum Geologists Bulletin* 57, 803-804.

Schroeder, C., Bois, A.P., Maury, V. and Halle, G. (1998) Water/Chalk (or Collapsible Soil) Interaction: Part II. Results of Tests Performed In Laboratory On Lixhe Chalk to Calibrate Water/Chalk Models, *SPE/ISRM Rock Mechanics in Petroleum Engineering. Society of Petroleum Engineers*, Trondheim, Norway.

Sharma, M.A., Z. P., Fredriksen, S. B., Fernø, M. A., Graue, A. (2019) Foam for CO2 EOR in a Carbonate Reservoir: Scale-up from Lab to Field, in: Singh, K.H., Joshi, R.M. (Ed.), *Petro-physics and Rock Physics of Carbonate Reservoirs*. Springer Singapore, Singapore.

Skovbjerg, L.L., Hassenkam, T., Makovicky, E., Hem, C.P., Yang, M., Bovet, N. and Stipp, S.L.S. (2012) Nano sized clay detected on chalk particle surfaces.(Report). *Geochim. Cosmochim. Acta* 99, 57.

Snow, S.E. and Brownlee, M.H. (1989) Practical and Theoretical Aspects of Well Testing in the Ekofisk Area Chalk Fields, *SPE Annual Technical Conference and Exhibition. Society of Petroleum Engineers,* San Antonio, Texas.

Solberg, J.K. and Hansen, V. (2007) *Innføring i transmisjon elektronmikroskopi*. s.n., S.l.

Strand, S., Hognesen, E.J. and Austad, T. (2006) Wettability alteration of carbonates - Effects of potential determining ions (Ca2+ and SO42-) and temperature. *Colloid Surf. A-Physicochem. Eng. Asp.* 275, 1-10.

Sulak, R.M. and Danielsen, J. (1989) Reservoir Aspects of Ekofisk Subsidence. *Journal of Petroleum Technology* 41, 709-716.

Surlyk, F., Damholt, T. and Bjerager, M. (2006) *Stevns Klint, Denmark: Uppermost Maastrichtian chalk, Cretaceous-Tertiary boundary, and lower Danian bryozoan mound complex*.

Surlyk, F., Stemmerik, L., Ahlborn, M., Harlou, R., Lauridsen, B., Rasmussen, S., Schovsbo, N., Sheldon, E. and Thibault, N. (2010) *The cyclic Rordal Member - a new lithostratigraphic unit of chronostratigraphic and palaeoclimatic importance in the upper Maastrichtian of Denmark*.

Tang, G.-Q. and Firoozabadi, A. (2001) Effect of Pressure Gradient and Initial Water Saturation on Water Injection in Water-Wet and Mixed-Wet Fractured Porous Media. *SPE Reservoir Evaluation & Engineering* 4, 516-524.

Teufel, L.W., Rhett, D.W. and Farrell, H.E. (1991) Effect of Reservoir Depletion And Pore Pressure Drawdown On In Situ Stress And Deformation In the Ekofisk Field, North Sea. *American Rock Mechanics Association*.

Thiel, V. (2011) Coccolithophores, in: Reitner, J. (Ed.), *Encyclopedia of Geobiology*. Springer, Dordrecht pp. 277-278.

Torsaeter, O. (1984) An Experimental Study of Water Imbibition in Chalk From the Ekofisk Field, *SPE Enhanced Oil Recovery Symposium. Society of Petroleum Engineers,* Tulsa, Oklahoma.

Tucker, M.E., Wright, V.P. and Dickson, J.A.D. (1990) *Carbonate sedimentology*. Blackwell, Oxford.

Vinningland, J.L., Jettestuen, E., Aursjø, O., Madland, M.V. and Hiorth, A. (2017) *Mineral Dissolution and Precipitation Rate Laws Predicted from Reactive Pore Scale Simulations*.

Wang, W., Madland, M.V., Zimmermann, U., Nermoen, A., Korsnes, R.I., Bertolino, S.R.A. and Hildebrand-Habel, T. (2016) Evaluation of porosity change during chemo-mechanical compaction in flooding experiments on Liège outcrop chalk. *Geological Society, London, Special Publications* 435.

Wei, L. (2012) Sequential Coupling of Geochemical Reactions With Reservoir Simulations for Waterflood and EOR Studies. *Society of Petroleum Engineers*.

Wright, E. (1987) Stratification and paleocirculation of the Late Cretaceous Western interior seaway of North Americal. *Geological Society of America Bulletin* 99, pp. 480-490.

Xia, F., Brugger, J., Chen, G., Ngothai, Y., O'Neill, B., Putnis, A. and Pring, A. (2009) Mechanism and kinetics of pseudomorphic mineral replacement reactions: A case study of the replacement of pentlandite by violarite. *Geochim. Cosmochim. Acta* 73, 1945-1969.

Zhang, P., Tweheyo, M.T. and Austad, T. (2007) Wettability alteration and improved oil recovery by spontaneous imbibition of seawater into chalk: Impact of the potential determining ions Ca 2+, Mg 2+, and SO 4 2−. *Colloids and Surfaces A: Physicochemical and Engineering Aspects* 301, 199-208.

Zimmermann, U., Madland, M.V., Nermoen, A., Hildebrand-Habel, T., Bertolino, S.A.R., Hiorth, A., Korsnes, R.I., Audinot, J.-N. and Grysan, P. (2015) Evaluation of the compositional changes during flooding of reactive fluids using scanning electron microscopy, nano-secondary ion mass spectrometry, X-ray diffraction, and whole-rock geochemistry. *AAPG Bulletin* 99, 791-805.